ABSTRACT

HOSEIN, ALTHEA MARIA. Survival of *Escherichia coli* O157:H7 in Acidified Foods: A Predictive Modeling Approach. (Under the direction of Dr. Charles E. Smith and Dr. Frederick Breidt Jr.)

Since the initial outbreak reported in 1982, there have been numerous cases of illness associated with *Escherichia coli* O157:H7. Epidemiological reports estimate that 20,000 cases of *E. coli* related illness are seen each year. A study of the O157:H7 outbreaks in the United States from 1982-2002 revealed that food-borne related illness accounts for roughly 50% of the reported cases [Emerging Infectious Diseases 11:4 2005 pp. 603-609]; thus the survival of *E. coli* O157:H7 in food systems is of great concern.

Predictive microbiology aims to create and evaluate appropriate mathematical models for describing microbial growth and survival in food systems. In this dissertation, mathematical models are developed and assessed for their ability to characterize the survival of *E. coli* O157:H7 in acidic environments similar to those exhibited in acidified food products. The classic Weibull model was used as a primary model to characterize the linear and nonlinear killing kinetics of *E. coli* exposed to acid and salt. Analysis of the nonlinear survival and the intracellular physiology revealed a significant correlation between the killing kinetics and the intracellular pH. A secondary linear model was additionally able to describe the time needed to achieve a 5-log reduction in viable cell counts; however this secondary model underestimated the times to achieve a 5-log reduction in validation experiments.

A mechanistic model of *E. coli* acid inhibition based on chemical composition of the intracellular matrix was derived. This model predicts the change in intracellular pH when

cells are subjected to increasing concentrations of acetic acid. The survival of *E. coli* in solutions of different salts was also studied and an in-depth model comparison is presented here. Finally, a modeling consideration of the use of a nonlinear, autonomous differential equation or a linear, non-autonomous one for Gompertzian growth and inactivation is examined. While for a single dataset with a fixed initial condition yields an indistinguishable curve, the models can be distinguished if a second initial condition is used in a follow up experiment. Tumor growth and *E. coli* survival datasets were used to illustrate these issues. The modeling and experimental approaches presented in this dissertation reveal possible methods for controlling the survival of *E. coli* in low-pH
($pH < 4.6$) environments.

Survival of *Escherichia coli* O157:H7 in Acidified Foods: A predictive Modeling Approach

by
Althea Maria Hosein

A dissertation submitted to the Graduate Faculty of
North Carolina State University
in partial fulfillment of the
requirements for the Degree of
Doctor of Philosophy

Biomathematics

Raleigh, North Carolina

2010

APPROVED BY:

Dr. Charles E. Smith Chair of Advisory Committee	Dr. Fred Breidt Jr. Co-Chair of Advisory Committee
Dr. Roger McFeeters	Dr. Mansoor Haider

DEDICATION

To my husband for his endless support.

To my mother, late father, sister, and brother for always believing in me.

BIOGRAPHY

Althea Maria Hosein was born to Beverley Rosanna Draggon and Millard Joseph Smith in Kingston, Jamaica. She is the youngest of 3 children who include her brother David and sister Diana. At the age of 2, her family moved to Queens, New York. Althea loved mathematics and it was always the first homework assignment she would complete each night. Althea also loved music and the performing arts. As a child she was very active in dance and later attended Bayside High School for vocal performing. After graduating high school, knowing that she wanted to stay in New York for college, she enrolled in Stony Brook University. It is while at Stony Brook she met and shared classes with her future husband Leslie. Midway into completing a research project in Dr. John Reinitz's laboratory, she was convinced that she wanted to attend graduate school for biomathematics. She graduated Stony Brook University cum laude with a B.S. in Mathematics and in 2004 entered the Biomathematics Program at North Carolina State University. She later obtained a Masters of Science in Biomathematics in the Summer of 2007. Since 2007 she has continued in the Biomathematics Program, completing her Ph.D. in the Fall of 2010.

ACKNOWLEDGMENTS

It is my faith in God which has gotten me through graduate school. His grace and mercy has given me the courage and resilience needed to complete this degree.

I would like to acknowledge the unfailing support of my research co-advisors Drs Charles E. Smith and Frederick Breidt Jr. Their patience, scientific guidance and encouragement have made this dissertation possible. I am greatly honored to have worked with them throughout my graduate career. I would also like to thank Dr. Roger McFeeters for his biochemical expertise and providing funding towards completing this degree; and Dr. Mansoor Haider for his insight, contributions and serving on my committee. Lastly, I would like to acknowledge Dr. Sharon Lubkin for her contributions in developing the models presented in Chapter 3 of this dissertation.

I would like to acknowledge all current and former members of the USDA ARS Food Science Research Unit all of whom have been very helpful and willing to share their advice. They have never failed to offer help or answer questions related to developing new laboratory protocols.

I would like to thank the co-principal investigators, Drs. Laura Bottomley and Karen Hollebrands, of the RAMP-UP program for providing funding for three years of graduate school. It was an honor to be a RAMP-UP Fellow and provide a valuable resource to the Wake County community. Special gratitude is extended to former and current RAMP-UP staff members; especially Mrs. Elizabeth Parry for being a great mentor and advisor and Ms. Lynn Albers for being very supportive, reliable and an awesome team member.

My family and friends have supported me emotionally through this journey. My mother has always given words of encouragement and my brother and sister have always offered their support even though we don't see each other very often. Special thanks are extended to Mrs. Shelly-ann Love and Ms. Merle Craig for their encouraging words, humor and candor; and Ms. DaJuanicia Holmes for her support and opening her home to me for my extended stay in Raleigh, North Carolina. I would also like to thank my in-laws for giving me words of encouragement and praying for me along this journey.

Finally, this degree would have not been possible if it was not for the love and sacrifice of my husband Leslie. He has read all chapters of this dissertation, offered constructive criticism and fruitful discussions about this work. I am grateful to have him in my life.

TABLE OF CONTENTS

LIST OF FIGURES ix
LIST OF TABLES xiv
LIST OF NOMENCLATURE xv
1 Introduction 1

1.1 Modeling Microbial Responses 1

1.1.1 Predictive Microbiology 3
1.1.2 Survival Models 4
1.1.3 A Note on Mechanistic Models 17

1.2 *ESCHERCHIA COLI* O157:H7 18

1.2.1 Microbiology 18
1.2.2 Epidemiology 27
1.2.3 Clinical Manifestations and Treatment 30

1.3 Acidified Vegetables and Food Safety 31
1.4 Proposed Research 33

2 Modeling the Effects of Salt, Acetic Acid and Intracellular pH on the Survival of *Escherichia coli* O157:H7 34

2.1 Abstract 34
2.2 Introduction 35
2.3 Materials and Methods 37

2.3.1 Bacterial Strain and Growth Conditions 37
2.3.2 Acetic acid and NaCl Treatments 38
2.3.3 Intracellular pH 39
2.3.4 Modeling and Statistical Analysis 41

2.4 Results 42

2.4.1 Survival 42
2.4.2 Effects of Acid and Salt on 5-log Reduction Time 43
2.4.3 Intracellular pH 43
2.4.4 Intracellular pH and Survival 44

2.5 Discussion 46
2.6 Acknowledgements 50
2.7 Supplementary Materials 58

3 Mathematical Modeling of the Intracellular pH of *Escherichia coli* 61

3.1 Introduction 61
3.2 A Simple Mechanistic Intracellular pH Model 62

3.2.1 Chemical Equilibrium 62
3.2.2 Material and Methods 63
3.2.3 Model Development 64
3.2.4 Methods 66
3.2.5 Results and Discussion 69

3.3 Modifying the Mechanistic Intracellular pH Model 72

3.3.1 Activity Coefficients 72
3.3.2 Results and Discussion 75

4 Models for Describing *E. coli* Inactivation by Various Salts 78

4.1 The Effects of Salt on *E. coli* O157:H7 Survival in Acidic pH 78

4.1.1 Introduction 78
4.1.2 Materials and Methods 80
4.1.3 Results 82
4.1.4 Discussion 88

4.2 Deterministic Inactivation Models 90

4.2.1 Introduction 90
4.2.2 Weibull Model 91
4.2.3 Gompertz Model 91
4.2.4 Logistic Model 93
4.2.5 Cole Model 94
4.2.6 Goodness-of-fit Criteria 94
4.2.7 Results 98
4.2.8 Discussion 103

4.3 A Note on Stochastic Inactivation Models for Describing Single Cell Behaviors 105

4.3.1 Weibull Distribution 106
4.3.2 Multi-Target Model 107
4.3.3 Results 108
4.3.4 Discussion 110

5 Autonomous and Non-autonomous Models for Describing Growth and Survival Behaviors 111

5.1 Introduction 111
5.2 Material and Methods 112
5.3 Mathematical Models 113

5.3.1 Gompertz Model 113
5.3.2 Logistic Model 114

5.4 Results 117
5.5 Discussion 122

6 Conclusions 124

REFERENCES 127
APPENDIX... 142

LIST OF FIGURES

Figure 1.1 Phases of bacterial growth. 2

Figure 1.2 Semi-logarithmic plot which is representative of first order linear decay for a microbial population. 6

Figure 1.3 Examples of nonlinear survival curves. Panels (A) and (B) were created using a Weibull model, (C) was created by using a Fermi-like model and (D) was created by using a modified Gompertz model. 8

Figure 1.4 The time to reach inactivation for a cell that is sensitive to inactivation treatment (A.1) compared to a cell that is resistant to the same treatment (A.2). For the Fermi distribution (panels B.1 and B.2) the red curves represent a change in the inactivation time (t_c) and the blue curves represent a change in the model parameters. For the three parameter Weibull distribution (panels C.1 and C.2), the blue curves represent a change in the model parameters and red dashed curves represent a change in the inactivation time relative to the solid red curves. 12

Figure 1.5 *Escherichia coli* O157:H7, 1000X magnification with phase contrast 18

Figure 1.6 Schematic representation of an organic acid accumulation in a typical *E. coli* cell. 20

Figure 2.1 Survival of *E. coli* O157:H7 exposed to 2% NaCl (open circles) or 4% NaCl (closed circles) with 0-40 mM of protonated acetic acid. The solid lines represent the Weibull prediction curves. 53

Figure 2.2 Response surface plot showing the 5-log reduction times as influenced by the protonated acetic acid concentration and the NaCl concentration, created by using equation (2.7) (see text). Several measured 5-log reduction times are also shown (black circles). 54

Figure 2.3 Intracellular pH of *E. coli* O157:H7 exposed to 2% salt and incubated at 25°C for 30 minutes with a buffered acid treatment and either ^{14}C-benzoate (Grey bars) or ^{14}C-salicylate (Black bars). Data represents the mean values of two independent replicates; errors bars represent the standard deviation. Letters within the same protonated acetic acid concentration indicate no significant ($P < 0.05$) difference. 55

Figure 2.4 Intracellular pH for *E. coli* O157:H7 exposed to no acetic acid, 5 mM, or 40 mM protonated acetic acid in the presence of 2 % salt or 4 % salt at 25°C. Cells were incubation with acid treatment for 5 minutes (white bars), 15 minutes (grey bars), 30 minutes (striped bars) or 60 minutes (black bars). The extracellular pH was 3.2. Data are mean values from three independent replicated experiments. Error bars represent the standard deviations of these replicates. Identical letters over error bars within the same acid treatment indicate that there is no significant difference ($P \geq 0.05$) between incubation time (minutes). 56

Figure 2.5 The intracellular pH (triangles) and estimated 5- log reduction times (circles) for 2% NaCl (open symbols) and 4% NaCl (filled symbols) and treatments. The lines represent linear regression of the protonated acid concentration and the intracellular pH (solid line, R^2= 0.99) or 5-log reduction time (dashed line, R^2 = 0.90), for the 2% NaCl treatment only. The error bars represents the standard error for three independent replications. Note that only three data points for the 5-log reduction time were predicted for the 4% NaCl treatment. 57

Figure 2.6 One hour log reduction for *E. coli* O157:H7 subjected to acetic acid and either 2% (black bars) or 4% (grey bars) NaCl at pH 3.2. Error bars represents the standard deviation of three independent replications. 59

Figure 2.7 Intracellular pH as a function of protonated acetic acid concentration for *E. coli* O157:H7 exposed to 1% (black bars) or 3% (grey bars) NaCl at pH 3.2. Error bars represents the standard deviation of three independent replications. 60

Figure 3.1 Intracellular pH as a function of protonated acetic acid for *E. coli* O157:H7 exposed to various concentrations of NaCl. Error bars represent the standard deviation of 3 independent replications. 63

Figure 3.2 Cross validation with removing 1 replication of the entire dataset with 4 salt levels. The other 2 replications are used to train the model. In (A) replicate 2 was removed, in (B) replicate 3 was removed and in (C) replicate 1 was removed. 68

Figure 3.3 Sensitivity of intracellular pH model parameters with respect to increasing concentrations of protonated acetic acid. 70

Figure 3.4 Predictions of the intracellular pH using the simple mechanistic intracellular pH model and a linear model for describing the decrease in intracellular pH as a function of the protonated acetic acid. 71

Figure 3.5 pK_a of acetic acid at 25^{o}C as a function of ionic strength. The points represent the pK_a's at the ionic strengths of the extracellular buffers used in this study. 74

Figure 3.6 Intracellular pH calculations for the 4 levels of NaCl assuming that the pK_a is at 0 ionic strength or adjusted pK_a based on ionic strength. 76

Figure 4.1 *E. coli* O157:H7 survival after exposure to various salts (LiCl, NaCl, KCl, RbCl, CsCl, $MgCl_2$, $CaCl_2$) at an ionic strength of 0.342 (A) or 0.684 (B). 20 mM gluconic acid (black square) is also shown here as a control. The concentration of the divalent ions are ¼ the concentration of the monovalent cations. The error bars represent the standard deviation of two or more independent replications and the trend lines are shown here as a visual aid. 83

Figure 4.2 Intracellular pH for various salts at 2 levels of ionic strength at 25^{o}C. Error bars represent the standard deviation from 2 independent replications. The same letters within the same ionic strength indicate no significant ($P < 0.05$) difference. The vertical line separates the monovalent and divalent salts which differ in concentration. 84

Figure 4.3 Intracellular pH for cells exposed to various concentrations of KCl. The ionic strength was held constant at 0.342 by the addition of NaCl. Error bars represent the means of 2 independent replicate experiments, however the 100-300 mM concentration experiments were performed once.. 85

Figure 4.4 The effects on salt and temperature on the intracellular pH for *E. coli* O157:H7 at pH 3.2 and ionic strength 0.342. Error bars represent the standard deviation from 2 independent replications. The same letters within the same salt type indicate no significant ($P < 0.05$) difference in temperature.. 86

Figure 4.5 The effects of salt type and temperature on the survival of *E. coli* O157:H7 at pH 3.2, ionic strength 0.342. Error bars represent the standard deviation from 2 independent replications. The same letters within the same salt type indicate no significant ($P < 0.05$) difference in temperature. 87

Figure 4.6 Modifications of accuracy and bias factors. 97

Figure 4.7 At ionic strength 0.342, model fits for NaCl (A) and CsCl (B) survival data. Error bars represent the standard deviation of 2 or more independent replicates. 99

Figure 4.8 A sample (the first 24) of the residuals for data created using equations (4.21)-(4.24) and fitted with the Weibull, Gompertz, Logistic and Cole models. A total of 8 symbols for each time point represent a different model iteration... 101

Figure 4.9 Model Misspecification. Weibull data (blue circles) was generated using a Weibull model based on the approximation of NaCl survival data at ionic strength 0.342. The generated Weibull data was then fit with a Logistic Model (red), Gompertz model (green) and a Cole model (magenta)... 102

Figure 4.10 Cumulative Weibull distribution and Multi-hit model for describing the inactivation of *E. coli* O157:H7 exposed to a NaCl solution at ionic strength 0.342 at pH 3.2. 108

Figure 4.11 Variance estimates for the Weibull distribution and Multi-hit model assuming a binomial distribution for the probability that *n* cells are alive at time *t*............................... 109

Figure 5.1 Log tumor weight time series for dataset 1 (TG1). The initial tumor weight for these data is 63mg.. 117

Figure 5.2 Log tumor weight time series for dataset 2 (TG2). The initial tumor weight for these data is 108mg.. 118

Figure 5.3 Comparison of autonomous and non-autonomous Gompertz fits of tumor growth datasets with different initial conditions (refer to materials and methods section 5.2). In (A) the initial tumor weight is 63mg and in (B) the initial tumor weight is 108mg. Green curves represent the autonomous Gompertz model fit. When the initial conditions are changed (see text) red curves represent the new autonomous Gompertz model fit and blue curves represent the new non-autonomous Gompertz fit.. 119

Figure 5.4 Comparison of autonomous and non-autonomous Gompertz solutions to fit *E. coli* O157:H7 inactivation when cells are exposed to NaCl at pH 3.2 and ionic strength 0.342 (circles). Green curves represent the autonomous Gompertz model fit. When the initial conditions are changed (see text) red curves represent the new autonomous Gompertz model fit and blue curves represent the new non-autonomous Gompertz model fit. 120

Figure 5.5 (A) Fit of the TG1 dataset with an autonomous Gompertz model whose parameters were estimated using TG2 data (red curve) shown with the original autonomous Gompertz model fit (green curve). (B) Fit of the TG2 data with an autonomous Gompertz model whose parameters were estimated using TG1 data (blue curve) shown with the original autonomous Gompertz model fit (green curve). 121

Figure 5.6 (A) Fit of the TG1 dataset with a non-autonomous Gompertz model whose parameters were estimated using TG2 data (red curve) shown with the original non-autonomous Gompertz model fit (green curve). (B) Fit of the TG2 data with a non-autonomous Gompertz model whose parameters were estimated using TG1 data (blue curve) shown with the original non-autonomous Gompertz model fit (green curve)...................... 122

Figure A. 1 Accuracy factor histograms of 10,000 Weibull models (A), Gompertz models (B), Logistic models (C) and Cole models based on approximations of the NaCl data at ionic strength 0.342..144

Figure A. 2 Bias factor histograms of 10,000 Weibull models (A), Gompertz models (B), Logistic models (C) and Cole models (D) based on approximations of the NaCl data at ionic strength 0.342. 145

Figure A. 3 Weibull data was generated using 10,000 Weibull models based on the approximation of NaCl (ionic strength 0.342) data, with error from a normal distribution (mean 0, variance from the approximation of the Weibull fit). The generated Weibull data was then approximated with a Gompertz model (B), a Logistic model (C), or a Cole model (D) and the accuracy factor was then calculated. 146

Figure A. 4 Weibull data was generated using 10,000 Weibull models based on the approximation of NaCl (ionic strength 0.342) data, with error from a normal distribution (mean 0, variance from the approximation of the Weibull fit). The generated Weibull data was then approximated with a Gompertz model (B), a Logistic model (C), or a Cole model (D) and the bias factor was then calculated. 147

LIST OF TABLES

Table 1.1 Examples and applications of primary survival models. The notation for the formulas used in this table originates in the reference listed. 13

Table 2.1 Weibull model parameters and 5-log reduction estimate (RT5) with standard errors (SE) for each acid/salt treatment. 51

Table 2.2 Intracellular pH and the total intracellular acetic acid concentration for acid/salt treatment. 52

Table 3.1 Simplified intracellular pH model parameters and variables. 66

Table 3.2 Predicted parameters values for determining intracellular pH of *E. coli* O157:H7 and the 95% confidence interval (CI) associated with each parameter estimate. 69

Table 3.3 Comparisons of the mean square error (MSE) for models in which the pK_a was at zero ionic or adjusted based on the intracellular sodium and potassium concentration. 77

Table A. 1 Diagnostics for comparing models within a salt and ionic strength treatment. Values in red represent the diagnostics which are optimal. 143

LIST OF NOMENCLATURE

Acidulant A chemical having an acid quality such that when added to another substance results in an equilibrated pH value of 7 or below.

Anion An ion with an overall negative charge (76).

Buffer An aqueous solution consisting of a weak acid and its conjugate base. Buffer solutions have the property of resisting changes in pH when small amounts of strong acid or base are added.

Cation An ion with an overall positive charge (76).

Intracellular/internal pH pH of the inner matrix of a cell.

Ionic strength A measure of the average electrostatic interactions among ions in an electrolyte solution. It is equal to one-half the sum of the terms obtained by multiplying the molarity of each ion by its valence squared as in the following expression

$$I = \frac{1}{2}\sum C_i z_i^2 .$$

pH A logarithmic quantity that indicates the acidity of a solution. pH is defined as the negative logarithm of the hydrogen ($[H^+]$) concentration (76).

1 Introduction

The survival of bacterial pathogens in food systems is an increasing public health concern. *Escherichia coli* (*E. coli*) O157:H7 has become an emerging food-borne pathogen. The illness it produces can result in kidney failure and potentially death. To combat these growing concerns of food-related illnesses, microbiologists have applied mathematical modeling techniques for quantitative prediction of the growth and survival of microorganisms in foods. This review focuses on quantifying and understanding the survival of *E. coli* in foods. As an aid to the reader, there is a list of nomenclature for defining terminology used in this review on page xv.

1.1 Modeling Microbial Responses

As early as the 1940's, the growth of a bacterial culture was defined by several distinct phases (114). These include a lag phase where no growth is found; an exponential or log phase where the growth rate is constant; a stationary phase where there is no growth; and a phase of decline where the growth rate is negative (114) (see Figure 1.1). Modeling approaches mainly attempt to quantify growth (lag and log phases) or the death (i.e. inactivation) phase relative to environmental conditions (e.g. pH, water activity, temperature, acid concentration).

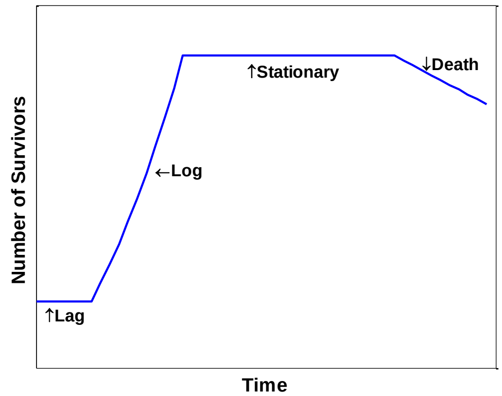

Figure 1.1 Phases of bacterial growth.

Since Chick (48) first used first-order kinetics to describe the survival of anthrax spores, many significant mathematical models have been developed aiding in a comprehensive understanding of microbial inactivation. In the context of microbial modeling it is usual to classify the applied models into empirical and mechanistic (8). Empirical models are descriptions of observed data, usually including polynomial and power-law models (72) and are often used for interpolation and or extrapolation. Often the parameters in empirical models have no physical meaning. Conversely, mechanistic models are based on a presumed molecular or physical mechanism. Mechanistic models can be further categorized into those which are deterministic and those which are probabilistic (stochastic). As noted by Nisbet and Gurney (117) to model the variation in a population, deterministic models can describe the trend of the dynamic behavior, while stochastic models can describe the trend and the fluctuations of the dynamic behavior within the population. The most important property of a deterministic model is that if the history of the population is known up to the present time, the exact behavior in the future can be predicted (117). Stochastic models, on the other hand, can only predict the probability that at a given time the population will have reached a particular size (117). In Chapter 4 deterministic and stochastic models are presented to describe the inactivation of *E. coli* by various salt solutions.

1.1.1 Predictive Microbiology

According to Ross and McMeekin (137)

> "Predictive microbiology is based upon the premise that the responses of populations of microorganisms to environmental factors are reproducible, and that by considering environments in terms of identifiable dominating constraints it is possible, from past observations, to predict the responses of those microorganisms."

Food microbiologists have long turned to mathematical modeling for advancing food safety objectives, however the wide use of modeling techniques did not present themselves until the 1980's. As noted by McClure (104), the true power of predictive microbiology is that once models are validated, they can used to predict with confidence the responses of organisms under a variety of conditions. Moreover, as reviewed by Skinner and Larkin (151) the benefits of using mathematical models include estimating the shelf-life, reducing time-consuming experimentation, and aiding with ensuring food safety.

1.1.2 Survival Models

Mathematical survival models pertaining to predictive microbiology have been classified into three categories: primary, secondary and tertiary (163). As Whiting (163) argues, “classification will aid modelers and model users to describe various stages of the overall modeling process”. Primary models describe microbial growth or survival over time under particular environmental and cultural conditions and aims to fit growth/survival curves and estimate parameters (98). Secondary models describe the response of primary model parameters as a function of environmental conditions, for example temperature, acid concentration, pH and water activity (98). Finally, tertiary models are applications of one or more secondary models to create a system for predictions to non-modelers (163). Using the framework of microbial survival, in the following sections the utility of each model categorization is discussed. These sections are outlined similar to Chapter 2 in McKellar and Lu (108).

Primary Models

Linear Models

The first-order kinetic model is what is commonly referred to as the traditional approach. Based on an analogy of first order chemical equations, Chick (48) suggested using first order kinetic models for describing the inactivation of anthrax spores (as reviewed in (168)). Additionally, in the 1920’s first order kinetic models were employed by Esty and Meyers (72) to describe the inactivation of thermal resistant spores. Microbial inactivation that obeys first-order kinetics assumes that the number of survivors per unit time is proportional to its death rate, resulting in the following relation

$$\begin{cases} \dfrac{\mathrm{d}N(t)}{\mathrm{dt}} = -kN(t) & (0 \le t < +\infty) \\ N(0) = N_0 & (N_0 > 0; t = 0) \end{cases} \tag{1.1}$$

with $N(t)$ (Colony forming units per mL (CFU/mL)) as the number of microorganisms, N_0 (CFU/mL) as the initial population density and k (time^{-1}) as the decay rate. Another convention for expressing the survivors in time is the survivor ratio $S(t)$, where

$$S(t) = \frac{N(t)}{N_0} \ . \tag{1.2}$$

Integrating equation (1.1) with considering the initial conditions ($N(0) = N_0$) results in

$$N(t) = N_0 \exp(-kt) \ . \tag{1.3}$$

Taking the natural logarithm of both sides of equation (1.3)

$$\ln N(t) = \ln N_0 - kt . \tag{1.4}$$

Microbiologists work in logarithm base 10, thus it is customarily to express equation (1.4) as

$$\log N(t) = \log N_0 - \frac{1}{\ln(10)} kt \tag{1.5}$$
.

The decimal reduction time or *D*-value is the time required to achieve a 1-log reduction in the number microorganisms, i.e. a reduction in 90% of the population. Without loss of generality the *D*-value is equal to the inverse slope of the inactivation curve such that $D = 1/k'$ (where $k' = k/\ln(10)$). Here one should note that by definition, k is a positive constant. Figure 1.2 is a semi-logarithmic plot of microbial inactivation assuming first order kinetics. The *D*-value can be multiplied by any constant to obtain the required log reduction time. The thermal death time τ , is the time required to destroy a certain concentration of cells (127). The most common thermal death times are $\tau = 12D$, used for sterilization processes and based on the inactivation of *Clostridium botulinum* and $\tau = 6D$ used for pasteurization (159). For acid juices, the US Code of Regulations (21 CFR part 120) requires a 5*D* reduction in the acid-resistant bacteria pathogens such as *E. coli* O157:H7 (24). Variations on equation (1.1) include decay rates which are functions of intrinsic or environmental factors such as temperature. Recently Klotz et al. (87) presented a first order linear kinetic model as a function of a time-varying parameter where, without loss of generality, $k = s(t) = st^{-0.5}$. Examples of other linear models describing microbial inactivation are detailed in Table 1.1.

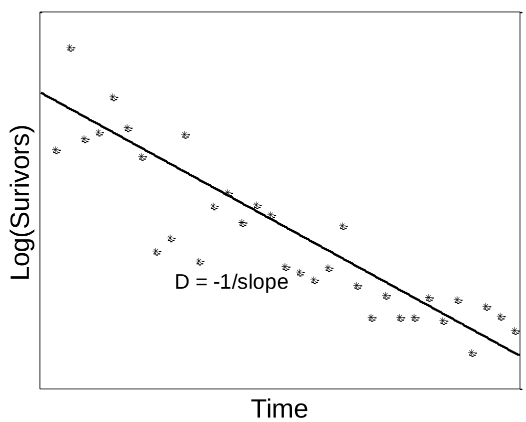

Figure 1.2 Semi-logarithmic plot which is representative of first order linear decay for a microbial population.

A mechanistic explanation for a population following first-order kinetics is that cells in a population have an equal, time independent, probability of inactivation (35). The question is now whether this is a reasonable assumption.

Nonlinear Models

The canning industry has widely accepted the logarithmic decay of microorganisms, and it is considered as the accepted dogma (108). As previously noted (18, 98, 125, 128, 159), in many instances microbial semi-logarithmic survival need not be linear. The common explanation for the observed non-linear behavior is that the microbial population consists of a number of subpopulations each with their own survival kinetics (159).

Commonly observed nonlinear behaviors are inactivation curves with shoulders, tails, or both shoulders and tails (sigmodial) as illustrated in Figure 1.3. Shoulders can be thought of as a lag of inactivation due to clumping in colony forming units (as reviewed in (168)). Li et al. (98) argues that in thermal processing, a shoulder phase is often observed before the exponential decline, thus a linear model was not appropriate for describing the inactivation. Tails can be a result of buildup resistance to the lethal agent (as reviewed in (167)). Chen and Hoover (46) found that linear models are not useful for predicting the strong tailing of the survival curves association with the pressure inactivation of *Yersinia enterocolitica*, hence nonlinear models were employed. In addition to shoulders and tailing, nonlinear survival behavior has shown 2 types of concavity: upward and downward (Figure 1.3 (A) and (B) respectively). Tailing behaviors imply that the inactivation treatment (e.g. temperature, pressure or chemicals) may not achieve the required decimal reduction time within a reasonable amount of processing time. This is particularly dangerous because pathogens which have a low infection dose such as *E. coli* O157:H7, will exist for periods of time, potentially causing food-related illness. Table 1.1 summarizes commonly used primary inactivation models used to describe microbial survival, where the notation in the cited papers is used.

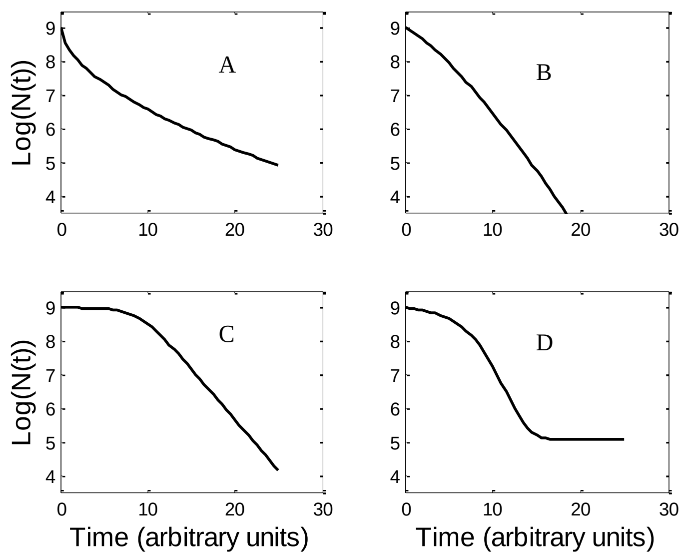

Figure 1.3 Examples of nonlinear survival curves. Panels (A) and (B) were created using a Weibull model, (C) was created by using a Fermi-like model and (D) was created by using a modified Gompertz model.

Survival Distributions

Distributions used for predicting microbial survival are based on the assumption that lethal events are probabilistic rather than deterministic (108). Hence there is heterogeneity between the cells within the same population of microorganisms (159). The resulting survival curve can be seen as a cumulative form of the underlying distributions of individual inactivation times (35, 159).

In the absence of injury, the survival curve for an individual cell is characterized by the time of its death or inactivation (124). If there are only two states, life and death, the survival curve for a cell in the population is a step function

$$N_i(t) = \begin{cases} 1 & \text{(alive) for } t < t_{ci} \\ 0 & \text{(dead) for } t \geq t_{ci} \end{cases} \tag{1.6}$$

where t_{ci} is the inactivation time of the i^{th} cell (108) and t_c is the population inactivation time. The discrete relationship described in equation (1.6) can approximated by the Fermi distribution (124). The Fermi distribution has been used to describe inactivation curves with extreme lags (124) (Figure 1.4). This behavior is usually found in spores, where there is a delay in the inactivation due to outgrowth; nonetheless vegetative cells also can exhibit this lag behavior. The Fermi cumulative distribution function is symmetric and the mirror image of the logistic equation with the general form

$$N(t) = \frac{N_0}{1 + \exp\left(\frac{t}{a}\right)} \tag{1.7}$$

where a represents the broadness of the distribution (125). Considering the time until inactivation, the Fermi survivor distribution function can be expressed as

$$N_i(t) = \frac{N_0}{1 + \exp\left(\frac{t - t_{ci}}{a}\right)}. \qquad (1.8)$$

Thus, the probability density function associated with the Fermi distribution is

$$PDF_{Fermi} = \frac{\exp\left(\frac{t}{a}\right)}{\left(1 + \exp\left(\frac{t}{a}\right)\right)^2}. \qquad (1.9)$$

Considering the inactivation time, this probability density function is extended to

$$PDF_{Fermi,t_c} = \frac{\exp\left(\frac{t - t_c}{a}\right)}{\left(1 + \exp\left(\frac{t - t_c}{a}\right)\right)^2}. \qquad (1.10)$$

The Weibull distribution, used in reliability engineering to predict failure time of airplane and automobile parts, has shown to have wide capability of predicting microorganism survival (108). As noted by van Boekel (159) the survivor density function has the form

$$N(t) = N_0 e^{-\left(\frac{t}{\alpha}\right)^\beta}. \qquad (1.11)$$

where α is the scale parameter with units time and β is non-dimensional shape parameter. Considering the time until inactivation, the Weibull survivor density function can be expressed as

$$N_i(t) = N_0 e^{-\left(\frac{t - t_{ci}}{\alpha}\right)^\beta}. \qquad (1.12)$$

Thus, the distribution of the inactivation times follows the following Weibull probability density function

$$PDF_{Weibull} = \frac{\beta}{\alpha}\left(\frac{t}{\alpha}\right)^{\beta-1} e^{-\left(\frac{t}{\alpha}\right)^{\beta}} . \tag{1.13}$$

Considering the time for inactivation, the three parameter Weibull probability density function can be written as

$$PDF_{Weibull,t_c} = \frac{\beta}{\alpha}\left(\frac{t-t_c}{\alpha}\right)^{\beta-1} e^{-\left(\frac{t-t_c}{\alpha}\right)^{\beta}} . \tag{1.14}$$

Figure 1.4 illustrates the survival curves for a microbial population which is sensitive or resistant to an inhibitory substance and depicts the Fermi and Weibull probability density functions as examples of the microbial frequency. Microbial populations that are resistant, naturally take a longer time to be inactivated than sensitive populations. Increases in the broadness of the distribution parameter (*a*) for the two parameter Fermi model, decreases the expected frequency. For the three parameter Weibull distribution, decreasing the scale parameter increases the broadness of the frequency while decreasing the shape parameter changes the profile of the frequency (Figure 1.3 (C)).

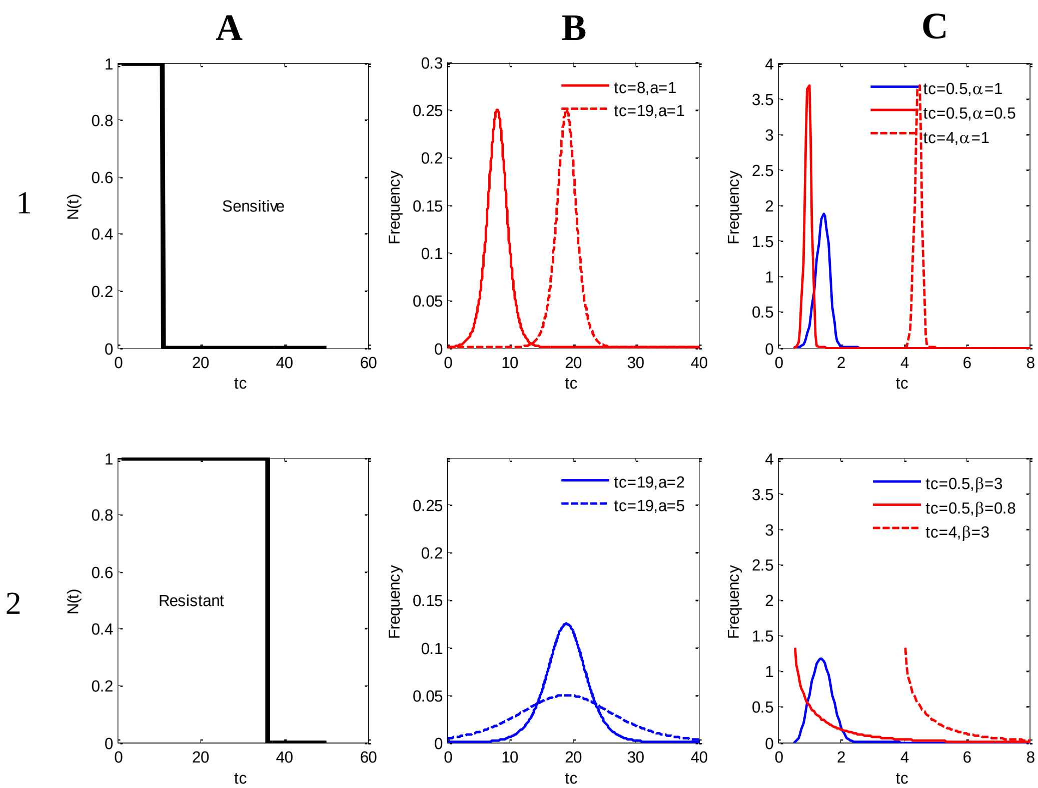

Figure 1.4 The time to reach inactivation for a cell that is sensitive to inactivation treatment (A.1) compared to a cell that is resistant to the same treatment (A.2). For the Fermi distribution (panels B.1 and B.2) the red curves represent a change in the inactivation time (t_c) and the blue curves represent a change in the model parameters. For the three parameter Weibull distribution (panels C.1 and C.2), the blue curves represent a change in the model parameters and red dashed curves represent a change in the inactivation time relative to the solid red curves.

Table 1.1 Examples and applications of primary survival models. The notation for the formulas used in this table originates in the reference listed.

Model (References)	Formula	Application
Cerf (43)	$\frac{N(t)}{N_0} = fe^{-k_1 t} + (1-f)e^{-k_2 t}$	Thermal inactivation of *Clostridium botulinum (C. botulinum)* spores.
Modified Gompertz (16, 69)	$\log N(t) = A - Ce^{-e^{-B(t-M)}}$ or $\log N(t)/N_0 = Ce^{-e^{BM}} - Ce^{-e^{-B(t-M)}}$	*C. botulinum (growth), Listeria monocytogenes (L. monocytogenes).*
Cole (Log-logistic) (50)	$\log N(t) = \alpha + \frac{\omega - \alpha}{1 + e^{4\sigma(\tau - \log(t))/(\omega - \sigma)}}$	Pressure inactivation *of Yersinia enterocolitica* in milk. Thermal inactivation of *C. botulinum.*
Kamau (84)	$\log N(t)/N_0 = \frac{2}{1+e^{\beta t}}$	*L. monocytogenes and Staphylococcus. aureus.*
Membre (110)	$\log N(t) = (1 + \log N_0) - e^{kt}$	*Salmonella tyhimurium (S. tyhimurium)* in reduced calorie mayonnaise
Weibull (65, 126)	$\log N(t) = N_0 e^{\left(\frac{t}{\alpha}\right)^{\beta}}$ or $\log N(t)/N_0 = -bt^n$	Thermal resistance of *Bacillus cereus* in a vegetable substrate. Pressure inactivation of *Yersinia enterocolitica* (*Y. enterocolitica*) in milk.
Buchanan (32)	$\log N(t) = \begin{cases} \log N_0 & (t \le t_{lag}) \\ \log N_0 - \frac{t - t_{lag}}{D} & (t > t_{lag}) \end{cases}$	Chemical (salt, acid) and thermal inactivation of *L. monocytogenes*.
Baranyi (8)	$N(t) = N_{\min} + (N_0 - N_{\min})e^{-k_{\max}(t - B(t))}$	Thermal inactivation of *L. monocytogenes* Scott A.
Modified Weibull (2)	$\gamma(t/\delta) = (N_0 - N_{res})10^{\left(-\left(\frac{1}{\delta}\right)^{p}\right)} + N_{res}$	Thermal inactivation *Bacillus pumilus in egg powder, Bacillus cereus* in dairy products.

Secondary Models

A secondary model based on the first-order kinetics parameter *k* is the *z*-value, defined as the increase in temperature that would produce a reduction in *D* by a factor of 10 (159). Calculating the *D*-value at several temperatures in thermal processing allows the *z*-value to be determined (18). Another widely considered secondary model in microbiology is the Arrhenius equation. The decay rate constant *k* describing logarithmic inactivation in equation (1.1) is related to temperature via the Arrhenius equation such that $k = N_0 e^{\left(-\frac{E_a}{RT}\right)}$ where E_a is the activation energy, *R* is the universal gas constant, and *T* is the temperature in degrees Kelvin (108).

Polynomial models are the most commonly used secondary models used in predictive microbiology to describe inactivation parameters of primary models (for examples refer to (35, 46, 50, 79, 90, 158, 160, 162)). These models are usually functions of environmental factors including, but not limited to, pH, temperature, NaCl/water activity, CO_2, organic acids, nitrite and natural antimicrobials (108). As noted by Ross (137) polynomial models are usually of the form of a multivariate quadratic equation.

Whiting (162) developed models for describing decreases in bacterial populations during storage at various temperatures in media containing varying concentrations of lactic acid, sodium chloride and sodium nitrite. Polynomial regression models were created to describe the inactivation of *Listeria monocytogenes* and *Salmonella* in these environments. It was observed that 86% of the variation in the 4D reduction time for *Listeria monocytogenes* could be explained by changes in temperature, NaCl concentration, nitrate concentration and pH (162). Since only 86% of the 4D reduction could be explained by the measured environmental factors, there may be other unmeasured intrinsic factors, such as lactose utilization and production, contributing to the survival. Thus the predictability of regression models is highly constrained by experimental design. More recently, polynomial models were used to describe the dependence on temperature, pH and essential oil concentration on the Baranyi model (8) parameters for the survival of *Salmonella enteridis* in food (90). In Chapter 2 a secondary model is used to describe the dependence of salt and acid concentration on the Weibull model's parameters. An excellent review of other secondary models for describing microbial responses can be found in Chapter 3 of McKellar and Xu (108).

Artificial neural networks (ANNs) are algorithms that define relationships between predictor variables, a series of hidden levels, and an output variable (108). Recently, ANNs have been used to generate secondary models for microbial inactivation parameters (e.g. see (74, 166)). Xie and Xiong (166) created a neural network to predict the parameters of a primary hyperbolic model used for quantifying the changes in dry peas during long cooking times. Compared to other secondary models (e.g. an Arrhenius model and a Davey's modified Arrhenius model) the performance of the neural network was better than that of the Davey's modified Arrhenius model. Horiuchi et al. (74) found that the ANN created to evaluate the pH changes in continuous anaerobic acidogenesis was successful in modeling the transient behavior in responses to changes in pH. Further research is needed in the application of ANNs in predictive microbiology, namely to elucidate the direct comparisons of the performance of different ANN techniques (108). It is increasingly important to obtain bounds on secondary models in which explanatory variables are related to physical measurements (e.g. temperature, time, pressure). For example, it is of interest in this dissertation to obtain an error bound on the 5-log reduction time. A method for obtaining the standard errors of the predicted 5-log reduction time is further discussed in Chapter 2.

Tertiary Models

User-friendly interfaces for non-modelers are in increasing demand. Their utility allows users to calculate changing conditions such as temperature after 5 days of storage, and compare microbial behaviors under several environmental conditions such as salt or pH (163). GInaFit developed by Geeraerd et al. (68) enables users to define the survival model, based on 8 common used inactivation curves (4-linear based, 2 biphasic, a convex curve and a concave curve based), to fit user-specific data. Recently, Corradini and Peleg (55) created a tertiary model based on an underling Weibull model which enables the user to predict survival under static or dynamic conditions. Other commercially available predictive modeling software include packages such as Food MicroModel (104) and the Pathogen Modelling Program (29).

1.1.3 A Note on Mechanistic Models

Unlike empirical models, mechanistic models are based on the underlying chemical and biological principles governing the system. This may include the pH, ATPase and temperature regulation. Mechanistic models are also widely used in predicting microbial growth and survival as shown in the models described above. However, it has proven difficult at times to produce pure mechanistic models for certain cellular processes are either difficult to measure or not yet biologically defined. Therefore, some models are classified as semi-mechanistic or pseudo-mechanistic, where the parameters or processes are estimated. In Chapter 3 the semi-mechanistic modeling approach described by Dougherty (61) to determine buffer composition of *E. coli* is discussed.

The principle of parsimony requires that the smallest possible number of parameters for adequate representation of the data should be strived for (159). This principle is also referred to as Occam's razor. In Chapter 4, inactivation models are compared and the principle of parsimony is discussed.

1.2 *ESCHERCHIA COLI* O157:H7

1.2.1 Microbiology

Escherichia coli (*E. coli*) is a gram negative rod shaped bacterium that is ubiquitous in the environment, though only certain serotypes are associated with human disease. The six classifications of diarrhea causing *Escherichia coli* include: enteropathogenic *E. coli* (EPEC), enterotoxigenic *E. coli* (ETEC), enteroinvasive (EIEC), diffuse-adhering *E. coli* (DAEC), enteroaggregative *E. coli* (EAEC) and enterohemorrhagic *E. coli* (EHEC) (62). This work focuses on enterohemorrhagic *E. coli*, in particular *E. coli* O157:H7 (Figure 1.5), due to its low infectious dose and frequent association with food borne illness. However, the results presented in this dissertation are likely to be applicable to other EHEC serotypes.

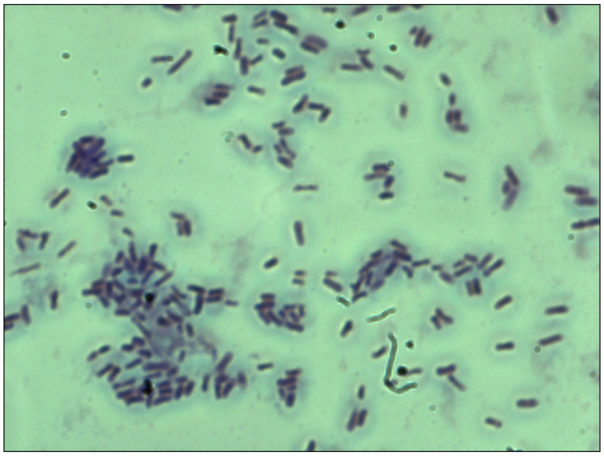

Figure 1.5 *Escherichia coli* O157:H7, 1000X magnification with phase contrast microscopy.

E. coli O157:H7 is physiologically distinguished from other *E. coli* strains by is its inability to ferment sorbitol, thus it is often plated on sorbitol-MacConkey agar. The O designates the somatic antigen and the H designates the flagellar antigen. *E. coli* O157:H7 has shown to produce two Shiga-like toxins: Shiga-like toxin I and Shiga-like toxin II both involved in pathogenesis. However, some strains have been shown to produce only one toxin while others can produce both toxins (155).

The growth and survival of *E. coli* in the presence of organic acids have been extensively studied (e.g. (17, 30, 51, 57, 82)). By definition, organic acids are weak non-polar acids. Studies have found that this non-polar property allows the uncharged acid to freely diffuse in and out of the cell membrane (145) (see Figure 1.6). Once inside the cell, these acids release protons and lower the intracellular pH thus explaining their observed antimicrobial property. To oppose lowering of the intracellular pH, the cell is able to remove excess protons at the expense of ATP (19). One hypothesis is that the energy required to remove these protons drains the cell of ATP, resulting in death (4). Alternatively, acid anions that become trapped in the cell cytoplasm accumulate inside the cell resulting in death (141). Despite attempts to control the survival of *E. coli* by using organic acids, certain strains (e.g. O157:H7) exhibit acid resistance mechanisms allowing the cell to survive under extreme acid stress. For instance, Russell and Diez-Gonzalez (57) found that *E. coli* O157:H7 can reduce the toxic accumulation of the acetate anion.

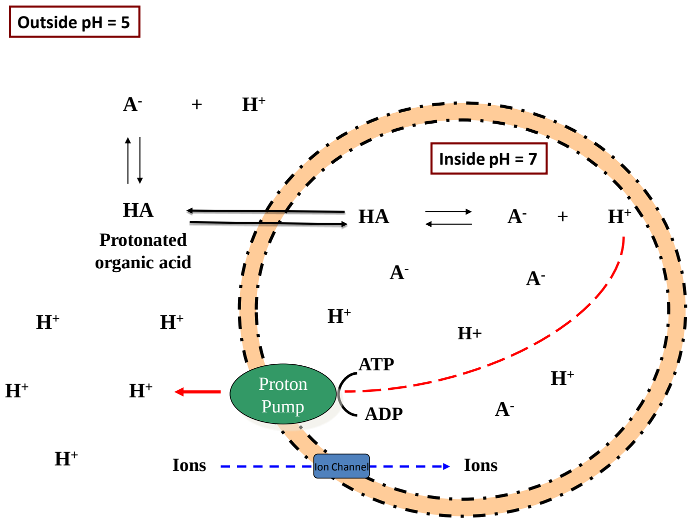

Figure 1.6 Schematic representation of an organic acid accumulation in a typical *E. coli* cell.

Acid Resistance and Acid Tolerance

According to Buchanan and Edelson (30), the term acid resistance (AR) or acid habituation can be used to refer to the extended exposure of a microorganism to moderately acidic conditions (e.g. 5.0) leading it to being able to withstand pH values of ≤ 2.5. On the other hand, acid tolerance response (ATR) refers to the enhanced survival of a microorganism exposed to pH values between 2.5 and 4.0 after a brief exposure to moderately acidic conditions (30). Lin et al. (99) makes note that is it hard to determine from the literature if the ATR and AR systems are truly different or reflect different ways of measuring the same system. The following does not attempt to distinguish the two systems, however it briefly discusses how both ATR and AR systems promote *E. coli* survival in acidic conditions.

Jordan and colleagues (82) investigated the survival of three population types of nontoxigenic *E. coli* O157:H7 at pH 3. Their results indicate that stationary-phase and acid-adapted exponential-phase cells showed elevated levels of acid tolerance relative to exponential-phase cells (82). Acid resistance of stationary-phase cells are generally defined by 4 systems. The acid resistance system 1 (AR1) is activated in slightly acidic media (5.5) in the absence of glucose, after which *E. coli* can survive after an acid shock as low as pH 2.5 (161). The acid resistance system 2 (AR2) is activated in *E. coli* during the stationary phase or by the log phase growth in acidic minimal media (132). This system requires the presence of extracellular glucose and glutamate and is dependent upon genes encoding glutamate decarboxylase (*gadAB*) and a glutamate:GABA antiporter (gabC). Under these conditions *E. coli* has shown to be acid resistant down to pH 2. Acid resistant system 3 (AR3) is activated under anaerobic conditions in a complex media in the presence of glucose, and requires increased expression of arginine decarboxylase and an arginine: agmatine antiporter for increased acid tolerance (161). Acid resistance system 4 (AR4) is lysine dependent and to date little information is known about this system. As noted by Richard and Foster (133), AR1 and AR4 systems are the least protective, AR3 provides moderate protection and AR2 is the most robust system providing the most protection. *E. coli* surviving in an acidic environment (pH 3.2) is of concern in this dissertation, thus *E. coli* O157:H7 is grown in the presence of 1% glucose in a defined media (Luria-Broth) to initiate acid resistance. In addition, *E. coli* O157:H7 are statically grown (grown without shaking) allowing the cells to ferment glucose and lower the pH of the media.

The extreme acid resistance and acid tolerance of *E. coli* is regulated by the RpoS regulatory factor; a sigma factor which is required for the transcriptional activation of genes essential for tolerance to environmental stresses (82). Cheville et al. (47) used a *rpoS* mutant of *E. coli* O157:H7 to determine the role of *rpoS*-regulated proteins in acid, heat, salt tolerance and survival in dry fermented sausage. Their results indicate that stationary phase-induced mechanisms governed by rpoS-regulated proteins exhibited cross-protection against heat and salt challenges and promoted survival of O157:H7 (47). According to Lin et al. (99) the RpoS-dependent system appears to be the stationary-phase general stress resistance system which includes resistance to low pH. However, the RpoS-regulated genes contributing to survival in low-pH environments are not yet fully understood.

There are numerous examples of *E. coli* acid resistance systems in the literature (27, 57, 59, 67, 97, 100). Garren et al. (67) determined whether ATR and or ASR (acid shock response) induces a sustained acid resistance when *E. coli* O157:H7 and non-O157:H7 are exposed to lactic acid. When there was a difference in the ATR and ASR responses, acid-shocked cells (cells exposed to lactic acid at pH 3.5 or 4.0) had a higher survival rate (usually less than 2 logs) than acid-adapted cells (cells exposed to pH 5.5 for an adaption period then challenged with acid at pH 3.5 or 4.0) (67). Brudzinski and Harrison (27) investigated the degree of acid tolerance when *E. coli* O157:H7 was exposed to acetate under static of agitated conditions at 25^{o}C and 32^{o}C. At pH 5.0 the ATR system allowed for a 1,000-fold increase in survival compared to survival of non-adapted *E. coli* O157:H7 at pH 4.0 (27).

The potential for *E. coli* O157:H7 surviving in a low pH (< 4.6) food exists. *E. coli* O157:H7 is found to be extremely acid resistant (pH 2) especially when acetate is the acidulant (59). O15:H7 also appears to be more acid-tolerant than other strains (e.g. K12) of *E. coli* (57). Lin et al. (100) studied the effects of organic acids on three acid resistance systems found in *E. coli* O157:H7 where they found that the arginine- and glutamate-dependent systems were both effective in protecting *E. coli* against the antimicrobial effects of several organic acids (benzoate, and a cocktail containing acetic, butyric and propionic acids). To date, however, there have been no outbreaks of disease from *E. coli* O157:H7 associated with acidified foods (pH < 4.6).

<u>Intracellular pH</u>

Intracellular pH maintenance is essential for cellular metabolism, as it plays an important role in processes such as DNA transcription and translation, protein synthesis and enzyme activities (146). An early study revealed that *E. coli* regulates intracellular pH (92). The authors conclude that *E. coli* can sense their intracellular pH; the pH gradient exerts a feedback regulation on intracellular pH; the mechanism of this regulation was found not to depend on sodium ion, and that potassium transport may be involved in raising the intracellular pH (92).

There is evidence that intracellular pH maintenance is associated with survival as seen for *E. coli* (57, 82) lactic acid bacteria (77, 105, 121, 146) and *Streptococcus* (142). Diez-Gonzalez and Russell (57) examined intracellular pH regulation for *E. coli* O157:H7 and *E. coli* K12 in the presence of acetate. Their results indicate the tolerance of acetate can be explained by the ability for this strain to lower its intracellular pH. Jordan et al. (83) studied the effects of lactate and ethanol on the survival of *E. coli* O157 in a low-pH environment. In their study, the killing kinetics in the presence of these compounds alone or in combination were consistent with the decline in the intracellular pH, however the lowering of the intracellular pH itself was not sufficient to cause cell death (83). Additionally, Jordan et al. (82) showed a strong correlation between increased acid tolerance and decreased permeability of the cell envelop to protons, implying that acid-resistant populations have a greater ability to maintain intracellular pH. However, the relationship between intracellular pH maintenance and survival for acid resistant *E. coli* is unclear. This concept will be further examined in Chapter 2.

O'Sullivan and Condon (121), found that intracellular pH regulation was a major factor for the acid tolerance response in exponentially growing *Lactococcus lactis*. In addition, their study revealed that exposure to a mild acid also cross-protected against other lethal agents such as heat, ethanol, sodium chloride and hydrogen peroxide (121). McDonald et al. (105) studied the acid tolerance of *Leuconostoc mesenteroides* and *Lactobacillus planturum* by examining growth limits and intracelllular pH. Their study revealed that for both microorganisms the intracellular pH regulated the growth, and they proposed that a minimum intracellular pH required for growth (105). Shabala et al. (146) also studied the responses to acid stress and glucose availability in *Listeria monocytogenes* by examining intracellular pH and survival. They found that the ability of stationary phase *Listeria monocytogenes* to maintain the transmembrane proton gradient depends on the glucose availability and the inability to maintain this gradient below a critical intracellular pH corresponds to loss of viability (146). This is contrary to Richard and Foster (132) who noticed that maintenance of a specific intracellular pH may not be essential to cell survival.

Common methods used for determining the intracellular pH in bacteria include using pH-dependent fluorescent probes (22, 33, 113, 135, 148), using ^{31}P- nuclear magnetic resonance (NMR) (91, 116, 144, 152) and using radioactive labeled weak acids or bases (52, 58, 111, 115, 134, 138). The benefits of using fluorescent probes include achieving a real-time single cell measurement. Riondet et al. (135) claim that fluorescent probes can achieve high-time resolution and that this technique is simpler to use than radioactively labeled weak acids. However, as Booth (19) notes, it may be difficult to interpret the signal from these systems. Alternatively, using ^{31}P-NMR has the advantage of simultaneously determining the intracellular pH and other metabolites (116). In this study the acid-distribution method for determining the intracellular pH as detailed by Rottenberg (138) and Riebeling et al. (134) was used. This method achieved reliable determinations of intracellular pH. However, one drawback of this method is that the determination depends on the pK_a of the radiolabeled acid and that the intracellular pH is not a physical measurement.

There have been very few attempts to model intracellular pH regulation. One effort was shown in Kobayashi's (88) work where a mechanistic model for intracellular pH was based on the ATPase activity. In Chapter 3, a semi-mechanistic model for intracellular pH determination based on intracellular buffer composition is presented.

Transmembrane Potential and Proton Motive Force

In addition to altering the intracellular pH, the influx of protonated organic acids may also impede with maintenance of the charge across the cell membrane. The transmembrane potential ($\Delta\psi$) is defined as the charge separation across a membrane that results from differences in the ionic concentrations on the two sides of the membrane (76).

It can be calculated using the Nernst equation using a probe that distributes across the cell membrane based on charge:

$$\Delta\psi = \frac{RT}{zF}\ln\left(\frac{[\Pr obe_{ex}]}{[\Pr obe_{in}]}\right).$$

Methods for determining the transmembrane electrochemical gradient are extensively reviewed by Rottenberg (139) in 1975. The proton motive force (PMF or Δp) is the combined influence of a difference in the concentration of protons on the two sides of the membrane and the electrical charge difference across the membrane (76). It produces a driving force that causes protons to move across the membrane. It can be calculated in the following manner:

$$\Delta p = \Delta\psi - \frac{2.303 * RT}{F}\Delta pH .$$

As early as 1981, the role of cation transport on the intracellular pH regulation in *E. coli* was determined (93). For stationary-phase *E. coli* K-12, potassium is a significant regulatory cation in controlling the intracellualr pH. Kroll (93) thus hypothesized that the role of the K^+ is to lower the transmembrane potential changing the re-entry of H^+ leading to an increase in the intracellular pH.

1.2.2 Epidemiology

<u>*Incidence*</u>

The first recognized outbreak of disease associated with *E. coli* O157:H7 was in 1982 and since then this pathogen has been an important public health concern (130). *E. coli* O157:H7 is particularly virulent because of its low infectious dose. It is believed that roughly 10 to 100 cells can cause an infection. However, according to the US Food and Drug Administration's bad bug book (64), the true infective dose is unknown. In fact, a study of an *E. coli* O157:H7 outbreak in Washington State and California from dry fermented salami found that of the four case patients who ate a particular brand of salami, the infectious dose ranged from 2 to 45 bacteria (157).

E. coli O157:H7 is notably the common cause of bloody and non-bloody diarrhea and there are reports estimating 20,000 infections in the United States (20). Each suspected case is required to be reported to the Center of Disease and Control and Prevention. However, since the most laboratories do not culture samples for *E. coli* O157:H7 isolates, the true incidence of infection is unknown. The disease usually is present in young children less than 10 years old and adults 50-59. According to Su and colleagues (155), the elderly- especially those in institutional settings- have the highest morbidity and mortality rates. For example, in 1984 *E. coli* O157:H7 was found in a nursing home where 34 of the residents developed diarrhea and 14 out of 34 were hospitalized and 4 out of 34 died (143). Nonetheless everyone is susceptible.

Geographical and Seasonal Factors

Most illness associated with *E. coli* O157:H7 has occurred in the United States, Canada, and Great Britain; however cases have been documented in over 30 nations including Australia, Chile, Japan and South Africa (155). According to Park et al. (123), the number of cases of *E. coli* O157:H7 in Europe have been increasing in recent years. For example, in 1996 the largest O157 outbreak occurred in Scotland which resulted in 496 cases with 20 reported deaths (123). In the United States, cases are more frequently reported in the northern states than in southern states (20). Moreover, reported cases tend to be seasonal and with a peak incidence from June through September (155). There is also less information on O157 infections in South America compared to North America, which appears to due to the lack of surveillance systems as in the case in many other developing countries (123).

Transmission

Healthy cattle are the main reservoir for human infections (71, 109), though *E. coli* O157:H7 has been shown to be able to colonize the gastrointestinal tract of sheep, goats, deer (49). In 2006, there was an outbreak of *E. coli* O157:H7 associated with baby spinach originating on a cattle farm where free roaming feral swine were observed (80). An investigation by Jay and others (80) found that isolates from feral swine, cattle, surface water, sediment and soil at one ranch matched the outbreak strain. Food-borne disease have been associated with contaminated cattle products including undercooked ground beef (42) and unpasteurized dairy products (3). Hamburger meat has been the cause of major outbreaks in recent years (9), where the sources originated in restaurants, schools, picnics or camps and at individual residences (130). Yet, the last reported hamburger fast-food outbreak was in 1995. This is believed to be associated with the restaurant industry's increased food safety compliance. In recent years, other beef products including salami (37, 164) have been associated with *E. coli* O157:H7 illness.

Fresh produce can also be a vehicle of transmission for *E. coli* O157:H7. It is believed that the manure used in cultivation, wild deer passing through fields, poor sanitation and hygiene by field workers can result in contamination of produce. Moreover, the enteric pathogens are able to attach to these foods using a variety of mechanisms including biofilm production and the use of fimbriae or flagella (56). Products such as apple cider (13) and apple juice (49), lettuce (1), and sprouts (112) have all been sources of outbreaks in recent years. For example, in 1996 there was a large outbreak of *E. coli* O157:H7 infection in school children in Japan which was associated with the consumption of white radish sprouts (112). Additionally, in 1997 outbreaks of O157:H7 infections in Michigan and Virginia were associated with alfalfa sprouts (41). The work by Taormina and Beuchat (156) suggest that the recommended procedures for sanitizing alfalfa seeds fail to eliminate *E. coli* O157:H7. Brackett (21) concludes that maintaining bacterial safety of fresh fruits and vegetables requires a systematic approach including monitoring production, processing, distribution, and use.

Outbreaks can also have non-food related vehicles. Child care centers and chronic-care facilities have been associated with person-to-person transmission of *E. coli* O157:H7. Unchlorinated recreational waters such as lakes, ponds and swimming pools; drinking waters are also reported as the cause of illness. Additionally, there are few reports of disease caused by animal contact and laboratory exposure. Yet still many of the outbreaks are reported as an unknown source (130).

1.2.3 Clinical Manifestations and Treatment

Illness associated with an *E. coli* O157:H7 infection ranges from being asymptomatic, to hemorrhagic colitis, hemorrhagic uremic syndrome, and thrombotic thrombocytopenia purpura or death. Hemorrhagic colitis is a clinical syndrome associated with *E. coli* O157 which manifestations include abdominal cramps and diarrhea which further becomes bloody (155). After ingesting *E. coli* O157:H7 the average interval between exposure and illness is 3 days as the disease progresses it presents itself as hemorrhagic colitis (109). The illness usually resolves after 1 week and patients recover with no obvious sequelae, however about in 5% of patients with hemorrhagic colitis symptoms progress into hemorrhagic uremic syndrome (109).

Hemolytic uremic syndrome (HUS) symptoms include bloody or non-bloody diarrhea, abdominal cramps, vomiting, fever, and renal failure. Manifestations of HUS may also affect the central nervous system resulting in lethargy, seizures, and in some cases coma (155). HUS occurs mostly in infants and young children, and it is the common cause of acute renal failure in children (155). The mortality rate associated with hemolytic uremic syndrome is 3 to 5 percent (20).

Thrombotic thrombocytopenia purpura (TTP) is the less common syndrome associated with *E. coli* O157:H7. TTP presents itself with the same sequelae as HUS but also includes fever and neurological symptoms (155). Kidney failure associated with TTP is less severe than that associated with HUS and the neurological involvement is more prominent (20). TTP usually affects adults – especially the elderly where the mortality rate is high.

Treatment for *E. coli* O157:H7 related illness is mainly supportive. HUS is treated with managing fluids and electrolytes (12) and in 50% of the cases dialysis is necessary (109). Other therapies include plasma infusion, intravenous immunoglobulin, vitamin E, and Shiga toxin inhibitors; however these methods have not proven to be effective (12). Future treatments may include the use of oral Shiga toxin-binding resins and toxin-neutralizing antibodies (109).

Research suggests avoiding the use of antibiotics for treating *E. coli* O157:H7 infections. One study found that the use of antibiotics to treat children with *E. coli* infection actually increased the risk of hemolytic uremic syndrome (165). The major arguments against their use is that antibiotics can rid the intestine of the natural microflora, promoting growth of *E. coli* O157:H7 or that antibiotics can lyse these pathogens and liberate the Shiga-like toxins (155). Antimotility agents have also been found to advance *E. coli* O157:H7 illness (10). In addition, the use of antimotility agents has shown to increase the risk of neurological manifestations in HUS patients (12).

1.3 Acidified Vegetables and Food Safety

Acidified vegetables include products such as cucumber pickles, pimentos and pickled peppers. Acetic acid is the most commonly used acidulant in these products. The natural microflora on freshly harvested pickling cucumbers can range anywhere from 10^4 t0

10^6 colony forming units (CFU) per gram (26). Various pathogens, including but not limited to *Salmonella spp., Shigella spp., Staphylococcus aureus, Listeria monocytogenes*, and *Escherichia coli*, may be present on fresh vegetable products (14). As reported by Beuchat (15), fruits and vegetables can be contaminated with pathogenic bacteria while growing in the fields, during harvesting, postharvest handling, processing and distribution. Removal of these pathogens has proved difficult since these microbes can attach to the surface of the fruit enhancing their survival during washing and or sanitizing treatments (26). However, the simultaneous use of inhibitory measures such as pH, salts, organic acids, sugar (to lower the water activity) and temperature (known as the hurdle theory) may rid processed vegetables of possible contaminants. For instance, with roughly 0.5 to 2% acetic acid these products are pasteurized to prevent spoilage and to ensure safety (26).

The Code of Federal Regulations for acidified (21 CFR part 114) foods was established by the United States Food and Drug Administration (USDA) to institute safety standards for these foods. According to the CFR an acid food is define as a food that naturally has a pH of 4.6 or below. Acid foods include products like apple juice, orange juice, and mayonnaise. Acidified foods are defined as low-acid foods to which acid or acid food ingredients have been added. These foods have a water activity of greater than 0.85 and have an equilibrium pH of 4.6 or below. These measures were established to prevent the growth of botulism and do not reference a concentration or type of acidulant needed to meet this 4.6 pH requirement. Examples of acidified foods include cucumbers, beans, cabbage, cauliflower, puddings, tropical fruit and peppers. In recent years acid foods have been associated with food-borne pathogens. Instances include outbreaks of disease from *Escherichia coli* O157:H7 in apple cider (38) and *Salmonella enterica* in orange juice (39), which typically have pH values between 3.5 and 4.0. Thus, the potential for *E. coli* O157:H7 illness associated with acidified foods exists.

1.4 Proposed Research

The main objectives of this research were to use mathematical modeling to further understand the survival of *E. coli* O157:H7 in environments similar to an acidic vegetable product. In Chapter 2 the goal was to understand the effects of sodium chloride and acetic acid concentration on O157:H7 intracellular pH maintenance and survival. A primary Weibull model was used and subsequent secondary models were created to characterize the relationship between intracellular pH and survival. In Chapter 3, a mechanistic model for describing intracellular pH was examined. In Chapter 4 the effects of environmental salt composition on the survival and intracellular pH of *E. coli* O157:H7 in a low-pH environment was determined. Primary models appropriate for describing *E. coli* inactivation in these environments were also compared in this chapter. In Chapter 5 the role of mathematical model assumptions in predicting survival and growth behavior was examined. In this chapter, tumor growth and microbial inactivation were used as case studies. Conclusions about this work and further research suggestions are made in Chapter 6.

2 Modeling the Effects of Salt, Acetic Acid and Intracellular pH on the Survival of *Escherichia coli* O157:H7[1]

2.1 Abstract

Microbiological safety has become a critical issue for acid and acidified foods since it became clear that acid-tolerant pathogens, such as *Escherichia coli* O157:H7 can survive (even though they are unable to grow) in the pH range of 3-4, typical for these classes of food products. The primary antimicrobial compounds in these products are acetic acid and NaCl, which can alter the intracellular physiology of *E. coli* O157:H7, leading to cell death. For combinations of acetic acid and NaCl at pH 3.2 (a pH value typical for non-heat processed acidified vegetables), survival curves were described by using a Weibull model. The data revealed a protective effect of NaCl concentration on cell survival for selected acetic acid concentrations. The intracellular pH of an *E. coli* O157:H7 strain exposed to acetic acid concentrations up to 40 mM and NaCl concentrations between 2% to 4% were determined. A reduction in the intracellular pH was observed for increasing acetic acid concentrations with an external pH of 3.2. Comparing intracellular pH with Weibull model predictions showed that decreases in intracellular pH were significantly correlated with the corresponding times required to achieve a 5-log reduction.

[1] This chapter shares the same title as a manuscript submitted and accepted (November 2010) to the Journal of Applied and Environmental Microbiology with co-authors Frederick Breidt Jr. and Charles E. Smith. The contents in this chapter are the foundation for the submitted manuscript.

2.2 Introduction

Since an initial outbreak in 1982, *Escherichia coli* O157:H7 has been a serious public health concern. It has been reported that there are 20,000 infections each year in the United States (20). In the majority of the cases the illness resolves in a week, however in about 5% of patients the disease progresses to hemolytic uremic syndrome which may result in kidney failure, neurological sequelae and death (109). While cases of food borne illness associated with acidified foods are rare, the FDA has expressed concern about these products, based upon disease outbreaks caused by *E. coli* O157:H7 in apple cider (13, 40) and *Salmonella enterica* in orange juice (53). The U.S. acidified food regulation (21 CFR part 114) requires that vegetative microbial pathogens are killed and organisms of non-public heath significance cannot grow in commercial acidified vegetable products.

E. coli O157:H7 has been found to be the most acid resistant vegetative pathogen of concern in acidified vegetables (25, 27). At pH 3 and 30^{o}C, Jordan et al. (82) showed that O157:H7 strains survived up to 3 days. A study by Breidt et al. (24) revealed that, depending on the temperature, O157:H7 strains needed 2 to 6 days to achieve a 5-log reduction at pH 3.3 in acetic acid solutions (at 25^{o}C and 10^{o}C, respectively). The organism may survive even longer in acidified vegetables acidified vegetables that are not heat processed at refrigeration temperatures (4^{o}C) (F. Breidt, unpublished). Therefore, it would be of importance to quantify the effects of antimicrobials used in preventing the survival of O157:H7 in acidified vegetables products. Mathematical models for microbial inactivation by heat, pressure and chemicals have been extensively studied (2, 25, 45, 46, 54, 160). Traditional approaches to measure the killing of bacteria by environmental stress uses first order kinetics (46). However, this does not account for deviations from linearity such as shoulders or tails in killing curves (107), which are evident in organic acid killing data (25).

The antimicrobial activity of organic acids is thought to be due to the ability of the undissociated acid to freely cross the cell membrane and release protons inside the cell (28, 145). The lowering of pH is opposed in the cell by removal of excess protons at the expense of ATP (19). The energy required to rid the cytoplasm of these protons drains the cell of ATP, resulting in death (4). An alternative explanation of the toxicity of organic acids is that acid anions become trapped in the cell cytoplasm and accumulate inside the cell, raising ionic strength, and potentially disrupting metabolism (141). Decreasing intracellular pH results in a low transmembrane pH gradient (57), and may therefore reduce anion levels inside the cell. This may result in reduced metabolic activity, because enzymes in the cytoplasm may not function well below neutral pH. It has been suggested that *Lactobacillus plantarum* predominates in vegetable fermentations because it can tolerate a lower intracellular pH better than competing lactic acid bacteria (105). The prolonged survival of *E. coli* O157:H7 in acidic conditions has been explained mainly by the existence of acid resistance (AR) systems (66), which help to maintain a high intracellular pH, in some cases around pH 7 (161). Because of the apparent conflicting survival mechanisms, i.e. lowering intracellular pH to prevent acid anion accumulation, or maintaining high pH to optimize metabolic enzyme function; it is unclear how intracellular pH and cell survival are related.

Acidified vegetables typically contain 2% to 4% NaCl and varying concentrations of acetic acid, up to 400 mM. There is evidence that sodium may increase acid sensitivity for *E.*

coli (140), but it also aids in recovery from stress and enhances cell growth (81). We determined the effects of salt (NaCl) and acetic acid on the survival and intracellular cell physiology of *E. coli* O157:H7 and the relationship of these variables to killing kinetics. Using a Weibull model, we report a significant correlation between intracellular pH and cell survival data. In addition, we found that NaCl may provide a protective effect on survival at pH 3.2 for concentrations of 20 mM or less protonated acetic acid and 4% NaCl compared to similar acid concentrations with 2% NaCl.

2.3 Materials and Methods

2.3.1 Bacterial Strain and Growth Conditions

E. coli B241 (strain O157:H7, 28RC1, bovine isolate) were used in this study. This strain was chosen based on its acid resistance properties (122). The stock culture was stored at -80^{o}C in Luria-Bertani broth (Difco Labs, Detroit, MI) supplemented with 20% glycerol and 1% glucose (Sigma Chemical Co., St. Louis, MO). Cultures were grown statically in 50 mL of Luria-Bertani + 1% glucose (LBG) for 18 h at 37^{o}C to induce acid resistance. Cultures were then harvested by centrifugation (25^{o}C, 10 min, 5000 x g) and concentrated 25 fold by resuspending in 2 mL of sterile saline (8.5 g/liter NaCl). Cells were enumerated by serial dilution in 0.85% NaCl and plating on Luria-Bertani agar (LB) using a spiral plater (model 4000, Spiral Biotech, Inc., Norwood, MA). After 24 h incubation at 37^{o}C, colonies were counted using an automated plate reader (QCount, Spiral Biotech).

2.3.2 Acetic acid and NaCl Treatments

The acetic acid (Sigma) solutions used in this study ranged from 0 mM to 60 mM protonated acid species. All acid solutions contained 20 mM D-gluconic acid sodium salt (Sigma), which functioned as a non-inhibitory buffer (pK_a = 3.8) (23). The ionic strength of the acid solutions (either 0.342, 0.684, or 1.027) was held constant by using NaCl, designed using pHTools software (61); a custom MATLAB routine. Additionally, the pH of the acetic acid solutions was held constant at pH 3.2 by the addition of HCl or NaOH. A final volume of 0.8 mL (for intracellular pH studies) or 1.6 mL (acid killing curves) of the acid solution in a 2 mL microcentrifuge tube contained 0.1 or 0.2 mL (respectively) of the concentrated cell suspension (as described above), gave an initial cell concentration of approximately 5 x 10^9 CFU/mL. For the killing curves, 50 uL samples were removed at the indicated time intervals and immediately diluted into 0.45 mL of 0.1 M MOPS buffer (3-morpholinopropane-1-sulfonic acid, Sigma) at pH 7.0 to neutralize the acid. Cells were enumerated following serial 10 fold dilutions in 0.85% NaCl and plating on LB agar as described above.

The relationship between the log of the 5-log reduction time, acid and salt concentrations was described by the following model:

$$\log RT_5 = c_0 + c_1 salt + c_2 acid + c_3 acid \times salt \qquad (2.1)$$

Regression parameters for equation (2.1) were estimated by using the general linear model procedure in SAS (see below). Based on this model, a response surface was generated with the 5-log reduction times for cells exposed to 20, 30 and 40 mM of acetic acid with either 2%, 4% or 6% NaCl. A total of 9 measured 5-log reduction times were used to create the response surface. For the validation of this model, survival experiments were performed for cells were exposed to 1% NaCl with 40 mM acetic acid, 2% NaCl with 60 mM of acetic acid, or 4% NaCl with 60 mM acetic acid.

2.3.3 Intracellular pH

Intracellular pH was determined using a radioactive acid distribution method (134). *E. coli* B241 were grown and washed as previously described. All radionuclides were obtained from the American Radiolabeled Chemicals, Inc. (St. Louis, MO). For the time course experiments, cells were incubated at 25^{o}C with a buffered acid treatment containing 0 mM, 5 mM or 40 mM acetic acid, and either 7-^{14}C-benzoate (50-60 mCi/mmol) or 1,2-^{14}C-polyethylene glycol (0.1-1 mCi/g), and $^{3}H_2O$ (1 mCi/mL) for either 5, 15, 30 or 60 min. The ^{14}C-benzoic acid was used to measure intracellular pH by acid partition and the ^{14}C-polyethylene glycol (PEG) was used to measure external cell pellet water space. Alternatively we used 7-^{14}C-salicylate (40-60 mCi/mmol) for the intracellular pH measurement and D-^{14}C(U)-sorbitol (250-350 mCi/mmol) or 1,2-^{14}C-taurine (30-60 mCi/mmol) for the external cell water space measurement. For determining dry weights, the cells pellets were digested overnight in a 3M HNO3, dried in a vacuum system (Speed Vac Concentrator, SVC 100, Savant Inst. Inc. Farmingdale, NY) and weighed.

To measure intracellular pH, cell cultures were incubated at 25^{o}C with the buffered acid treatments described above, containing approximately 1 uCi of 7-^{14}C-benzoic acid or 1,2-^{14}C-polyethylene glycol (^{14}C-PEG) in combination with tritated water ($^{3}H_2O$, to measure total cell pellet volume) for 30 min. After the indicated incubation period, 500 uL samples from the acid treatment were centrifuged through a silicone oil mixture (65:35 mix of Dow

Chemical Co. type 550 and 556) in a microcentrifuge (13, 000*g*, 15 min) at 4^{o}C. An aliquot (100 uL) of the supernatant was removed. Cell pellets under the silicone layer were frozen for a minimum of 40 min at -80^{o}C to solidify the silicone and then the pellets were cut from the bottom of the tube with dog nail clippers. A detergent solution containing 50 mM Tris (Sigma) and 0.5 % Tween 80 (Fisher Scientific, Pittsburgh, PA) at pH 7.0 was used to resuspend pellet samples. Pellet samples or 100 uL of the supernatant were added to 600 uL or 500 uL respectively of the detergent solution into a 7 mL scintillation vial (Perkin Elmer, Waltham, MA; cat # 6000167). After resuspension of the cell pellet from the microcentrifuge tube fragment by vortexing, 5 mL of scintillation fluid (Scintisafe from Fisher) was added and disintegrations per minute for ^{14}C and ^{3}H of the radionuclides were determined by dual label counting using a scintillation counter (model LS600, Beckman Coulter, Inc., Fullerton, CA). DPM values were determined from CPM using ^{14}C and ^{3}H quench standards (Beckman). Intracellular cell volume was determined by subtracting the calculated external pellet water volume from the total pellet volume, based on ^{14}C-PEG (which does not enter the cell) and $^{3}H_2O$ (total pellet volume) DPM in the pellet fraction. Intracellular pH was calculated using the intracellular/extracellular DPM ratio for ^{14}C-benzoate, based on the intracellular volume determined from the pellet and the supernatant ^{14}C counts with the Henderson-Hasselbalch equation, assuming an intracellular pK_a for benzoic acid of 4.21.

2.3.4 Modeling and Statistical Analysis

A Weibull model was used to describe the log reduction in microbial population and to estimate the 5-log reduction in the number of bacteria. The survivors, measured in colony forming units per milliliter (CFU/mL) over time (hours) was described by

$$N(t) = N_0 e^{(-t/\alpha)^{\beta}} \qquad \text{with} \qquad N(0) = N_0 \tag{2.2}$$

where *N(t)* is the concentration of bacteria over time, N_0 is the initial bacterial load, α is the scale parameter with units of time, and β is the dimensionless shape parameter. For $\beta > 1$ the survival curve is convex, for $\beta = 1$ the survival curve is linear (on a logarithmic scale) and for $\beta < 1$ the survival curve is concave. The log (base 10) of the number of survivors is thus written as follows

$$\log N(t) = \log N_0 - \frac{1}{\ln(10)}\left(\frac{t}{\alpha}\right)^{\beta} \tag{2.3}$$

and the 5-log reduction time as a function of alpha and beta can be written as

$$RT_5 = \alpha\left(5\ln(10)\right)^{1/\beta}. \tag{2.4}$$

Statistical analysis for the Weibull model was determined using the NLIN procedure of SAS software (SAS Institute Inc., Cary, NC). For all acid treatments, the parameters N_0, α, and β were estimated. Solving for α in equation (2.4),

$$\alpha = \left(5\ln(10)\right)^{1/\beta} / RT_5. \tag{2.5}$$

Then the 5-log reduction time was estimated and the corresponding standard error of these estimates determined by re-parameterizing the Weibull model,

$$\log N(t) = \log N_0 - 5\left(\frac{t}{RT_5}\right)^{\beta}. \qquad (2.6)$$

As discussed by Breidt et al. (25) the result (equation (2.6)) is a nonlinear regression model that has additive, normally distributed errors that have equal variance. Model parameters were estimated using a non-linear protocol (PROC NLIN) in SAS.

For the radionuclide acid distribution experiments and the time course experiments, differences between the means in intracellular pH were carried out using a Tukey least significant difference method ($P < 0.05$) for pair-wise comparisons. The REG procedure of SAS was used for determining regression models of the 5-log reduction time and the CORR procedure of SAS was used to determine the correlation between the 5-log reduction time and the intracellular pH.

2.4 Results

2.4.1 Survival

The survival of *E. coli* O157:H7 exposed to 0 - 40 mM of protonated acetic acid and 2 or 4% NaCl at pH 3.2 was determined (Figure 2.1). A Weibull survival model was used to predict the time required to achieve a 5-log reduction (Table 2.1). As expected, an increase in the protonated acetic acid concentration decreased the number of survivors over time. There was no significant change in CFU/mL for all treatments during the first 30 min of incubation (not shown). After 60 min, survival curves were nearly linear or concave upward (Figure 2.1). With greater than 20 mM of protonated acetic acid, increasing the salt concentration decreased the predicted time for a 5-log reduction. With 0 to 10 mM acetic acid and 4% NaCl there was a pronounced tailing behavior, preventing accurate predictions of the 5-log reduction time, indicating NaCl has a protective effect on cell survival under these conditions, compared to 2% NaCl.

2.4.2 Effects of Acid and Salt on 5-log Reduction Time

A predictive model was developed using data collected from cells exposed to 20 - 40 mM acetic acid and 2-6% NaCl (Figure 2.2). The following model was appropriate to predict the 5-log reduction time based on these acid and salt concentrations:

$$\log RT_5 = 2.57^{****} - 1.49^{***} salt - 29.37^{**} acid + 22.63^{*} acid \times salt \quad . \tag{2.7}$$

Parameters that were significant are denoted with four stars ($P < 0.0001$), three stars ($P = 0.0008$), two stars ($P = 0.0017$) or one star ($P = 0.0196$). The coefficient of determination (R^2) for the equation was 0.9830. Validations for the predictive model (equation (2.7)) were performed using three selected salt and acid combinations and the results of these studies are illustrated in Figure 2.2. The predictive model for the three validation experiments underestimated the time required for a 5-log reduction.

2.4.3 Intracellular pH

To establish which radionuclides are appropriate for measuring intracellular pH, we compared ^{14}C-benzoate with ^{14}C-salicylate (Figure 2.3). A two-way ANOVA was performed for comparing the radioactive acid used for measuring pH and acetic acid concentration, where acetic acid concentration was found to be more significant than the choice of radionuclide. Radioactively labelled sorbitol (121), inulin (93), taurine (58), and PEG (52) were used for cell pellet external water volume measurements. We found that ^{14}C-sorbitol, ^{14}C-inulin, and ^{14}C-taurine gave inconsistent results, including negative calculated cell volumes (data not shown). PEG however, consistently gave cell volumes of approximately 1 µL/mg cell dry weight (data not shown).

For the intracellular pH measurements, all treatments showed a trend of declining pH with exposure time (Figure 2.4). No significant change in the viable cell count was observed for all treatments during the first 30 min acid incubation time. After 1 h incubation, the largest decline in cell numbers was a 0.36 log units, with 4% NaCl and 40 mM protonated acetic acid (data not shown). For the 4% NaCl treatment at pH 3.2 with no acetic acid, the intracellular pH decreased more than one pH unit, from greater than pH 6.5 to less than pH 5.5 during the 1 h of incubation. With 40 mM acetic acid for both 2% and 4% NaCl, the intracellular pH values showed only about 0.5 pH unit decrease, ranging from approximately pH 6.0 to pH 5.5, when incubation time increased from 5 to 60 min. Interestingly, only the 5 mM protonated acid treatment with 2% NaCl resulted in no significant change in the intracellular pH during the 60 min incubation.

2.4.4 Intracellular pH and Survival

Increasing the concentration of protonated acetic acid decreased the intracellular pH (Figure 2.5) with a linear trend (R^2 = 0.99) for the 2% NaCl treatment. The 5-log reduction time predicted by the Weibull model showed a similar trend for the 2% NaCl treatment, with the time decreasing from 195 h to 17 h (Table 2.1, Figure 2.5, $R^2 = 0.90$). With 2% NaCl data, the coefficient of determination for the relationship between intracellular pH or the calculated intracellular acetate anion concentration and 5-log reduction time was 0.95 and 0.89 (respectively, data not shown). For the pH 4% NaCl treatment, however, the relationship between protonated acetic acid, and intracellular pH and 5-log reduction time was not linear. Between 0 and 10 mM protonated acid intracellular pH increased from 5.7 to 6 (Table 2.2, Figure 2.5), and as protonated acid concentration increased from 10 to 40 mM, the intracellular pH declined to 5.7. The estimated alpha and beta parameters for the Weibull model both approached zero for survival curves when the protonated acid concentrations were below 10 mM with 4% NaCl, and a 5-log reduction time could not be reliably predicted (Table 2.1). This corresponded to survival curves with an extended tailing behavior (Figure 2.1). With 4% NaCl and protonated acetic acid concentrations above 10mM, the 5-log reduction times declined from 20 to 10 hours, which is similar to the trend seen with the 2% NaCl treatments (Figure 2.5).

2.5 Discussion

Acetic acid and NaCl are the primary barriers to survival of acid resistant pathogens in many acidified foods (23). For acidified vegetables with pH values above 3.3, a heat process is required to assure safety, but products below pH 3.3 rely on acetic acid for a 5-log reduction in cell numbers of vegetative microbial pathogens (24). A 5-log reduction (the standard used by FDA for process filings) for *E. coli* O157:H7 strains in pickled vegetable brines may take up to 6 days, depending on temperature (24). Little is known about the intracellular physiology of *E. coli* strains undergoing acid stress typical of acidified foods. We examined the effects of NaCl, acetic acid and intracellular pH on the survival of *E. coli* O157:H7 at pH 3.2, typical of non-heat processed acidified food products. These products can have up to 400 mM acetic acid, however, we used 0 to 40 mM protonated acetic acid for our studies because this allowed accurate measurements of intracellular pH. At higher acetic acid concentrations the lethal effects of the acid treatments prevented accurate measurements of intracellular pH, because of the accumulation of dead cells. With 0 to 40 mM protonated acetic acid, non-linear killing kinetics were observed. There was no significant decrease in CFU/mL was observed during the first 30 min of incubation for all treatments (data not shown). After the first 30 to 60 min, survival behavior was concave (up) or nearly log-linear. As in previous reports (25, 54, 78, 160), a Weibull model was used to describe the survival curves. *E. coli* O157:H7 exposed to 4% NaCl, and less than 20 mM acetic acid had survival curves with a remarkable tailing behavior. Under these conditions, approximately 0.1% (1 x 10^6 CFU/mL) of the initial population remained resistant to the acid solution, and survived for over 100 hours with little change in cell numbers (Figure 2.1). As discussed by Jordan et al. (26), these data emphasize the need for nonlinear models that predict conditions for eliminating pathogens from foods, where surviving subpopulations of viable cells can potentially cause disease outbreaks.

Intracellular pH measurements showed that pH decreased for most acid treatments during the first 60 min of incubation (Figure 2.4). To correlate intracellular pH with cell survival, we chose the 30 min; during this time no significant change in cell number occurred. After 60 min a decrease of 0.36 $\log_{10}$ CFU/ml was seen for the 4% NaCl treatment with 40 mM acetic acid. Therefore the 30 min time was chosen to correlate intracellular pH changes with subsequent cell survival. The two radionuclide compounds used, ^{14}C-Benzoic and ^{14}C-Salicylic acid, have different pK_a values (4.2 and 3.0, respectively), but gave similar intracellular pH values measurements. Similar results were observed by Russell (141) where he found no apparent difference in the intracellular pH determination when using radioactively labeled benzoate or acetate. For our studies we chose ^{14}C-benzoate for intracellular pH measurements because the pK_a of this acid was closer to the measured intracellular pH values.

Increasing the acetic acid concentrations decreased cell survival within a given NaCl concentration, which is consistent with previous literature (57). However, data from Figure 2.1 shows that with protonated acid concentrations of 10 mM or less, long term survival (between 50 and 100 hours) was better with 4% NaCl that with 2% NaCl. At higher protonated acetic acid concentrations (Figure 2.2) survival decreased as NaCl and protonated acetic acid increased. Modeling the 5-log reduction time with acid concentrations of 20 mM or greater (equation (2.7)) underestimated the 5-log reduction time, and would therefore not be appropriate for food safety applications without modification. However, the model did show that 98% of the variability could be explained by NaCl concentration, acetic acid concentration and the interaction between the salt and acid concentrations. The consequences of salt relative to the survival of *E. coli* has been investigated (36, 44, 63, 81). Chapman et al. (44) has shown *E. coli* SERL 2 in the presence of sucrose with pH ranging from 3.2 to 4, increasing NaCl concentrations (1 to 3%, wt/wt) increased the time required for a 3 $\log_{10}$ reduction resulting in a protective salt effect. A similar observation was reported for growing *E. coli* O157:45 where, in combination with acid, NaCl conferred a protective effect against the bacteriocidal acid pH (36). However, the protective salt effect was not observed in our study when the protonated acid concentration was 20 mM or greater (Figure 2.1). Our results suggest that a protective salt effect is only apparent with low-acid (10 mM or less) conditions and 4% NaCl. At these salt concentrations our intracellular pH measurements did not follow the same trend as was seen with 2% NaCl, being lower than expected, as described below. Casey and Codon (36) reported that the protective salt effect may be a result of the increased osmolarity or may be due to increases in the cytoplasmic pH of the cells. At 4% NaCl and less than 20 mM of acetic acid, the observed tailing behavior was correlated with a lower intracellular pH 30 min after the start of incubation in the acid solution (Figure 2.5, Table 2.2), possibly reducing the accumulation of the acid anion and cell death. Additional research to examine the function of Na^+ antiporters at low concentrations of acetic acid may help with understanding protective salt behavior.

By examining intracellular pH for selected conditions (2% and 4% NaCl, and 0, 5, 10, 20, and 40 mM protonated acetic acid) we sought to identify how internal cell physiology was altered by the external environment, and how those changes may lead to cell death. The relationship between intracellular pH and survival of *E. coli* has been previously considered (27, 83, 145). In the presence of lactic acid, lowering the intracellular pH for *E. coli* was not sufficient to cause cell death (83). Brudzinski and Harrison (27) examined the acid tolerance response for *E. coli* O157:H7 when exposed to acetic acid at various temperatures and pH, and concluded cell death may have resulted from a reduction in intracellular pH. As reviewed by Jordan et al. (82), several studies have attempted to identify the factors contributing to increased acid tolerance in *E. coli*. Diez-Gonzalez and Russell found that intracellular acetic acid accumulation in *E. coli* O157:H7 was limited by the ability of these organisms to lower the intracellular pH (57).

For all the 2% NaCl treatments, we found that lower intracellular pH correlated (R^2 = 0.95, not shown) with a decrease in the observed 5-log reduction time, suggesting that lowering intracellular pH reduced survival. For the same data set, increasing intracellular acetate anion, based on the protonated acid concentration and calculated from the intracellular pH data (Table 2.2), was also found to correlate with a decrease in survival (R^2 = 0.89, not shown). At 4% NaCl and 0 to 10 mM protonated acetic acid, the intracellular pH increased, and prolonged survival of a subpopulation of cells was apparent from the data shown in Figure 2.1. Enhanced survival of *E. coli* O157:H7 was previously reported for these salt and acid conditions (17). However, the intracellular pH value with 4% NaCl and 5 mM protonated acetic acid was similar to the intracellular pH with 2% NaCl and 40 mM protonated acid (around pH 5.8), although the corresponding cell survival data was very different (Figure 2.1). The relationship between the intracellular pH, acetic acid anion concentration and cell survival remains unclear. Future work may include separating live and dead cell populations for intracellular pH measurements of the surviving cells at different times of incubation with acid solutions. It is likely that other factors, including the transmembrane motive force which is determined by proton flux, may also help elucidate the relationship between the internal physiology of *E. coli* O157:H7 and cell death.

2.6 Acknowledgements

The authors thank Dr. Roger F. McFeeters for helpful discussions about this work, Mrs. Sandra Parker for excellent secretarial assistance, and Mr. Donald Fornea for the HPLC analyses performed. This work is partial supported by grant from the Pickle Packers International Inc.

Table 2.1 Weibull model parameters and 5-log reduction estimate (RT5) with standard errors (SE) for each acid/salt treatment.

NaCl Concentration	Protonated Acetic Acid (mM)	N_0 (SE)[a]	α (SE)[b]	β (SE)[c]	RT5 (SE)[d]
2%	0	9.61 (0.25)	0.50 (0.58)	0.41 (0.20)	194.92 (70.70)
	5	9.22 (0.13)	1.54 (0.59)	0.52 (0.43)	173.49 (10.46)
	10	9.18 (0.14)	2.58 (0.83)	0.62 (0.52)	131.52 (6.49)
	20	9.57 (0.35)	0.94 (0.70)	0.63 (0.39)	44.95 (6.08)
	30	9.59 (0.30)	0.58 (0.38)	0.63 (0.41)	27.91 (3.99)
	40	9.64(0.37)	0.19 (0.15)	0.54 (0.35)	17.16 (3.10)
4%	0	10.22 (1.84)	4.28E-25 (2.85E-23)	0.04 (0.03)	ND
	5	9.33 (0.39)	8.26E-11 (1.04E-9)	0.08 (0.03)	ND
	10	9.07 (0.23)	6.88E-4 (1.48E-3)	0.18 (0.03)	ND
	20	9.61 (0.30)	0.07 (0.05)	0.43 (0.05)	20.33 (3.22)
	30	9.57 (0.26)	0.28 (0.16)	0.65 (0.45)	12.39 (1.20)
	40	9.56 (0.26)	0.32 (0.14)	0.71 (0.53)	9.65 (0.81)
6%	10	9.04 (0.26)	0.01 (0.02)	0.37 (0.08)	9.33 (1.79)
	20	9.05 (0.18)	0.001 (0.004)	0.28 (0.07)	9.31 (2.77)
	30	9.42 (0.30)	0.004 (0.006)	0.33 (0.07)	6.90 (1.40)
	40	9.37 (0.32)	0.09 (0.071)	0.56 (0.09)	7.29 (0.95)

[a] Initial bacterial counts in units of CFU/mL
[b] Weibull scale parameter in units of hours
[c] Weibull dimensionless shape parameter
[d] 5-log reduction time in units of hours

Table 2.2 Intracellular pH and the total intracellular acetic acid concentration for acid/salt treatment.

NaCl Concentration	Protonated Acetic Acid (mM)	Calculated Extracellular Acetate Anion (mM)[a]	Intracellular pH (SE)[b]	Calculated Intracellular Acetate Anion (mM)[c]
2%	0	0.00	6.35 (0.03)	0.00
	5	0.78	6.25 (0.03)	154.57
	10	1.02	6.13 (0.02)	233.22
	20	3.13	5.93 (0.04)	298.67
	30	4.64	5.77 (0.02)	306.49
	40	4.28	5.65 (0.06)	312.34
4%	0	0	5.67 (0.05)	0.00
	5	0.36	5.73 (0.03)	47.17
	10	0.71	5.97 (0.05)	162.50
	20	1.82	5.92 (0.03)	289.20
	30	3.63	5.80 (0.05)	328.24
	40	4.31	5.71 (0.01)	353.20

[a] Calculated from the total protonated acetic acid concentration using HPLC
[b] Mean intracellular pH from 3 independent replicates with the standard error in parenthesis
[c] Calculated using the Henderson-Hasselbalch equation

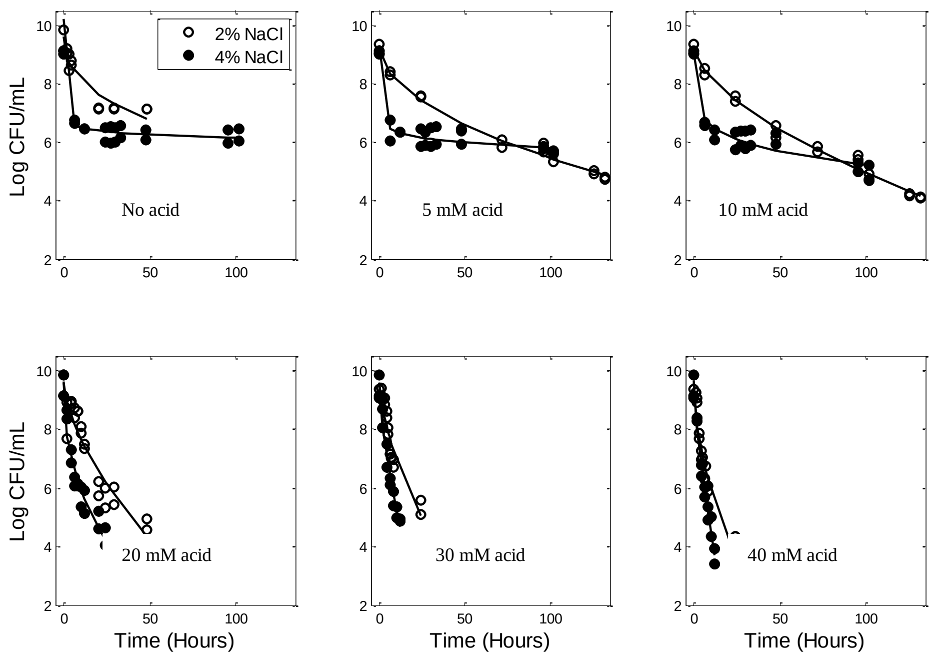

Figure 2.1 Survival of *E. coli* O157:H7 exposed to 2% NaCl (open circles) or 4% NaCl (closed circles) with 0-40 mM of protonated acetic acid. The solid lines represent the Weibull prediction curves.

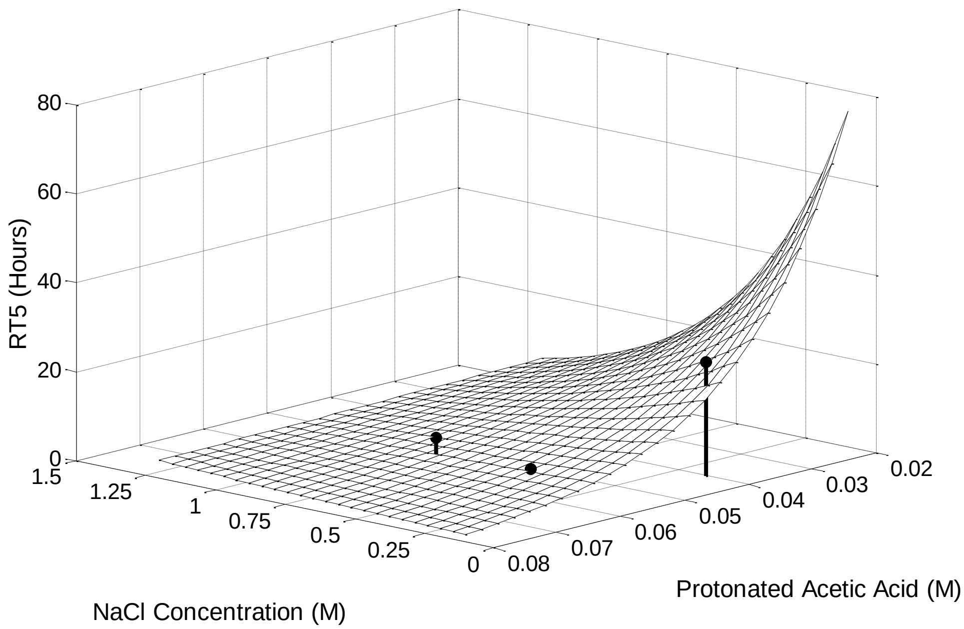

Figure 2.2 Response surface plot showing the 5-log reduction times as influenced by the protonated acetic acid concentration and the NaCl concentration, created by using equation (2.7) (see text). Several measured 5-log reduction times are also shown (black circles).

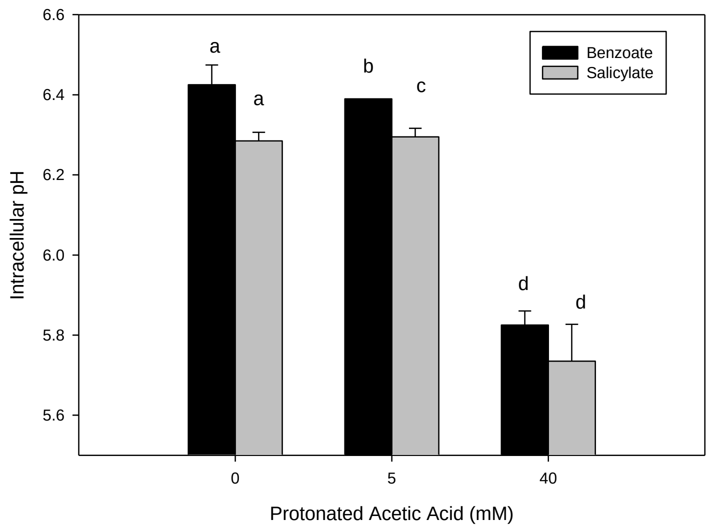

Figure 2.3 Intracellular pH of *E. coli* O157:H7 exposed to 2% salt and incubated at 25°C for 30 minutes with a buffered acid treatment and either ^{14}C-benzoate (Grey bars) or ^{14}C-salicylate (Black bars). Data represents the mean values of two independent replicates; errors bars represent the standard deviation. Letters within the same protonated acetic acid concentration indicate no significant (P < 0.05) difference.

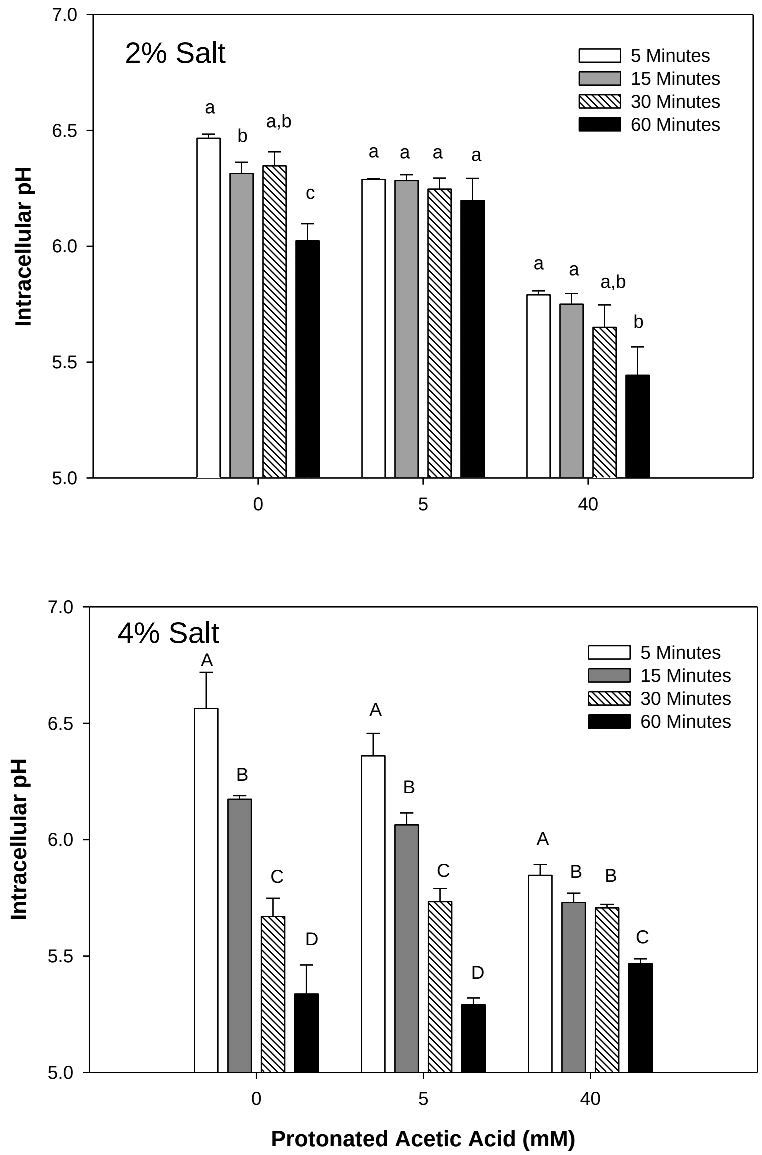

Figure 2.4 Intracellular pH for *E. coli* O157:H7 exposed to no acetic acid, 5 mM, or 40 mM protonated acetic acid in the presence of 2 % salt or 4 % salt at 25^{o}C. Cells were incubation with acid treatment for 5 minutes (white bars), 15 minutes (grey bars), 30 minutes (striped bars) or 60 minutes (black bars). The extracellular pH was 3.2. Data are mean values from three independent replicated experiments. Error bars represent the standard deviations of these replicates. Identical letters over error bars within the same acid treatment indicate that there is no significant difference ($P \geq 0.05$) between incubation time (minutes).

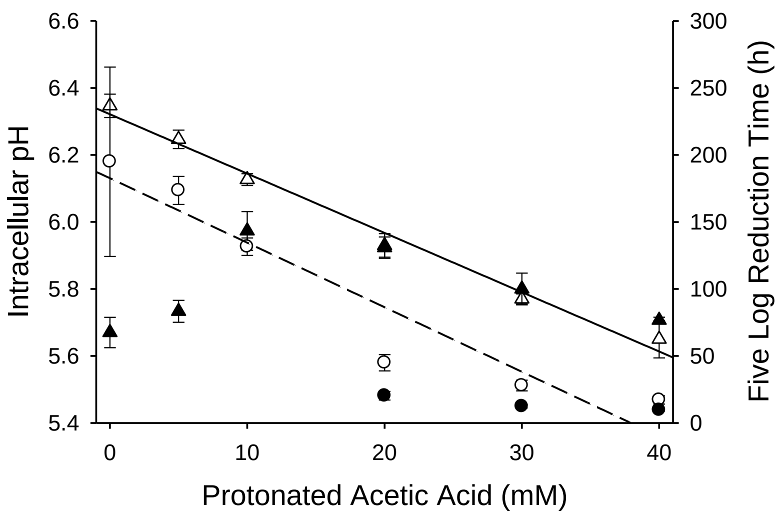

Figure 2.5 The intracellular pH (triangles) and estimated 5- log reduction times (circles) for 2% NaCl (open symbols) and 4% NaCl (filled symbols) and treatments. The lines represent linear regression of the protonated acid concentration and the intracellular pH (solid line, R^2= 0.99) or 5-log reduction time (dashed line, R^2 = 0.90), for the 2% NaCl treatment only. The error bars represents the standard error for three independent replications. Note that only three data points for the 5-log reduction time were predicted for the 4% NaCl treatment.

2.7 Supplementary Materials [2]

Integral to intracellular pH measurement is the density of live cells present during this measurement. Thus, the survival within the first 30 minutes and 60 minutes for cells subjected to protonated acetic acid was determined. With exposure to 2% or 4% salt with acetic acid concentration ranging from 0 to 40 mM, there were no significant differences in the means between the initial population and the population after 30 minutes. The maximum log reduction in 30 minutes was 0.27 (± 0.01 standard deviation, 2 independent replicates). In addition, the log-reduction for O157:H7 exposed to 2% or 4% salt solutions with 0, 5, or 40 mM acetic acid after 1 hour was determined. There was no decrease in the number of viable cells after 1 hour and the maximum log reduction obtained was 0.36 (± 0.07 standard deviation, 3 independent replicates) (see Figure 2.6) . This data indicates that within 1 hour the intracellular pH can be determined.

[2] This section will present the materials pertaining to *E. coli* O157:H7 survival in the presence of acetic acid and salt (NaCl) solutions which are not a part of the manuscript (Section 2.1 to 2.6) submitted to the Journal of Applied and Environmental Microbiology for publication.

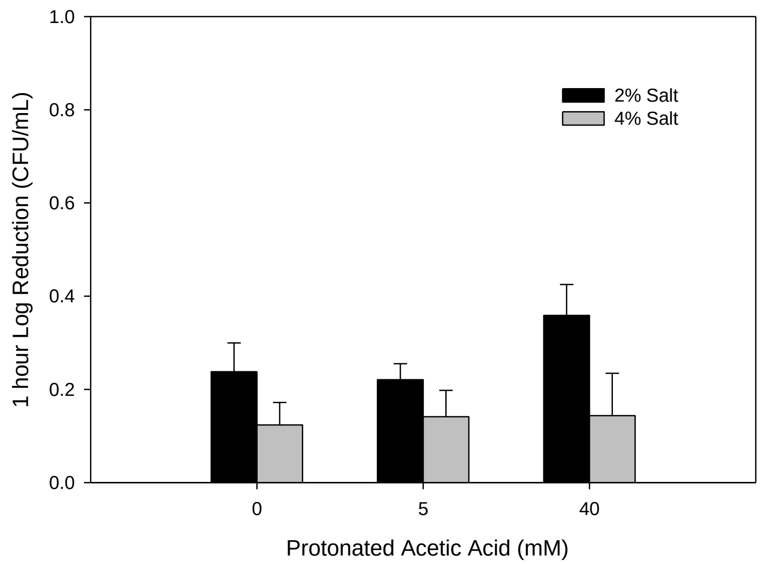

Figure 2.6 One hour log reduction for *E. coli* O157:H7 subjected to acetic acid and either 2% (black bars) or 4% (grey bars) NaCl at pH 3.2. Error bars represents the standard deviation of three independent replications.

To describe the relationship between the survival parameters secondary linear models were created from data where cells were exposed to 20-40 mM acetic acid and 2-4% NaCl; the Weibull shape and scale parameters can be described such that

$$\hat{\alpha} = 3.41^{++} - 83.87^{++}\,acid - 5.36^{++}\,salt + 144.97^{+}\,acid \times salt \qquad (2.8)$$

$$\hat{\beta} = 0.98^{+++} - 382.42^{+}\,acid^{2} - 1.71^{+}\,salt + 56.43^{+}\,acid \times salt\,. \qquad (2.9)$$

The coefficient of determination for alpha and beta were $R^2_{alpha} = 0.99, R^2_{beta} = 0.98$ respectively, and parameters that were significant are denoted by one (P < 0.02), two (P <0.01), or three (P = 0.003) plus signs. Modeling the Weibull parameters revealed the significance of the measured inhibitory factors on the dependency of survival, yet there may be other explanatory variables, not examined in the current investigation, which are contributing to survival.

The intracellular pH was also determined for additional salt concentrations. The results for *E. coli* O157:H7 exposed to 1% and 3% NaCl with 10-40 mM are depicted in Figure 2.7. Increasing the protonated acetic acid concentration with either 1% or 3% NaCl decreased the intracellular pH for *E. coli* O157:H7 at pH 3.2. These results are consistent with the observations made for cells exposed to 2% and 4% salt. Experiments using higher concentrations of salt (6 and 8%) were attempted; however the silicone oil used for separating the pellet from the supernatant, was less dense than these high salt solutions.

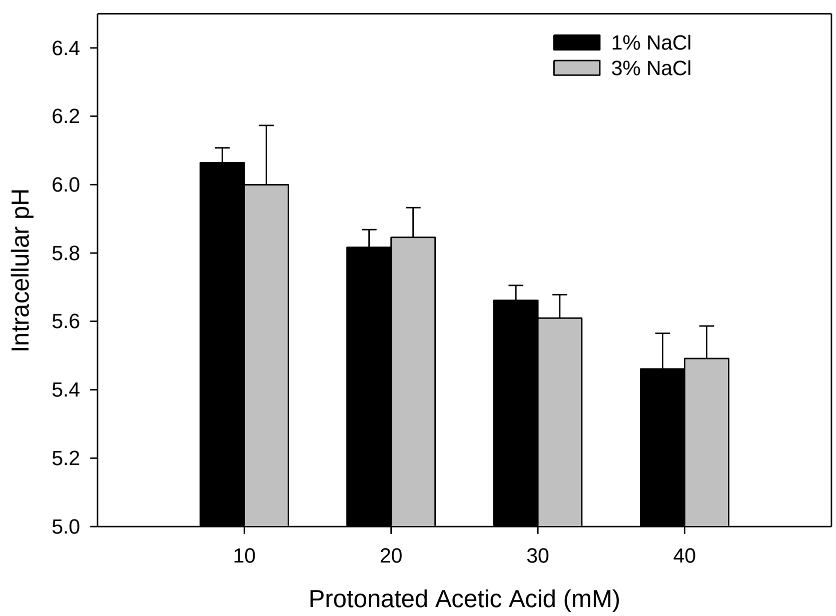

Figure 2.7 Intracellular pH as a function of protonated acetic acid concentration for *E. coli* O157:H7 exposed to 1% (black bars) or 3% (grey bars) NaCl at pH 3.2. Error bars represents the standard deviation of three independent replications.

3 Mathematical Modeling of the Intracellular pH of *Escherichia coli*

3.1 Introduction

The intracellular composition of a bacterial cell is complex. The cytoplasmic membrane is essential for maintain optimal internal conditions for metabolism and energy transduction (89). The cytoplasmic pH is an important aspect of bacterial cell physiology and is highly regulated (19). However, the regulation of intracellular pH for *Escherichia coli* (*E. coli*), particularly in an acidic environment, is not yet fully understood.

In this chapter a mathematical model was extended based on the work initiated by Dougherty et al. (60, 61) to predict the intracellular pH of *E. coli* in an acidic environment. This model is based on the chemical equilibrium established when the cell is exposed to a weak organic acid. However, simplifying assumptions are made because the intracellular cell composition is highly undefined. Sensitivity analyses were also performed to determine the effects of changing model parameters on the intracellular pH. As discussed in Chapter 2, there is significant correlation between intracellular pH and cell survival in the presence of acetic acid and NaCl, thus modeling the internal physiology can aid in predicting survival outcomes. Moreover, modeling the intracellular pH has practical use. Such models may eliminate the need for costly and time-consuming intracellular pH experiments which involve the use of radioactively labeled chemicals.

3.2 A Simple Mechanistic Intracellular pH Model

3.2.1 Chemical Equilibrium

The chemical equilibrium involved when organic acid is added to a buffer solution is considered here. A weak organic acid (HA) can be dissociated into an anion (A^-) and a proton (H^+) as written in the following chemical equilibrium

$$HA \longleftrightarrow H^+ + A^- .$$

In addition, the dissociation of the weak acid can be described as

$$K_a = \frac{[H^+][A^-]}{[HA]} \qquad (3.1)$$

where K_a is the dissociation constant of a weak monoprotic acid. Water, which dissociates into a proton and a hydroxyl ion (OH^-), at equilibrium can be written as

$$K_w = [H^+][OH^-] \qquad (3.2)$$

where K_w is the dissociation constant for water. It is worth noting that the dissociation constants depend on both temperature and ionic strength. These concepts will be further discussed in section 3.3.

3.2.2 Material and Methods

<u>*Intracellular pH Data Revisited*</u>

As explained in Chapter 2, the intracellular pH was obtained for *E. coli* O157:H7 cells subjected to 1%, 2%, 3% and 4% with acetic acid concentrations ranging from 10 to 40 mM. At each concentration there were 3 independent measurements taken; the results are presented in Figure 3.1.

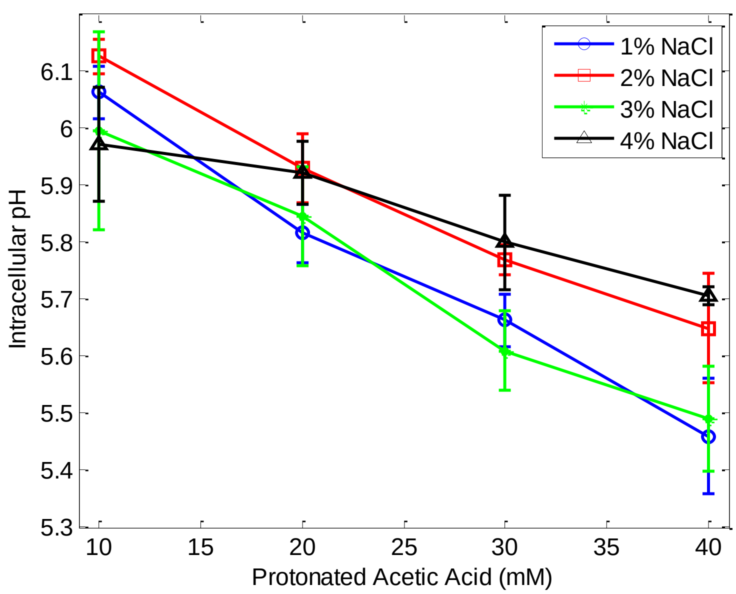

Figure 3.1 Intracellular pH as a function of protonated acetic acid for *E. coli* O157:H7 exposed to various concentrations of NaCl. Error bars represent the standard deviation of 3 independent replications.

3.2.3 Model Development

The model attempts to quantify the intracellular pH behavior as a weak organic acid (acetic acid) dissociates inside the cell. As presented in the above chemical rate equation, a weak organic acid can enter the cell and dissociate into an anion and a proton. The subsequent rate of dissociation is pH dependent. The protonated form of the acid can freely cross the membrane because of its uncharged state. However the anion cannot free cross the membrane unless coupled with another transport system. To accomplish this task of further understanding acid inhibition, one must consider mass balance of the organic acid. Thus, the total amount of the organic acid (C_{HA}) can be written as

$$C_{HA} = [A^{-}] + [HA]. \qquad (3.3)$$

The main hypothesis of this model is that there exists a charge balance of negative and positive ions in a buffer solution (the intracellular space) allowing for determination of pH.

Assumptions

In developing this model the following simplifying assumptions are made to describe the dissociation of a weak organic acid inside of a cell

(i) The intracellular composition of a cell is a weak monoprotic buffer solution, with an unknown composition.

(ii) The K_a of the weak organic acid in not a function of ionic strength.

If the intracellular charges sum to zero, then it is hypothesize the following model for determining the amount of protons inside the cell is appropriate

$$[H^+]+[Cation]=[B^-]+[A^-]+[OH^-]+[Anion] \qquad (3.4)$$

where $[Cation]$ is the total concentration of other positively charged ions (cations), $[B^-]$ is the buffer concentration, and $[Anion]$ is the total concentration of other negatively charged ions. To express equation (3.4) in terms of the proton concentration, equations (3.1) and (3.3) are combined to re-express the total concentration of organic acid inside the cell as

$$C_{HA}=[A^-]+\frac{[H^+][A^-]}{K_a}=[A^-]\left(1+\frac{[H^+]}{K_a}\right)=[A^-]\left(\frac{[H^+]+K_a}{K_a}\right). \qquad (3.5)$$

Solving equation (3.5) for $[A^-]$ results in

$$[A^-]=\frac{C_{HA}K_a}{K_a+[H^+]}. \qquad (3.6)$$

Similarly the buffer anion can be expressed as

$$[B^-]=\frac{C_{HB}K_b}{K_b+[H^+]} \qquad (3.7)$$

where C_{HB} is the total concentration of the buffer and K_b is the dissociation constant associated with this intracellular buffer.

The total ion concentration is regarded as the sum of cations and anions inside the cell, therefore

$$Ion_{Total}=[Cation]+[Anion]. \qquad (3.8)$$

The concentration of intracellular protons (and thus intracellular pH) can now be described by using the following model

$$[H^+]+[Ion_{Total}]=\frac{C_{HB}K_b}{K_b+[H^+]}+\frac{C_{HA}K_a}{K_a+[H^+]}+\frac{K_w}{[H^+]}, \qquad (3.9)$$

a cubic polynomial in $[H^+]$ with three unknown parameters. Table 3.1 summarizes the variable and parameter definitions for this simplified intracellular proton determination model.

Table 3.1 Simplified intracellular pH model parameters and variables.

Variable/Parameter	Description	Value	Range or value
$[H^+]$	Proton Concentration	Predicted variable (unknown)	10^{-7} to 10^{-5}
$[Ions_{Total}]$	Total Ion Concentration	Unknown parameter	0.2 to 1
$[C_{HB}]$	Total Buffer Concentration	Unknown parameter	0.2 to 1
$[K_b]$	Buffer dissociation constant	Unknown parameter	10^{-2} to 10^{-14}
$[C_{HA}]$	Total Organic Acid Concentration	Known variable	0 to 0.45
K_a	Organic Acid Dissociation constant	Known parameter	$10^{-4.76}$ (acetic acid)
Kw	Water Dissociation constant	Known parameter	10^{-14}

3.2.4 Methods

At each acid concentration, a Tukey test for multiple pairwise comparisons between mean intracellular pH values was performed for the 4 NaCl percentages at the alpha = 0.05 significance level. The analysis revealed no significant differences in the mean intracellular pH values among the 4 levels of NaCl when cells were exposed to 10 and 20 mM of acetic acid. For cells exposed to 30 mM of acetic acid, a 3% NaCl treatment was significantly different from cells exposed to 2% and 4% NaCl. For cells exposed to 40 mM acetic acid, the mean intracellular pH for cells exposed to 1% NaCl was significant different from the 4%

NaCl treatment. It is reasonable to assume that there is no significant among all the levels of NaCl used in this study. With this assumption, at each acid concentration the data is averaged over the levels of NaCl in this section.

Cross-validation is a method used to test how well a model will fit to a new dataset. As reviewed by Shao (147) the data is split into subgroups, those that are used to refine the parameters of the model and those that are used to determine how well the model fits. This is repeated for each subgroup of the data. The purposed models are then compared using the usually techniques (e.g. mean square error (MSE) or R^2).

The dataset consist of intracellular pH values for cells subjected to 1%, 2%, 3% and 4% salt and either 10, 20, 30 or 40 mM of acetic acid. At each salt/acid combination there are 3 independent replicates; thus there is a total of 48 measured intracellular pH values. Cross validation was performed three times and the data was split by replications where using all levels of salt, two replications were used to train the model and the other replication was used to validation model predictions. Subgroup A consisted of the first and second series of independent replications. Subgroup B consisted of the first and third independent replicates, and the second and third independent replicated comprised subgroup C. For all cross-validations, the unknown parameters as listed in Table 3.1 are estimated using nonlinear regression in MATLAB (nlinfit function) which assumes an additive error structure.

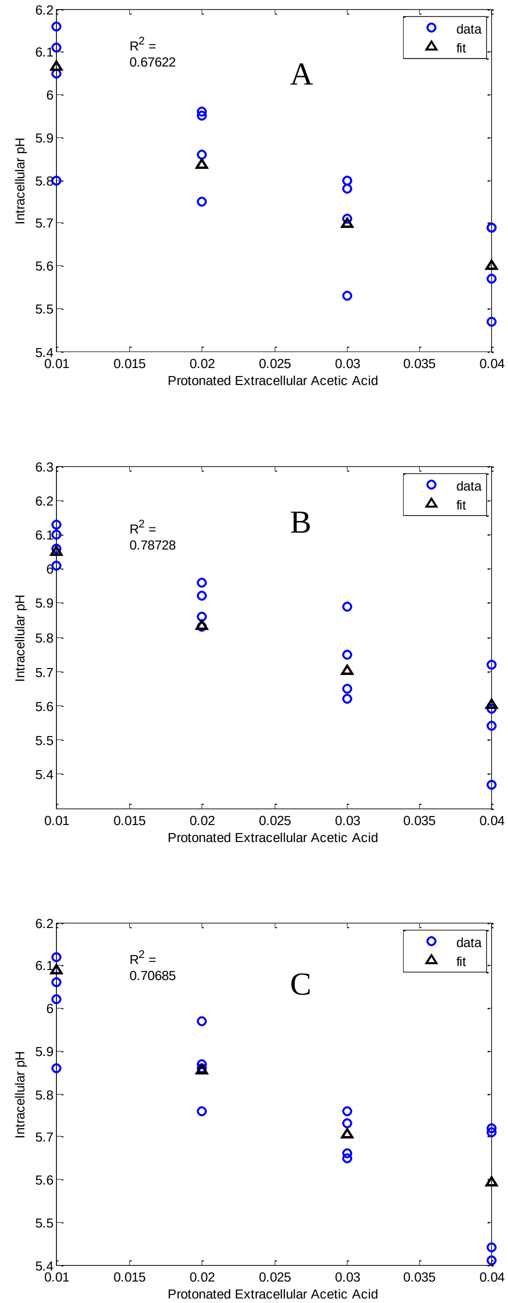

Figure 3.2 Cross validation with removing 1 replication of the entire dataset with 4 salt levels. The other 2 replications are used to train the model. In (A) replicate 2 was removed, in (B) replicate 3 was removed and in (C) replicate 1 was removed.

3.2.5 Results and Discussion

From the analysis obtained in the cross-validation method, the dataset which contained the independent replicate series 1 and 3 was able to predict independent replicate series 2 with the smallest residual sum of squares error when compared to splitting the data by the other defined subgroups. The parameters from the fit of independent replicate series 1 and 3 and their associated 95% confidence intervals are detailed in Table 3.2.

Table 3.2 Predicted parameters values for determining intracellular pH of *E. coli* O157:H7 and the 95% confidence interval (CI) associated with each parameter estimate.

K_b (95% CI)	C_{HB} (95% CI)	$Ions_{Total}$ (95% CI)
6.21(5.58,6.99)	0.35 (0.17, 0.48)	0.39 (0.03,0.60)

<u>Parameter Sensitivity</u>

Figure 3.3 illustrates the how responsive the intracellular pH determination is to changes in the estimated parameters for different acid concentrations. The most sensitive parameter appears to be the buffer dissociation constant K_b. For all levels of protonated acetic acid, decreasing K_b by 20% produced a near 1-log change in intracellular pH. On the other hand, the total buffer concentration (C_{HB}) appears to be the least sensitive parameter governing this system and perturbations in this parameter did not change with increasing protonated acid concentration.

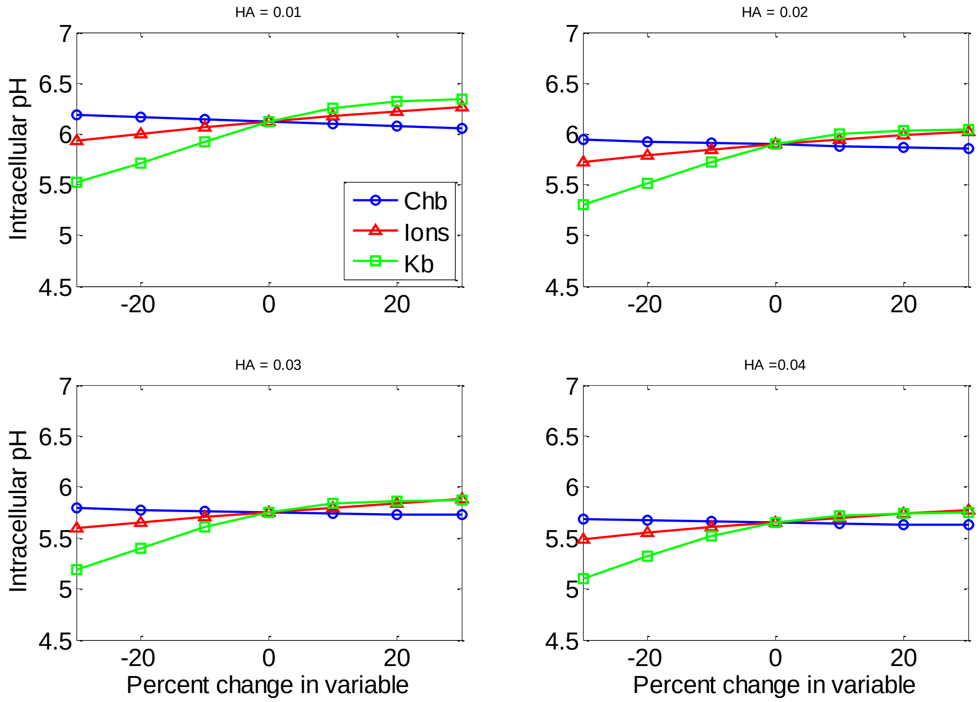

Figure 3.3 Sensitivity of intracellular pH model parameters with respect to increasing concentrations of protonated acetic acid.

Model Comparison

To assess whether this mechanistic model provides a better description of the intracellular pH than a linear model in acid concentration, the following regression model was introduced

$$pHin = r_0 + r_1[HA]. \qquad (3.10)$$

All parameters in this linear model (equation (3.10)) were statistically significant ($P < 0.0001$). The coefficient of determination for this model was 0.7161. Additional linear regression models were also considered, (e.g. include the main effects of salt and an interaction between salt and acid) however the additional model parameters were not statistically significant at the alpha = 0.05 level. A comparison of the fits of the simplified intracellular pH model and the linear model describing intracellular pH is illustrated in Figure 3.4.

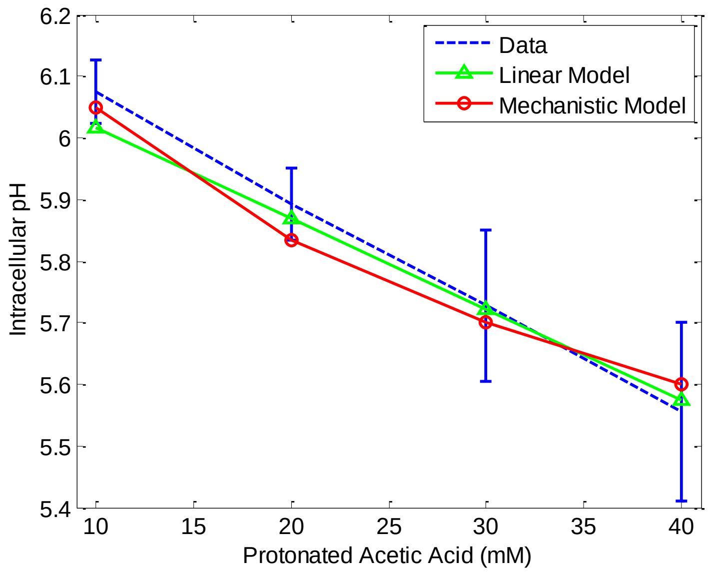

Figure 3.4 Predictions of the intracellular pH using the simple mechanistic intracellular pH model and a linear model for describing the decrease in intracellular pH as a function of the protonated acetic acid.

The simple mechanistic intracellular pH model presented here was able to describe the intracellular pH of *E. coli* O157:H7 pH when cells were exposed to varying concentrations of acetic acid. Assuming that the intracellular matrix of the cell behaves as a monoprotic buffer and that the pK_a of acetic acid does not depend on the ionic strength, the simple mechanistic model results in a better description of the intracellular pH as a function of acid ($R^2 = 0.7873$) than a linear model as a function of acid ($R^2 = 0.7161$). These assumptions may be very limiting, thus in section 3.3 the model assumptions are re-examined.

3.3 Modifying the Mechanistic Intracellular pH Model

3.3.1 Activity Coefficients

In the previous section, the contribution of ionic strength to the pK_a constant was ignored. This was a reasonable assumption because in at least two instances, at the same concentration of acetic acid, no significant differences in mean intracellular pH values were found at NaCl levels. Therefore increasing the ionic strength, which reflects the increase in NaCl concentration, did not affect the resulting intracellular pH. However, is this assumption truly reasonable? From the survival data it was seen that for more than 20 mM of acetic acid, increasing the salt concentration decreased the survival. If intracellular pH is truly correlated with survival, than increasing the salt concentration should in essence decrease the intracellular pH.

An activity coefficient can be thought of as a salting out factor which accounts for the deviations in ideal laws, which assumes that each particular behaves independently of any other in electrolyte solutions. By assuming that ions are point charges in a continuous medium of dielectric constant equal to that of water, Debye and Huckel were able to derive the theoretical expression for the activity coefficients in dilute solutions (34). Based on the Debye-Huckel theory the following limiting law holds in a sufficiently dilute solution for any completely dissociated electrolyte

$$-\log \gamma_{\pm} = A z_{+} z_{-} \sqrt{I} \,. \tag{3.11}$$

Here $\gamma_{\pm}$ is the geometric mean activity coefficient of the two ions, $z_{+}z_{-}$ are the charges of the two ions, and A is a constant that depends on the absolution temperature and the dielectric constant of the solvent (ε_d) such that

$$A = 1.825 \times 10^6 (\varepsilon_d T)^{-3/2} \tag{3.12}$$

at 25°C in water (34). In addition, the Davies extended the Debye-Huckle law to include spherical charges of ions of finite size instead of point charges as in the Debye-Huckle law. Now the mean activity of two ions is described by

$$-\log \gamma_{\pm} = A z_{+} z_{-} \left(\frac{\sqrt{I}}{1+\sqrt{I}} - 0.2I \right). \tag{3.13}$$

To account for changes in the pK_a due to ionic strength, the definition of the dissociation constant (K_a) is now generalized to

$$K_a = \frac{[H^+]\gamma_{+}[A^-]\gamma_{-}}{[HA]\gamma_0} \tag{3.14}$$

where the γ_i 's are the activity coefficients which depend on factors such as temperature, salt content of the solution, and the concentration of ions in the solution (129). Taking the logarithm of both sides of equation (3.13) results in

$$pKa = pK_a^0 + \log \gamma_{+} + \log \gamma_{-} - \log \gamma_0 \tag{3.15}$$

where pK_a^0 is the pK_a of the acid at zero ionic strength. As described in Butler and Cogley (34), the Davies equation can be used to evaluate $\log \gamma_{+}$ and $\log \gamma_{-}$. Using the Davies equation, the following relationship was developed

$$pKa = pK_a^0 + (2)(0.51)\left(\frac{\sqrt{I}}{1+\sqrt{I}} - b'I\right) - b^*I \qquad (3.16)$$

where b' is the Davies coefficient and b^* is the ionic strength coefficient. Using equation (3.16), with $b' = 0.3$ and $b^* = 0$ the relationship between ionic strength and pK_a is illustrated in Figure 3.5. Increasing the ionic strength by 1 unit nearly decreased the pK_a value by 2 units (see Figure 3.5).

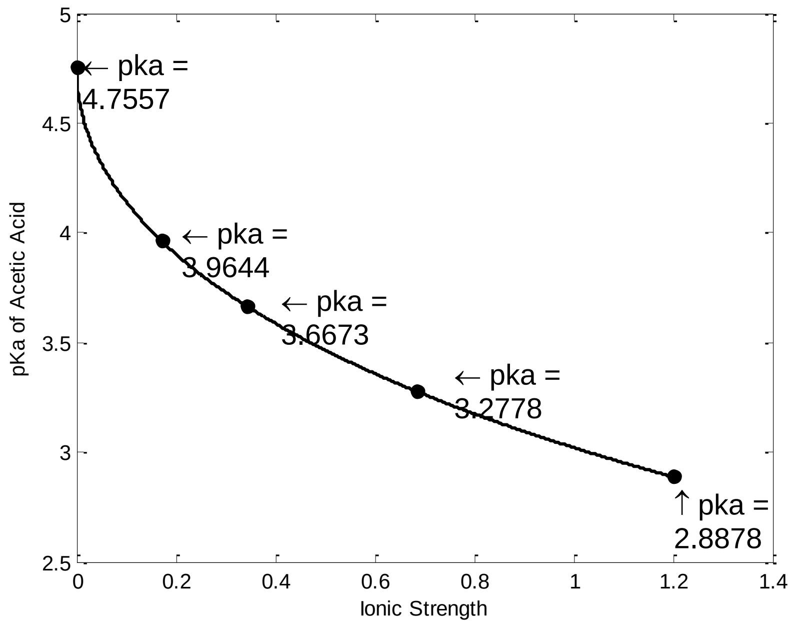

Figure 3.5 pK_a of acetic acid at 25°C as a function of ionic strength. The points represent the pK_a's at the ionic strengths of the extracellular buffers used in this study.

In this study the extracellular ionic strength is well defined and fixed experimentally, however the true ionic strength inside the cell is unknown. It has been documented that potassium is the major cation inside the cell and sodium regulates the growth of *E. coli*. Lo et al. (102) found that changing the external sodium concentration in the range of 1-85mM resulted in changes in the intracellular sodium concentration ranging from 5-14mM. In addition, Russell and Diez-Gonzalez (58) found that the intracellular potassium concentrations for *E. coli* O157:H7 ranged from 200 to 240 mM when the extracellular acetate concentration ranged from 0 to 250 mM. The intracellular ionic strength is this study will be estimated based on the predominant intracellular ions.

3.3.2 Results and Discussion

Assuming that the pK_a depends on the ionic strength, the pK_a was approximated using the Davies equation. The intracellular concentrations used to calculate the intracellular ionic strength based on the measured intracellular potassium and sodium concentrations detailed in Russell and Diez-Gonzalez (58) and Lo et al. (102) respectively. The maximum intracellular potassium concentration was assumed and the ratio between maximum intracellular and extracellular sodium concentrations was used to calculate the intracellular sodium concentrations in this study. Figure 3.6 compares the effect of including the pK_a dependence on intracellular ionic strength. As seen here and in Table 3.3, there was no improvement in the model predictions when the ionic strength was accounted for in the pK_a determination.

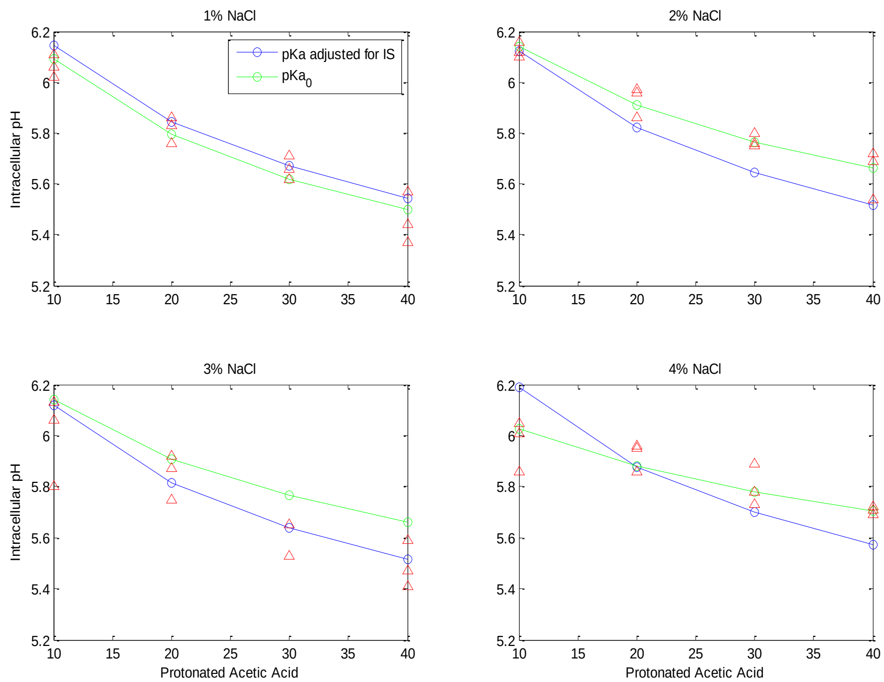

Figure 3.6 Intracellular pH calculations for the 4 levels of NaCl assuming that the pK_a is at 0 ionic strength or adjusted pK_a based on ionic strength.

Table 3.3 Comparisons of the mean square error (MSE) for models in which the pK_a was at zero ionic or adjusted based on the intracellular sodium and potassium concentration.

NaCl Percentage	MSE for Intracellular pH fit with pK_a adjusted for Ionic Strength	MSE for Intracellular pH fit with pK_a at zero Ionic Strength
1%	0.0066	0.0040
2%	0.0138	0.0026
3%	0.0128	0.0106
4%	0.0225	0.0045

From this study, we have shown that considering the effects of ionic strength on intracellular pH did not improve model estimates. However the analysis presented in this study are limited, because there is little information available on the concentration of the major ions inside the cell at pH 3.2. Further experiments will involve the use of inductively coupled plasma mass spectrometry to characterize the intracellular potassium, sodium and chloride concentrations. It worth noting that a complex buffer describing the intracellular matrix is still not determined here and is a suggested subject of future research.

4 Models for Describing *E. coli* Inactivation by Various Salts

4.1 The Effects of Salt on *E. coli* O157:H7 Survival in Acidic pH

4.1.1 Introduction

NaCl has been used as an antimicrobial in foods for thousands of years (154). The survival and growth of *E. coli* in foods depends on interaction of intrinsic (relating to the food) and extrinsic factors such as temperature, pH and water activity (31). Foods which are minimally processed (e.g. acidified vegetables) often present further challenges in inhibiting microbial growth. The simultaneous use of inhibitory measures such as pH, salts, organic acids, sugar and temperature (known as the hurdle theory) may rid processed vegetables products of possible food-borne pathogens. In this communication the effects of the type and concentration of salt on the survival of *E. coli* O157:H7 in a low-pH environment (pH 3.2) are compared.

The intracellular ion balance is essential for growth, motility ATP utilization, enzyme activity and other metabolic processes. It has been established that sodium (Na^+) and potassium (K^+) are essential to homeostasis. These ions are transported through the cell membrane via active and passive pathways. In addition, all living cells maintain a sodium concentration directed inward , thus cells have extrusion systems controlling Na+ uptake (85).

Antiporters are integral membrane proteins that allow the cotransport of two different species of ions of molecules in opposite directions across the cell membrane (76). It has been established that *E. coli* has two Na^+ antiporters. The NhaA and NhaB antiporters extrude Na^+ simultaneously with H^+ influx and this mechanism is dependent of the proton motive force (140). As reviewed by Karpel et al. (85) these Na^+/H^+ antiporters are specific to Na+ and Li^+; moreover there exist a third less antiporter which exchanges K^+, Li^+, Na^+ or Rb^+ for H^+. Another antiporter which has been implicated in intracellular pH homeostasis for *E. coli* is the K+/H antiporter which is essential for growth (86). It was shown that in the absence of net potassium, *E. coli* has limited capacity to raise intracellular pH (19).

A considerable amount of research has been devoted to studying the relationship between salt and acid tolerance/resistance for *E. coli* (e.g. 81, 140). Rowbury et al. (140) studied the sensitivity of *E. coli* exposed to NaCl after previously being grown in low-salt broths at pH 7. Their results indicate that on exposure to NaCl, *E. coli* (K-12) became highly acid sensitive. In addition, Richard and Foster (133) found that sodium and not potassium concentration coincides with decreased acid resistance and decreased expression of acid resistance genes. As described in Chapter 2, the synergistic effects of salt and acid on *E. coli* O157:H7 survival and intracellular pH maintenance was determined. The results indicate that for acetic acid concentration greater than 20 mM increasing the acetic acid concentration decreased both the viable cell count and intracellular pH. This chapter will not focus on the effects of weak acids however; it will examine the effects of salt type on intracellular physiology and survival in the presence of acid solution typical of acidified foods.

There is limited information available in the literature relating the cation contribution to survival of *E. coli* O157:H7. In the current study, the effects of Li^+, Na^+, K^+, Rb^+, Cs^+, Mg^{2+} and Ca^{2+} on killing kinetics at acidic pH are examined. The data presented here shows that KCl resulted in more killing of *E. coli* O157:H7 than NaCl in a similar environment. Moreover, it was demonstrated that the combined effects of KCl with NaCl did not produce a significant decrease in the intracellular pH when the concentration of KCl was increased from 10 t0 300 mM. The synergistic effects of salt and temperature on survival and intracellular pH will also be briefly discussed here.

4.1.2 Materials and Methods

Bacterial Strain and Growth Conditions

E. coli B241 (strain O157:H7, 28RC1, bovine isolate) were used in this study. The stock culture was stored at -80C in Luria-Bertani broth (Difco Labs, Detroit, MI.) supplemented with 20% glycerol and 1% glucose (Sigma Chemical Co., St. Louis, MO.). The culture was streaked from frozen stocks, plated on Luria-Bertani agar (Difco) supplemented with 1% glucose (LBG) and incubated at 37^{o}C for 24 hours. Colonies were transferred by loop inoculum and incubated statically in 50mL of LBG for 18 hours at 37^{o}C to induce acid resistance. Cultures were washed by centrifugation (25^{o}C, 10 min, 5 x 1000*g*) and finally resuspended in 2mL of sterile saline (8.5 g/liter NaCl). Cells were enumerated by plating on LBG agar using a spiral plater (model 4000, Spiral Biotech, Inc., Norwood, MA). After 24 hour incubation at 37^{o}C, colonies were counted using an automated plate reader (QCount, Spiral Biotech).

<u>Preparation of Salt Solutions</u>

The following salt solutions were used in this study: LiCl (Sigma), NaCl (Sigma), KCl (Sigma), RbCl (Acros organics, New Jersey, USA), CsCl (Cabot, Revere PA), MgCl2 (Sigma), CaCl2 (Sigma). In addition, all solutions contained 20 mM D-gluconic acid sodium salt (Sigma); a non-inhibitory buffer (23). The ionic strength (either 0.342 or 0.684) of the salt solutions was held constant as determined by using pHTools, a custom MATLAB routine as described in Dougherty et al., 2006 (61). The pH of the salt solutions was held constant at 3.2 by the addition of HCl and or NaOH.

<u>Intracellular pH</u>

Intracellular pH was determined using a radioactive acid distribution method (134). *E. coli* B241 were grown and washed as previously described. All radionuclides were obtained from the American Radiolabeled Chemicals, Inc. (St. Louis, MO.). For intracellular pH measurements cultures were incubated at 25^{o}C with a buffered salt treatment, [7-^{14}C]benzoate or [1,2-^{14}C]polyethylene glycol and $^{3}H_2O$ for 30 minutes. For determining the effects of salt and temperature on intracellular pH, cells were incubated with salt solutions containing either NaCl or KCl (ionic strength 0.342) at 10^{o}C or 30^{o}C for 30 minutes. After the incubation period samples were centrifuged through a silicone oil mixture (65:35 mix of Dow Chemical Co. type 550 and 556) in a microcentrifuge (13, 000*g*, 15 min) at 4^{o}C. An aliquot (100ul) of the supernatant was removed. Pellets were frozen for a minimum of 40 minutes or longer at -80^{o}C and then the pellets were cut from the bottom of the tube with dog nail clippers. Supernatant and pellet samples were added to a detergent solution of 50 mM

Tris Base (Sigma) + 0.5 % Tween 80 (Fisher Scientific, Pittsburgh, PA), followed by 5ml of scintillation fluid (Scintisafe from Fisher) in a 7ml scintillation vial (Perkin Elmer, Waltham, MA; cat # 6000167). Disintegrations per minute of the radionuclides were determined by using a scintillation counter (model LS600, Beckman Coulter, Inc., Fullerton, CA.). Intracellular volumes were determined from the difference between the DPMs in $^{3}H_2O$ and the [1,2-^{14}C]polyethylene glycol. Intracellular pH was determined from the intracellular/extracellular [7-^{14}C]benzoate distribution, the using the Henderson-Hasselbalch equation assuming an intracellular pK_a for benzoic acid of 4.21.

4.1.3 Results

Effects of Salt Composition on Survival

Figure 4.1 details the survival of *E. coli* O157:H7 exposed to several salts at pH 3.2. As seen here, the divalent salts conferred better survival than the monovalent salts at the same ionic strength. However, it is important remark that at the same ionic strength the concentration of divalent salts are ¼ the concentration of the monovalent salts. At ionic strength 0.342 NaCl and CsCl were found to be less inhibitory monovalent salts than LiCl, KCl and RbCl. At ionic strength 0.684, NaCl was a less inhibitory monovalent salt than LiCl, KCl, RbCl and CsCl. Over time, at ionic strength 0.342 $CaCl_2$ and $MgCl_2$ were not significantly different than the 20 mM gluconic acid solution. However at ionic strength 0.684, the $CaCl_2$ solution exhibited more killing than $MgCl_2$ and the control (20 mM gluconic acid).

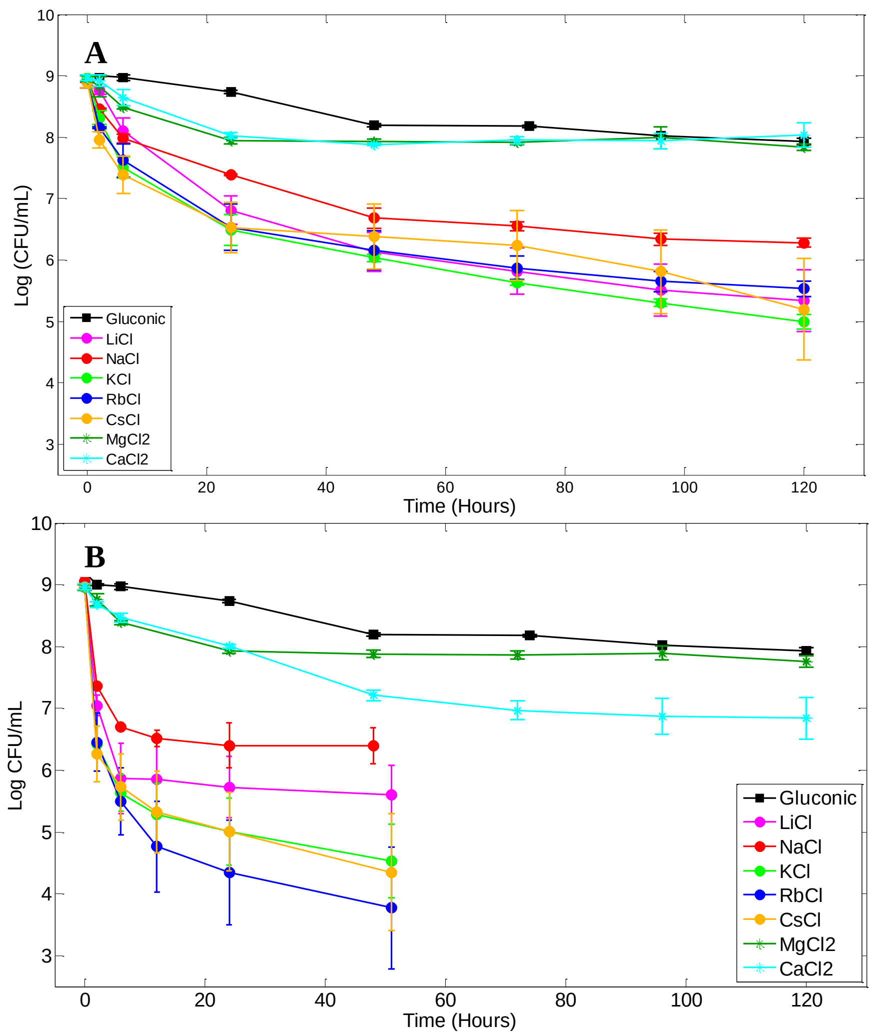

Figure 4.1 *E. coli* O157:H7 survival after exposure to various salts (LiCl, NaCl, KCl, RbCl, CsCl, $MgCl_2$, $CaCl_2$) at an ionic strength of 0.342 (A) or 0.684 (B). 20 mM gluconic acid (black square) is also shown here as a control. The concentration of the divalent ions are ¼ the concentration of the monovalent cations. The error bars represent the standard deviation of two or more independent replications and the trend lines are shown here as a visual aid.

Effects of Salt Composition on Intracellular pH

The intracellular pH was determined for *E. coli* O157:H7 exposed to LiCl, NaCl, KCl, $CaCl_2$ and $MgCl_2$ at ionic strengths 0.342 and 0.684 and RbCl at ionic strength 0.342. The intracellular pH could not be determined for cells exposed to CsCl and RbCl at ionic strength 0.684; for these solutions were denser than the silicone oil mixture used in our methods. The results indicate that for the monovalent salts, increasing the ionic strength decreased the intracellular pH by almost 1-log. This difference is not nearly as large for the divalent salts examined. Controlling for ionic strength, there was no significant difference in the mean intracellular pH values for cells exposed to LiCl, NaCl, KCl and RbCl.

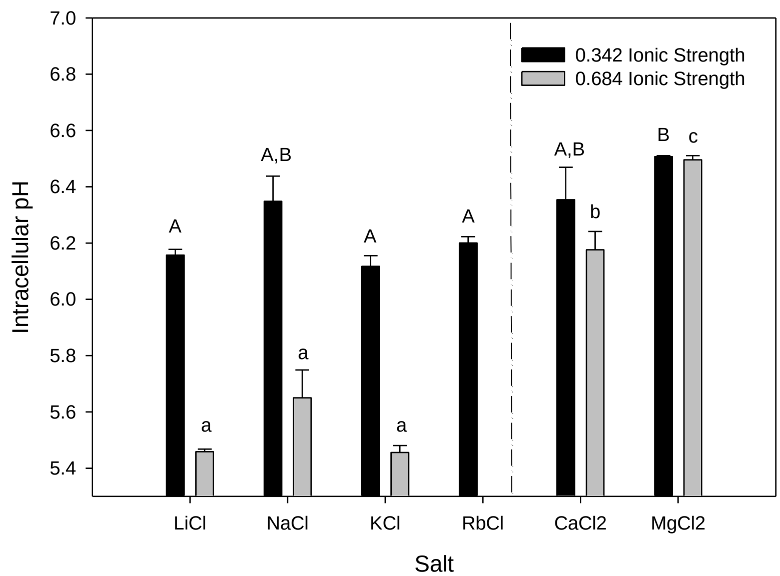

Figure 4.2 Intracellular pH for various salts at 2 levels of ionic strength at 25°C. Error bars represent the standard deviation from 2 independent replications. The same letters within the same ionic strength indicate no significant ($P < 0.05$) difference. The vertical line separates the monovalent and divalent salts which differ in concentration.

The effect of NaCl in combination with KCl on intracellular pH maintenance (Figure 4.3) was determined. Ionic strength of these KCl solutions was held constant at 0.342 with the addition of NaCl. Thus, as the concentration of KCl increases, the concentration of NaCl decreases. As seen in Figure 4.3, a 10-fold increase in the KCl concentration decreased the intracellular pH by almost 0.4 units, however subsequent increases in KCl concentration did not notably decrease the intracellular pH further.

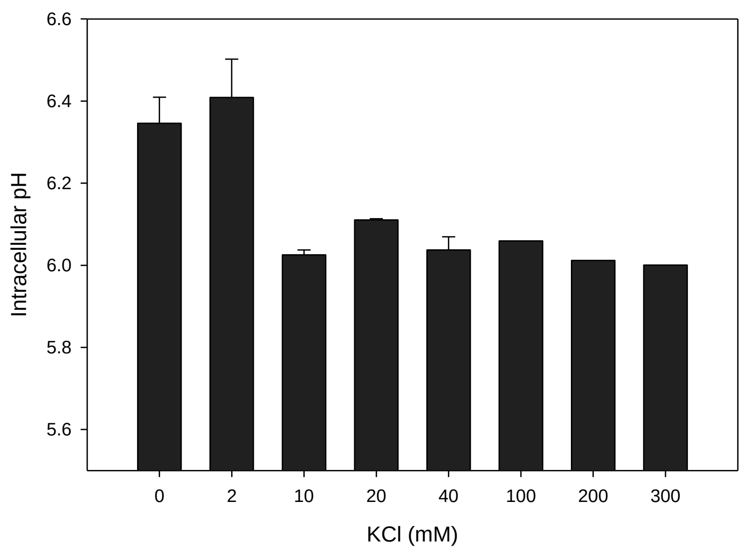

Figure 4.3 Intracellular pH for cells exposed to various concentrations of KCl. The ionic strength was held constant at 0.342 by the addition of NaCl. Error bars represent the means of 2 independent replicate experiments, however the 100-300 mM concentration experiments were performed once.

Combined Effects of Salt Composition and Temperature on Intracellular pH

A preliminary experiment assessed how temperature influences intracellular pH maintenance in *E. coli* O157:H7. The intracellular pH could be measured here at 30 minutes because there was no significant decrease in the number of viable cells after 1 hour (data not shown). Surprisingly there was no significant decrease in the intracellular pH when the temperature increased from 10^{o}C to 25^{o}C for cells subjected to NaCl or KCl at ionic strength 0.342. However, a 5 degree increase in temperature (from 25 to 30^{o}C) significantly decreased the intracellular pH by 0.6 and 0.4 units of the NaCl and KCl solutions respectively at ionic strength 0.342. Survival studies under the same conditions however revealed that for KCl treated cells, there was no significant decrease in the viable count in 24 hours in temperatures ranging from 10^{o}C to 30^{o}C (Figure 4.5).

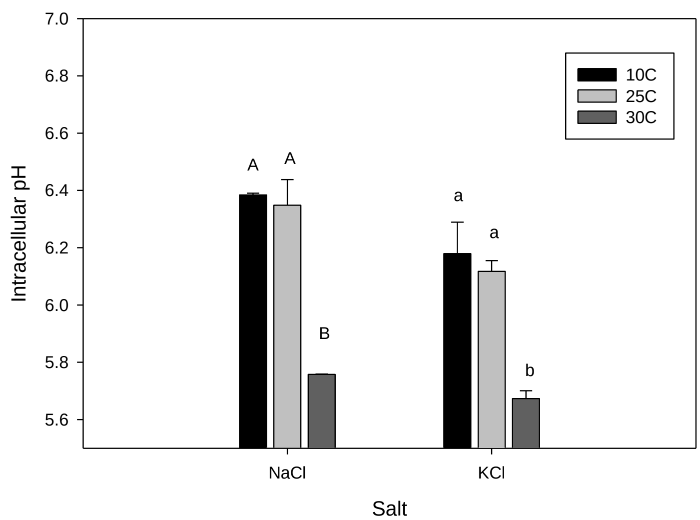

Figure 4.4 The effects on salt and temperature on the intracellular pH for *E. coli* O157:H7 at pH 3.2 and ionic strength 0.342. Error bars represent the standard deviation from 2 independent replications. The same letters within the same salt type indicate no significant (P < 0.05) difference in temperature.

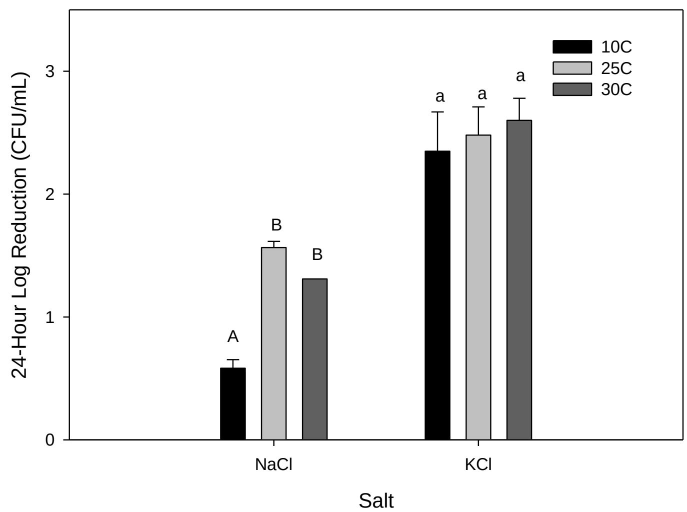

Figure 4.5 The effects of salt type and temperature on the survival of *E. coli* O157:H7 at pH 3.2, ionic strength 0.342. Error bars represent the standard deviation from 2 independent replications. The same letters within the same salt type indicate no significant ($P < 0.05$) difference in temperature.

4.1.4 Discussion

The results presented here support the idea that environmental salts confer different effects on survival and intracellular pH within the same ionic strength. The survival of *E. coli* O157:H7 in the presence of divalent salts was significantly greater than when exposed to monovalent salts at the same ionic strength. This may be solely due to the fact that the divalent salts are ¼ the concentration of the monovalent salts.

There was no apparent correlation between survival and intracellular pH mechanism after prolonged exposure to monovalent salts. As seen in Figure 4.1 (A) at ionic strength 0.342 and after 24 hours, NaCl exposure presents better survival than the other monovalent salts. Similarly there is evidence that NaCl exposure provides better survival than the other monovalent cations at ionic strength 0.684 after 6 hours. However, the intracellular pH determined at the same conditions revealed no significant differences in the mean intracellular pH values for NaCl and the other cations. This can be explained by the fact that the intracellular pH measurements for various salts at 2 levels of ionic strength at 25^{o}C were taken within the first 30 minutes of inactivation (Figure 4.2). Moreover, during this 30 minute period the survival patterns between the salt types are not significantly different.

A 10-fold increase in the KCl concentration decreased the intracellular pH by almost 0.4 units, however subsequent increases in KCl concentration did not notably decrease the intracellular pH further. This perhaps can be explained by fact that the intracellular potassium may be approaching a threshold intracellular pH concentration. At pH 5.6, the intracellular pH of *E. coli* O157:H7 is already on the order of 200 mM (58) and increasing the acetic acid concentration did not sustainably change the potassium concentration. Further research needs to examine the corresponding concentrations of cations inside the cell, given the concentrations of extracellular ions examined in this study. Such experiments may involve the using inductively coupled plasma mass spectroscopy techniques which can determine the parts per million of the cations in a sample.

A preliminary experiment on the effects of temperature on the intracellular pH showed that increasing the temperature from 25°C to 30°C significantly decreased the intracellular pH. Conversely, there was no significant decrease in the intracellular pH when the temperature decreased from 25°C to 10°C. This may be explained by the fact that at 10°C the cell membrane, which is comprised of lipid bilayer, is less fluid than at higher temperatures and is not allowing the salt to actively pass through the membrane. Unexpectedly, there was no decrease in the log survivors after 24 hour exposure to KCl when the temperature was increased from 25°C to 30°C. Further investigations along these lines may make clear the combined effects of salt (type and concentration) and temperature on the survival of *E. coli* O157:H7.

Of the four generally recognized as safe (GRAS) salts examined here (NaCl, KCl, CaCl2 and MgCl2), KCl provided the most killing for a given ionic strength (Figure 4.1). Previously, researchers have examined substituting NaCl with KCl in pickle products (11). Panel tasting revealed that the two sweet pickle products with KCl substituted for NaCl were almost as acceptable as the NaCl products. However the dill products with KCl substitutions reduced the overall acceptability of the product from "good" to "poor" when compared to products containing only NaCl (11). A more recent study by McFeeters and Fleming (106) showed that the flavor acceptability of dill pickles was rated higher ($P < 0.05$) than NaCl products when the NaCl concentration was reduced by 20% and replaced by KCl. The results presented here imply that food products with low-pH (3.2) which contain NaCl as the primary barrier against *E. coli* O157:H7 survival, substituting the KCl for NaCl may ensure safety.

4.2 Deterministic Inactivation Models

4.2.1 Introduction

Models for bacterial inactivation in the presence of NaCl have been widely investigated (e.g. (18)). Survival curves have shown to be sigmodial or semi-sigmodial with a shoulder and or tailing region, hence Gompertz and logistic models have shown to be applicable in such instances of inactivation (150). Additionally, the Weibull model (46, 127, 159) and Log-logistic models (18, 50, 101) have proven to adequately describe nonlinear inactivation behavior. These models can both be written as the cumulative distribution of inactivation that is stochastic in nature or as solutions to continuous deterministic differential equation. The latter is examined in this section where the survival data presented in section 4.1is used to compare and contrast 4 deterministic inactivation models: a Weibull, a Gompertz, a Logistic and a Log-Logistic. The results from these comparisons indicate that a three parameter nonlinear model provides a good description of *E. coli* inactivation by salt, however a two parameter nonlinear model is parsimonious and thus is preferred. The robustness of goodness of fit measures used in predictive microbiology namely the 'accuracy factor' and 'bias factor' are also compared here.

4.2.2 Weibull Model

The differential equation for the mean population size representing Weibull microbial inactivation can be written as follows

$$\frac{dN(t)}{dt} = -\frac{\beta}{\alpha}\left(\frac{t}{\alpha}\right)^{\beta-1} N(t)$$

with

$$N(0) = N_0 \tag{4.1}$$

where, $N(t)$ (Colony forming units per milliliter (CFU/mL)) is the number of bacteria alive at time t, α (in units of time) is the shape parameter, β (dimensionless) is the scale parameter and N_0 is the initial count in the microbial population. The solution to this separable differential equation (4.1) is the following

$$N(t) = N_0 e^{-\left(\frac{t}{\alpha}\right)^{\beta}} . \tag{4.2}$$

Microbiologists often work on a logarithm (base 10) scale resulting in the subsequent Weibull solution

$$\log(N(t)) = \log(N_0) - \frac{1}{\ln(10)}\left(\frac{t}{\alpha}\right)^{\beta} . \tag{4.3}$$

4.2.3 Gompertz Model

The Gompertz model for representing population dynamics was introduced by Benjamin Gompertz in 1825 (70). This model can be written as the following non-linear time invariant differential equation

$$\frac{dN(t)}{dt} = rN(t)\ln\left(\frac{K}{N(t)}\right) \tag{4.4}$$

with

$$N(0) = N_0 .$$

where r (time^{-1}) is the intrinsic decay rate and K (CFU/mL) is the microbial carrying capacity. Solving for $N(t)$ we arrive at

$$N(t) = Ke^{\ln\left(\frac{\mathrm{N}_0}{\mathrm{K}}\right)e^{-rt}} . \tag{4.5}$$

Alternatively, the Gompertz model can be written as the following time-varying linear differential equation

$$\frac{dN(t)}{dt} = a_G e^{-bt} N(t) \tag{4.6}$$

with

$$N(0) = N_0$$

where a_G (time^{-1}) is the initial decay rate and b (time^{-1}) is degradation rate of the decay rate. Continuing to solve for $N(t)$, we obtain

$$N(t) = N_0 e^{a_G/b} e^{-\frac{a_G}{b}e^{-bt}} . \tag{4.7}$$

Comparing equations (4.9) and (4.11), by allowing

$$K = N_0 e^{a_G/b} \tag{4.8}$$

and

$$r = b \tag{4.9}$$

the two forms of the solution agree. For fitting the data we will use the logarithm (base 10) of Gompertz solution represented in equation (4.5) namely

$$\log(N(t)) = \log\left(Ke^{\ln\left(\frac{N_0}{K}\right)e^{-rt}}\right). \tag{4.10}$$

4.2.4 Logistic Model

The well-known Verhulst-Pearl logistic differential equation for sigmodial population growth and decay was first introduced by Verhulst in 1838. The model is as follows:

$$\frac{dN(t)}{dt} = mN(t)\left(\frac{D - N(t)}{D}\right) \tag{4.11}$$

with

$$N(0) = N_0 .$$

where m (time^{-1}) is the natural decay rate and D (CFU/mL) is the carrying capacity (here, minimum attainable population size). Integrating equation (4.10) and solving for *N(t)* gives

$$N(t) = \frac{DN_0}{N_0 + e^{-mt}(D - N_0)} . \tag{4.12}$$

We will use the logarithm of the logistic model to fit the data as is the following equation

$$\log(N(t)) = \log\left(\frac{DN_0}{N_0 + e^{-mt}(D - N_0)}\right). \tag{4.13}$$

4.2.5 Cole Model

The log-logistic type model used to described inactivation of microorganisms was first described by Cole et al. (50) to illustrate the thermal inactivation of *Listeria monocytogenes*. The four parameter model for log survivors is logistic model (c.f. equation (4.11)) is written as

$$\log(N(t)) = \lambda + \frac{\omega - \lambda}{1 + e^{4\eta(\mu - \log_{10}(t))/(\omega - \lambda)}} \qquad (4.14)$$

with λ (CFU/mL) being the upper asymptote, ω (CFU/mL) the lower asymptote, μ (time) is the position of the maximum slope and η (CFU/mL/time) is the maximum slope. Statistical analyses for the deterministic models described above were carried out using the NLIN procedure of SAS software version 9.1 (SAS Institute Inc., Cary, NC).

4.2.6 Goodness-of-fit Criteria

MSE and R^2

The smaller the mean square error (MSE), the better the model is suited for describing the data (46), where the MSE is defined as

$$MSE = \frac{\sum (predicted - observed)^2}{n - P} \qquad (4.15)$$

where *n* is the number of observations and *P* is the number of parameters in the model.

The coefficient of determination (R^2) is a measure of the adequacy of the model to describe the data. The coefficient of determination can be defined in terms of the sum of squares total ($SST = \sum_{i=1}^{n}(observed_i - meanobserved)^2$) and the sum of squares error

($SSE = \sum_{i=1}^{n}(observed_i - predicted)^2$) such that

$$R^2 = 1 - \frac{SST}{SSE}. \qquad (4.16)$$

R^2 is interpreted as the proportion of the total observed variation due to variation in the predicted responses (131). The coefficient of determination ranges from 0 to 1.

AIC and SBC

The AIC is a measure of the goodness of fit of model and it depends on the number of parameters. The model with the lowest AIC is more suitable for the data in question. The Schwarz Bayesian criterion (SBC) is similar to the AIC however; the SBC takes more into consideration the sample size. Similarly, we choose models with the smallest SBC. Equations (4.17) and (4.18) defines the AIC and SBC respectively.

$$AIC = n\ln\left(\frac{SSE}{n}\right) + 2(P+1). \qquad (4.17)$$

$$SBC = n\ln\left(\frac{SSE}{n}\right) + (P+1)\ln(n). \qquad (4.18)$$

Accuracy Factor and Bias Factor

The accuracy factor concept was first described by Ross (136) and can be used to evaluate the performance of the model. It is defined as

$$A_f = 10^{\frac{\sum \left| \log_{10}(predicted/observed) \right|}{n}} \tag{4.19}$$

An accuracy factor can be explained as multiplicative factor to give an expected range of residuals (60). For example, a for an accuracy factor of 1.15 the expected range of residuals fall in the asymmetric interval (Predicted/1.15, Predicted*1.15). A large accuracy value implies a less accurate model and an accuracy value of 1 indicates a perfect fit of the model to the data (136).

The bias factor is the average ratio of the predicted and observed values and can be written as

$$B_f = 10^{\frac{\sum \log_{10}(predicted/observed)}{n}}. \tag{4.20}$$

A bias factor of 1 implies a perfect fit between the model and the observations, and hence it is unbiased. A bias factor less than one implies that the model under predicts (fail-dangerous) and a bias factor greater than one implies that the model over predicts (fail-safe).

Figure 4.6 illustrates the effects on the error assumptions on the determination of the accuracy and bias factor diagnostics. For an additive error assumption, increasing the error decreases the accuracy factor and increases the bias factor. Assuming the error is multiplicative; increasing the error increases the accuracy factor and decreases the bias factor.

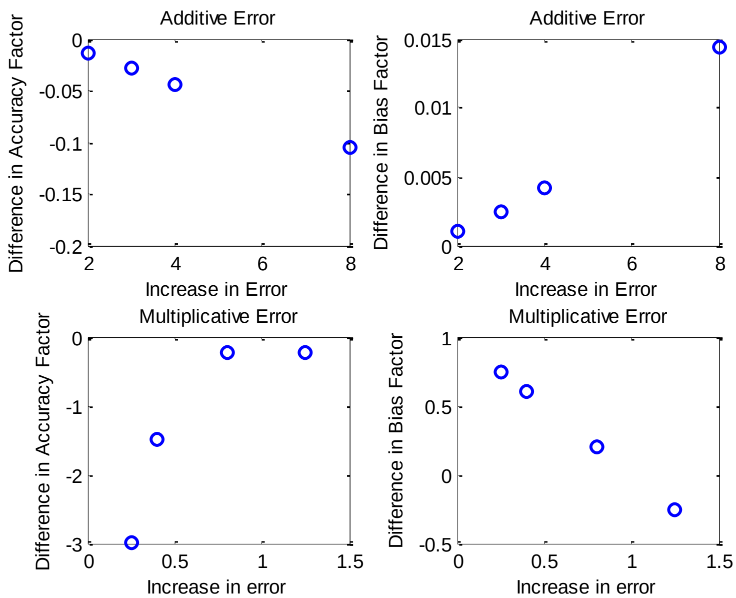

Figure 4.6 Modifications of accuracy and bias factors.

4.2.7 Results

Model Comparisons

The survival data (see section 4.1.3) was fit with a Weibull, Gompertz, Logistic or Cole model. For two salt solutions (NaCl and CsCl at ionic strength 0.342) the model fits are illustrated in Figure 4.7. The goodness-of-fit criteria for comparing these 4 model solutions are found in Table A. 1 (see the Appendix).

The MSE, R^2, AIC and SBC were determined by linear regression of the predicted values obtained in the fit to the true model equation. For the 14 salt solutions studied in section 4.2; based on the AIC criterion 11 were best approximated by using a Cole model, 2 were best approximated using a Logistic model (CsCl data) and 1 was best approximated using a Gompertz model ($CaCl_2$ data, ionic strength 0.684). When considering only the 2-parameter models, the Gompertz model was best fit for 7 salt solutions, the Logistic model was best for 4 salt solutions and the Weibull model was best fit for 3 salt solutions. An instance where the Cole model failed to describe the data is seen in Figure 4.7.

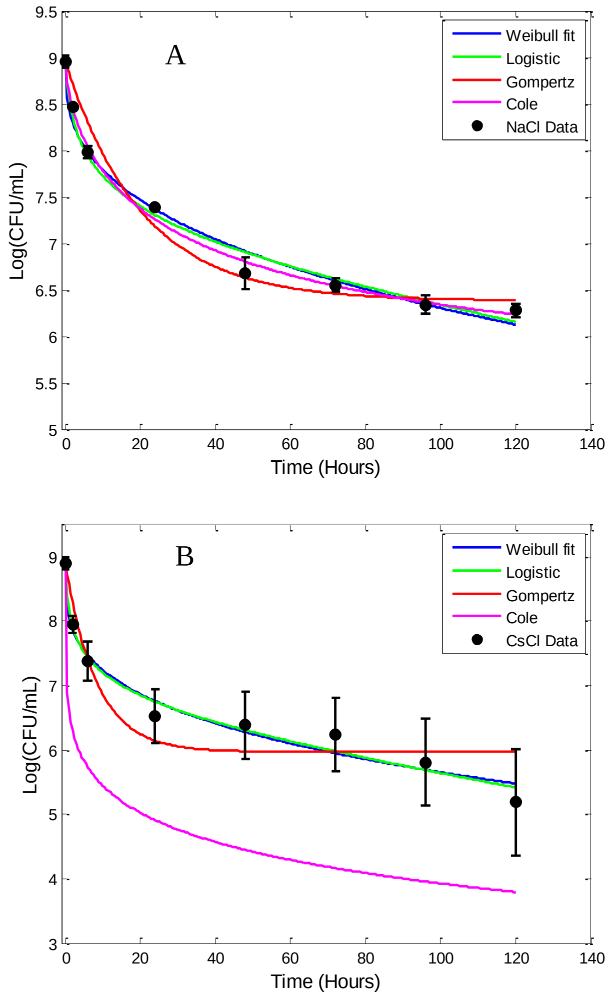

Figure 4.7 At ionic strength 0.342, model fits for NaCl (A) and CsCl (B) survival data. Error bars represent the standard deviation of 2 or more independent replicates.

To understand the distribution of the accuracy and bias factors 80,000 Weibull, Gompertz, Logistic and Cole predicted data points were generated based on the fit to the NaCl data (ionic strength 0.342). For $i = 1\ldots10{,}000$ and $t = 0, 2, 6, 24, 48, 72, 96, 120$; the data was created as follows

$$Weibull_{noise}(t,i) = \log(N_0) - \frac{1}{\ln(10)}\left(\frac{t}{\alpha}\right)^{\beta} + \varepsilon_{i,Weibull} \quad (4.21)$$

$$Gompertz_{noise}(t,i) = \log\left(Ke^{\ln\left(\frac{N_0}{K}\right)e^{-rt}}\right) + \varepsilon_{i,Gomperz} \quad (4.22)$$

$$Logistic_{noise}(t,i) = \log\left(\frac{DN_0}{N_0 + e^{-mt}(D - N_0)}\right) + \varepsilon_{i,Logistic} \quad (4.23)$$

$$Cole_{noise}(t,i) = \lambda + \frac{\omega - \lambda}{1 + e^{4\eta(\tau - \log_{10}(t))/(\omega-\lambda)}} + \varepsilon_{i,Cole} \quad (4.24)$$

where $\varepsilon_{i,Model} \sim N(0, \sigma_{Model})$ and σ_{Model} is the square root of the MSE obtained from a fit of the respective models to the NaCl (ionic strength 0.342) data. These data points where then fit to their respective originating models. The results are illustrated in Figure A. 1 and Figure A. 2 (see Appendix). Note that for clarity the bias factor for the Cole model is on a different scale than the Weibull, Gompertz and Logistic models. The accuracy factors generated were normally distributed and the Cole model produced the narrowest distribution of accuracy factors. The bias factors were all centered at 1 and the narrowest distribution was found with the Cole model. In addition to the calculated accuracy and bias factors, the residuals were also calculated. The observed residuals for the first 24 data points are displayed in Figure 4.8.

There is no clear pattern in the residuals for the models examined here, and the Cole model produced the smallest error.

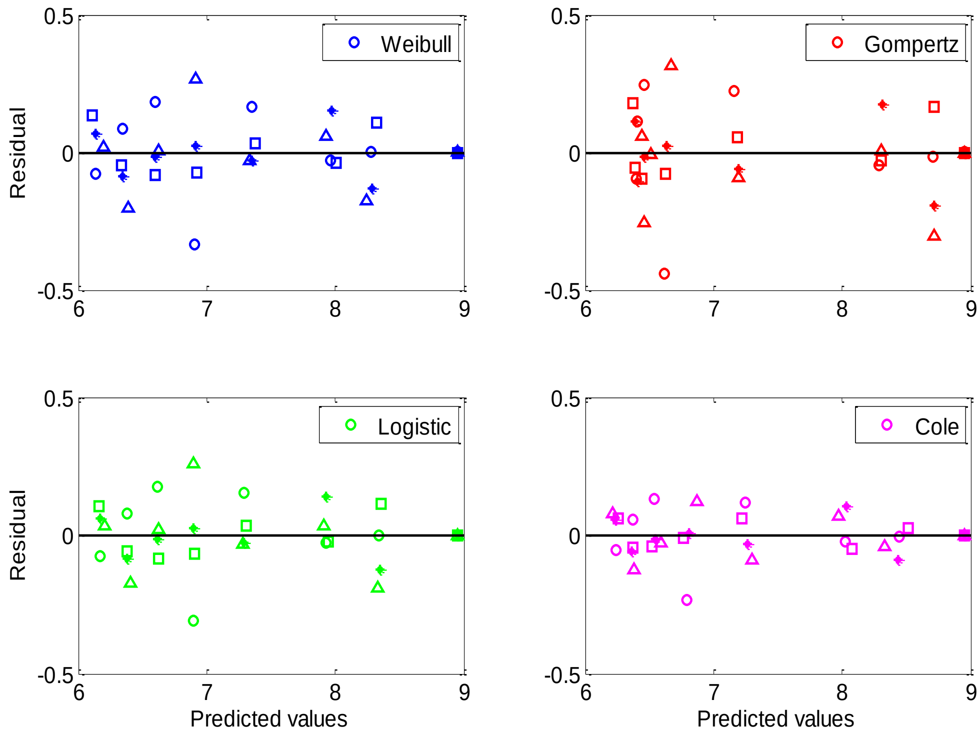

Figure 4.8 A sample (the first 24) of the residuals for data created using equations (4.21)-(4.24) and fitted with the Weibull, Gompertz, Logistic and Cole models. A total of 8 symbols for each time point represent a different model iteration.

Model Misspecification

The data was assumed to be modeled by Weibull equation and create a data set from the fit of NaCl (ionic strength 0.342) data. The Gompertz model, Logistic model and the Cole model is then used to fit this data set. The Logistic and Cole model produced almost indistinguishable fits while the Gompertz sigmodial curve was the worst approximation (Figure 4.9).

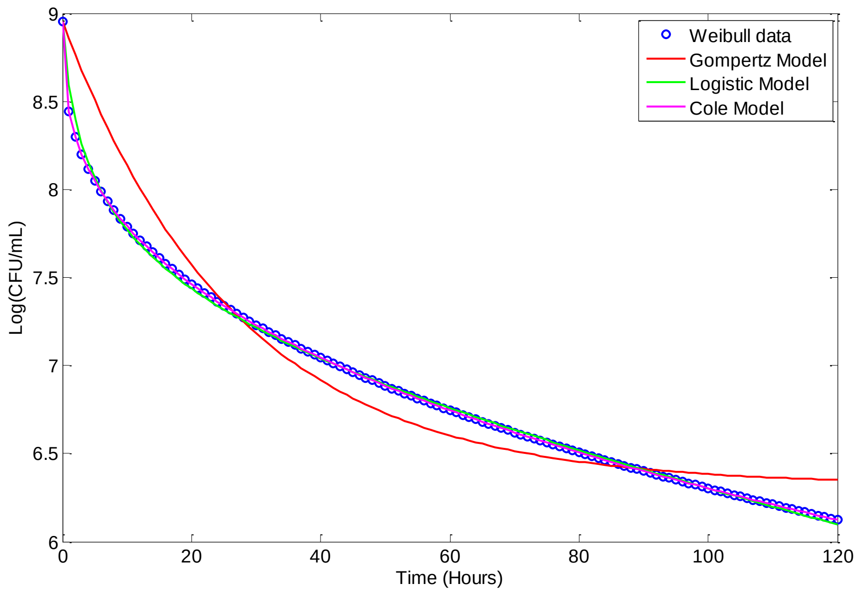

Figure 4.9 Model Misspecification. Weibull data (blue circles) was generated using a Weibull model based on the approximation of NaCl survival data at ionic strength 0.342. The generated Weibull data was then fit with a Logistic Model (red), Gompertz model (green) and a Cole model (magenta).

To assess how the accuracy and bias factors change when the model is misspecified, a data set of 80,000 Weibull observations was created as described by equation (4.42). The Gompertz, Logistic and Cole models were then used to approximate this dataset. The histograms of these accuracy and biased factors are seen in the Appendix (Figure A. 3 and Figure A. 4 respectively) based on the fit to the NaCl survival data at ionic strength 0.342. The Gompertz, Logistic and Cole accuracy factors means were all shifted to the right. The Gompertz model accuracy was the worse approximation of the data. Similarly the bias factors means were all shifted to the right, implying that the predictions and observations were dissimilar.

4.2.8 Discussion

Blackburn (18) used a log-logistic model to describe the thermal inactivation of *Salmonella enteritidis* and *E. coli* O157:H7 when exposed to several pHs, organics acids and NaCl. Their results indicate that a log-logistic approach provided a better description of the killing kinetics than compared to the used of first-order linear kinetics (18). The log-logistic modeling approach has also been applied to the survival of *Yersinia enterocolitia* (101). Chen and Hoover (46) compared the use of first order kinetics, log-logistic equation, a modified Gompertz equation and the Weibull model for describing the pressure inactivation of *Yersinia enterocolitia* in milk. The models were compared using the MSE, R^2, accuracy factors as goodness-of-fit criterion. Among these four models, the log-logistic model consistently provided the best fit to the all the survival curves; Weibull model was slightly worse but produced better fits than the modified Gompertz model (46). Moreover, Chen and Hoover (46) found that the Weibull model was beneficial for it allowed for predictions to be made through secondary models of the Weibull parameters as a function of the pressure and temperature. Models of the Weibull parameters based on the salt and acid concentration were already described in Chapter 2. The results presented here indicate that even though a pronounced shoulder is not present in the inactivation data, a log-logistic model is nonetheless appropriate. One can argue that the Cole log-logistic model maybe over-parameterizing the data, hence according to the principle of parsimony one would suggest using a Gompertz model to for a more appropriate description of *E. coli* inactivation in a salt environment.

Goodness-of-fit criterions have aided in model selection. Using the correlation coefficient and the root mean square error (RMSE), Xiong et al. (167) compared the use of a Baranyi model to the modified Gompertz model for describing the thermal inactivation for *Listeria monocytogenes* Scott A in infant formula. Their results indicate that Baranyi model was a better fit and robust model than the modified Gompertz model (167). The accuracy factor and bias factor concepts first developed by Ross (136), were posed to create a set of criteria in which a model can be said to have been validated. More specifically, his goal was to develop a set of indices in which can be readily interpretable and dimensionless so that models could be easily summarized and compared. Since their development the accuracy and bias factors have been widely employed (e.g. (7, 46)). However, distributions of these measures have not been examined or discussed previously. This study attempts to fill this gap (see histograms of accuracy and bias factors in the Appendix). The accuracy factor provides asymmetrical 95% confidence regions when the bias factor is close to 1. Additionally, when comparing the models (see Table A. 1 in the Appendix), we see here that the accuracy factor is not definitive and at times inconsistent with the other measures.

4.3 A Note on Stochastic Inactivation Models for Describing Single Cell Behaviors

It is increasingly important to describe the growth and survival of individual cells in a population. This is of particular interest when attempting to describe the survival of pathogenic microorganisms with low infectious doses. When using deterministic models, the residual error is often explained by the error in the parameter values. This unexplained error however, is not built into the model assumptions. Deterministic models can be obtained as the expected value of the stochastic processes describing the inactivation of individual cells (94). However, as noted by Baranyi (5) for growth models the underlying individual stochastic models cannot be retrieved from the deterministic stochastic models.

Stochastic models not only produce a mean population size over time but also give the variance and autocorrelation of the population size over time. While the population size is discrete, approximating the population size by a continuous variable and its differential equation is appropriate for the population sizes in this study. However, as mentioned above, for very small populations, a discrete stochastic model is more appropriate. In this section we discuss models with underlying stochastic assumptions used for describing the inactivation of *E. coli* O157:H7 in a NaCl solution. To describe the probability of that n cells are alive at time t, a binomial distribution of the success of life or death is used.

4.3.1 Weibull Distribution

The survivor function obtained from the Weibull distribution has been used to describe the inactivation of various microorganisms in a variety of food environments (e.g. (46, 127)). The Weibull probability density function is the following

$$f(t,\alpha,\beta) = \frac{\beta}{\alpha}\left(\frac{t}{\alpha}\right)^{\beta-1} e^{(-t/\alpha)^{\beta}} \tag{4.25}$$

where α and β are previously defined. The cumulative distribution function can be written as

$$F(t,\alpha,\beta) = 1 - e^{(-t/\alpha)^{\beta}} \quad . \tag{4.26}$$

The survivor function is the probability that the cells live. For the Weibull distribution the survivor function is

$$S(t,\alpha,\beta) = 1 - F(t,\alpha,\beta) = e^{-(t/\alpha)^{b}} \quad . \tag{4.27}$$

Other properties of the Weibull distribution are the hazard function (failure rate), the mean and variance functions which are described below

$$h(t,\alpha,\beta) = \frac{\beta}{\alpha}\left(\frac{t}{\alpha}\right)^{\beta-1} \tag{4.28}$$

$$Mean, \quad \mu_{Weibull} = \alpha\Gamma\left(1+\frac{1}{\beta}\right) \tag{4.29}$$

$$\text{Variance,} \quad {\sigma_{Weibull}}^{2} = \alpha^{2}\left[\Gamma\left(1+\frac{2}{\beta}\right) - \Gamma^{2}\left(1+\frac{1}{\beta}\right)\right] \quad . \tag{4.30}$$

The survival model is the same as in the solution to the deterministic equation model (c.f. equation (4.3)) which can be written as

$$\log(N(t)) = \log(N_0) + \log(1 - F(t, \alpha, \beta)) \tag{4.31}$$

which is equivalent to

$$\log(N(t)) = \log(N_0) - \frac{1}{\ln(10)}\left(\frac{t}{\alpha}\right)^{\beta}. \tag{4.32}$$

4.3.2 Multi-Target Model

Developed by Hermann and Horst (73), the Multi-Target model assumes that the each cell has q targets which are hit simultaneously. The times ρ_j ($j = 1\ldots q$) between the hits are independent, exponentially distributed variables with mean value $\rho = 1/\kappa$. The survival time of the i-th cell is written as

$$\tau_i = \max_{1 \le j \le q} \rho_j \tag{4.33}$$

and $F(t, q, \kappa) = (1 - e^{-\kappa t})^q$ where $q \ge 1$. The survival model is therefore described as

$$\log(N(t)) = \log(N_0) + \log(1 - F(t, q, \kappa)) \tag{4.34}$$

which is equivalent to

$$\log(N(t)) = \log(N_0) + \log(1 - (1 - e^{-\kappa t})^q). \tag{4.35}$$

This is generalization of the gamma distribution model used by Baranyi and Pin (6).

There are several ways to describe the probability that one cell is alive at time t. Here it is assumed that the number of cells alive at time t can be described by a binomial distribution. Statistical analyses for the probabilistic models described above were carried out using the NLIN procedure of SAS software (SAS Institute Inc., Cary, NC).

4.3.3 Results

The fit of the mean and variance of the Weibull and Multi-target hit stochastic models are shown in Figure 4.10 and Figure 4.11. The Multi-hit model was not able to explain the sigmodial behaviors of the mean NaCl data (Figure 4.11). We also note that neither the Weibull nor the Multi-hit model describe the values nor the shape of variances seen in the data when the underlying survival probability is described by a binomial distribution (Figure 4.11)

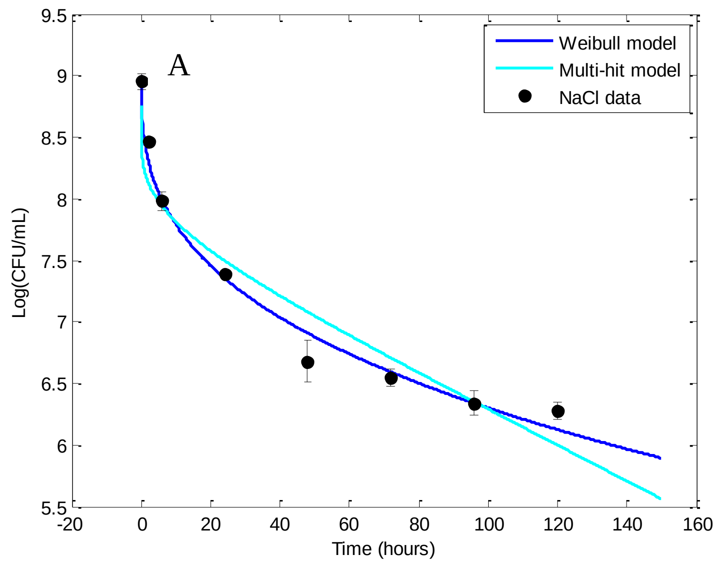

Figure 4.10 Cumulative Weibull distribution and Multi-hit model for describing the inactivation of *E. coli* O157:H7 exposed to a NaCl solution at ionic strength 0.342 at pH 3.2.

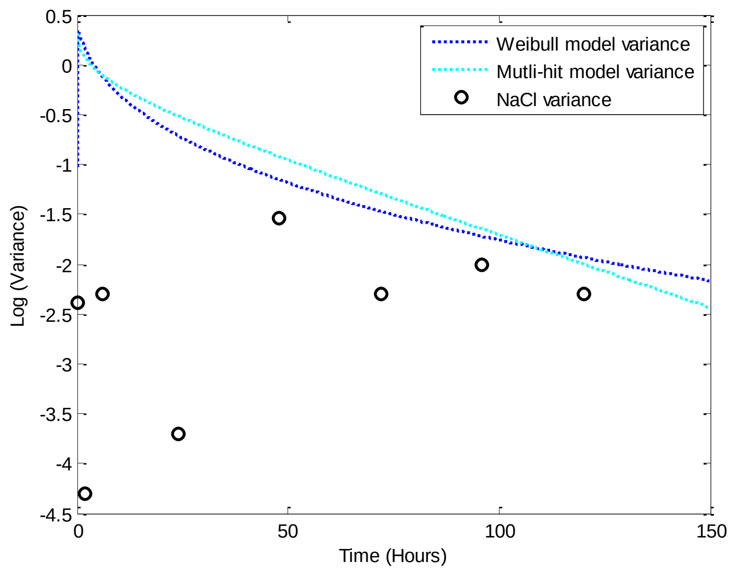

Figure 4.11 Variance estimates for the Weibull distribution and Multi-hit model assuming a binomial distribution for the probability that *n* cells are alive at time *t*.

4.3.4 Discussion

Using probabilistic models has the added advantage of modeling at the cellular level and may be useful for smaller population sizes. However, the stochastic models examined here were unable to estimate the temporal pattern of the variance observed in the data. The autocorrelation could not be measured over time because the constraints of the experimental methods used in this study (i.e. enumeration by plating). To address these concerns, future work may entail using a flow cytometer for counting single cells in a population.

Horowitz (75) used a probabilistic approach to stochastic birth-death model for describing microbial cell growth division and inactivation. As Horowitz (75) argues, their stochastic model may be useful for investigating growth and mortality of small populations where deterministic continuous models may be inappropriate. However, it is worth noting that the detection limit used in this investigation is on the order of 100 colony forming units per milliliter. Future work may elucidate the role of probabilistic models used for describing pathogenic bacteria inactivation such as *E. coli* O157:H7.

5 Autonomous and Non-autonomous Models for Describing Growth and Survival Behaviors

5.1 Introduction

Mathematical models used for population dynamics are capable of describing both growth and death solely by changing sign or parameter definitions. Examples of such models include the nonlinear Gompertz and Logistic models which were already presented in Chapter 4, to describe microbial inactivation. An autonomous model is a mathematical set of equations which is governed by independent variables and is an implicit function of time. Conversely non-autonomous models explicitly depend on time. In this chapter, autonomous and non-autonomous Gompertz and Logistic equations are presented and the Gompertz models are used to describe the tumor growth in rats and the chemical inactivation of *E. coli* O157:H7.

The Gompertz model has been used extensively to describe the growth of tumors (e.g. (95, 96, 103, 118, 119)). An early study by Laird (95) in 1964 showed the growth of a variety of tumors in mice, rats and rabbits was well described by using a Gompertz equation. Using a non-autonomous Gompertz growth equation Laird (96) suggest that when a tumor is implanted into a new host, it grows as though it is a community of cells derived from the host rather than as a population of independent tumor cells. The current trend for describing tumor growth is to use non-autonomous Gompertz growth models. However, the time-varying characteristic of this model may over or under estimate the tumor size. The objective of this chapter is to compare autonomous and non-autonomous assumptions where tumor growth data and *E. coli* survival data will be used to illustrate the differences. For ease to the reader, the Gompertz and Logistic models presented in Chapter 4 will be re-presented here.

5.2 Material and Methods

Tumor Growth Datasets

The tumor growth data used here was kindly provided by Simpson-Herren et al. (149); which is a subset of the data presented in their paper sorted by initial conditions. The data is for mammary adenocarcinomas (cancer of epithelia cells lining glandular tissue) which were induced by intra-gastric doses of DMBA (7,12-Dimethylbenz(a)anthracene) in female Sprangue-Dawley rats (153). DMBA is a widely used laboratory carcinogen which serves as a tumor initiator. The data is collected from two independent trails. In dataset 1, tumor weight (mg) is measured for 40 rats every 7 days over a period of 84 days. The initial tumor weight in dataset 1 is held constant at 63mg for all rats. In this study, dataset 1 was then modified to minimize missing data points and this new dataset consisted of 29 rats with tumors measured for 84 days (from here on it will be referred to as TG1). In dataset 2, tumor weight is measured for 20 rats every 7 days over a period of 84 days. The initial tumor weight in dataset 2 is held constant at 108mg for all rats. Similarly, dataset 2 was modified in this study to minimize missing data points and this new dataset consisted of 13 rats with tumors measured over 77 days (from here on it will be referred to as TG2).

E. coli O157:H7 *Inactivation Data*

E. coli O157:H7 inactivation data was taken from Chapter 4. Cells were exposed to a NaCl solution at an ionic strength of 0.342, pH 3.2 at 25^{o}C (refer to the materials and methods section 4.1.2. on page 80).

5.3 Mathematical Models

5.3.1 Gompertz Model

Autonomous Gompertz Model

As a review, the autonomous model describing growth and decay behavior can be written as the following non-linear time invariant differential equation

$$\frac{dN(t)}{dt} = rN(t)\ln\left(\frac{K}{N(t)}\right) \tag{5.1}$$

with

$$N(0) = N_0 .$$

where r (time^{-1}) is the intrinsic decay rate and K (CFU/mL) is the microbial carrying capacity. The solution to equation (5.1) is then

$$N(t) = Ke^{\ln\left(\frac{N_0}{K}\right)e^{-rt}} . \tag{5.2}$$

Non-autonomous Gompertz Model

The time-varying linear version of the differential equation for the Gompertz model is as follows

$$\frac{dN(t)}{dt} = a_G e^{-bt} N(t) \tag{5.3}$$

with

$$N(0) = N_0$$

where a_G (time^{-1}) is the initial decay rate and b (time^{-1}) is degradation rate of the decay rate. Continuing to solve for *N(t)*, results in

$$N(t) = N_0 e^{a_G/b} e^{-\frac{a_G}{b}e^{-bt}} . \tag{5.4}$$

As seen in Chapter 4, the solution to the non-autonomous Gompertz model is equivalent to the solution of the autonomous Gompertz model.

5.3.2 Logistic Model

Autonomous Logistic Model

The autonomous Logistic model can be written as follows

$$\frac{dN(t)}{dt} = mN(t)\left(\frac{D - N(t)}{D}\right) \tag{5.5}$$

with

$$N(0) = N_0$$

where m (time^{-1}) is the natural decay rate and D (CFU/mL) is the carrying capacity (here, minimum attainable population size). Integrating equation (5.11) and solving for *N(t)* gives

$$N(t) = \frac{DN_0}{N_0 + e^{-mt}(D - N_0)}. \tag{5.6}$$

<u>*Non-autonomous Logistic Model*</u>

Paralleling the presentation for the Gompertz models, here non-autonomous logistic equation is developed, with the same solution as (5.6) but now as a linear time-varying differential equation. The proposed model is

$$\frac{dN(t)}{dt} = \frac{cm}{N_0 e^{tm} + c} N(t) \tag{5.7}$$

with

$$N(0) = N_0$$

where c (CFU/mL) is the total change in population size. It is left to show is that the proposed differential has a solution and the solution is unique for $N(0) = N_0$.

Existence and Uniqueness Theorem

Let f and df/dt be continuous for all $(t, N(t))$ in a closed rectangle centered at (t_0, N_0). Then there exist a positive number h such that the initial value problem $$N(t)' - f(t, N(t)); \quad \mathrm{N(t_0)} = N_0$$ has a unique solution defined over the interval $(t_0 - h, t_0 + h)$. (120)

To be in accordance with the existence and uniqueness theorem, $f(t, N(t))$ is defined as

$$f(t, N(t)) = \frac{cm}{N_0 e^{tm} + c} N(t). \tag{5.8}$$

By taking the partial derivative with respect to $N(t)$

$$\frac{df(t, N(t))}{dN(t)} = \frac{cm}{N_0 e^{tm} + c}. \tag{5.9}$$

Notice that, $f(t, N(t))$ and $df(t, N(t))/dN(t)$ defined in equations (5.8) and (5.9) are continuous functions everywhere including $N(t) = N_0$; thus satisfying the existence and uniqueness theorem. Solving for $N(t)$ in equation (5.7) gives

$$N(t) = \frac{N_0(N_0 + c)}{N_0 + ce^{-tm}}. \tag{5.10}$$

By allowing $c = D - N_0$, the solution of the non-autonomous Logistic model is equivalent to the autonomous Logistic model.

5.4 Results

Time series data collected for tumors with initial weight of 63 or 108mg are shown in Figure 5.1 and Figure 5.2 respectively. There appears to be large variations in tumor weights between rats (denoted in the figure as a series number).

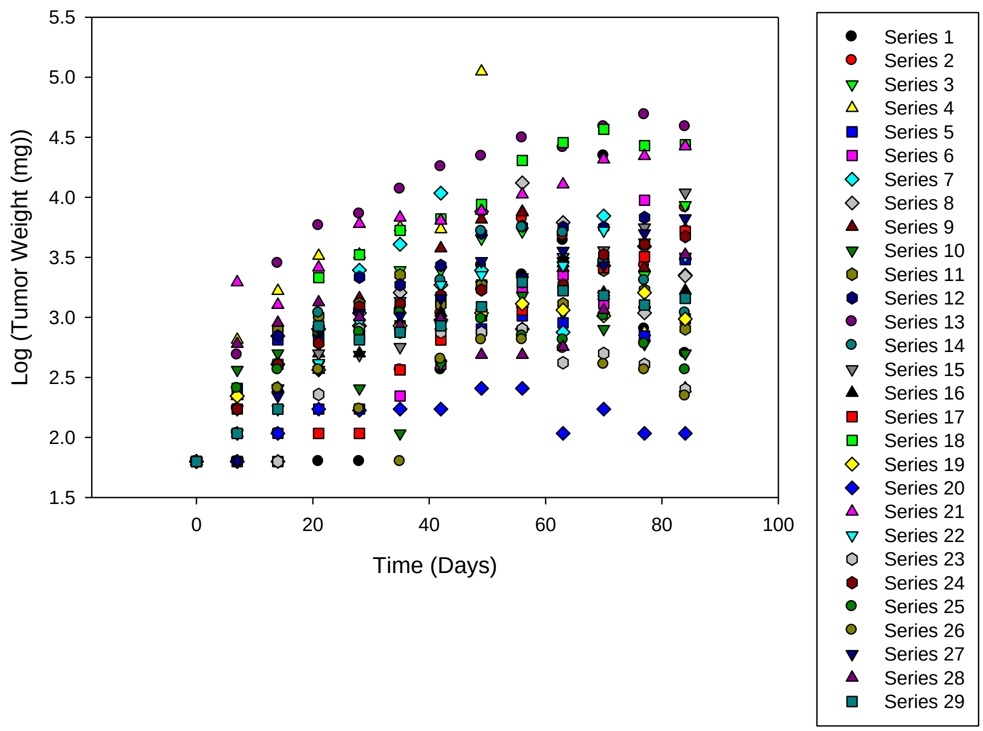

Figure 5.1 Log tumor weight time series for dataset 1 (TG1). The initial tumor weight for these data is 63mg.

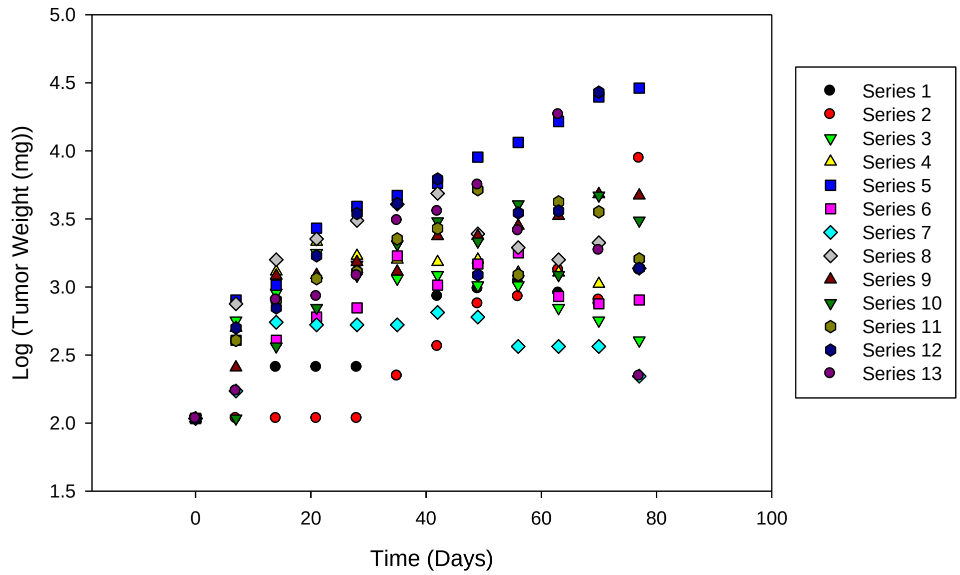

Figure 5.2 Log tumor weight time series for dataset 2 (TG2). The initial tumor weight for these data is 108mg.

Autonomous and non-autonomous Gompertz models were used to describe tumor growth and bacterial inactivation data. By construction the solution to the autonomous Gompertz model is equivalent to the non-autonomous Gompertz model. When initial conditions are changed to the mean value of the fourth (tumor growth) or second observation (*E. coli* inactivation), the autonomous Gompertz solution approaches the carrying capacity over time (red curves in Figure 5.3 and Figure 5.4). This is in contrast to the time-varying non-autonomous model which approaches a new asymptotic carrying capacity (blue curves in Figure 5.3 and Figure 5.4).

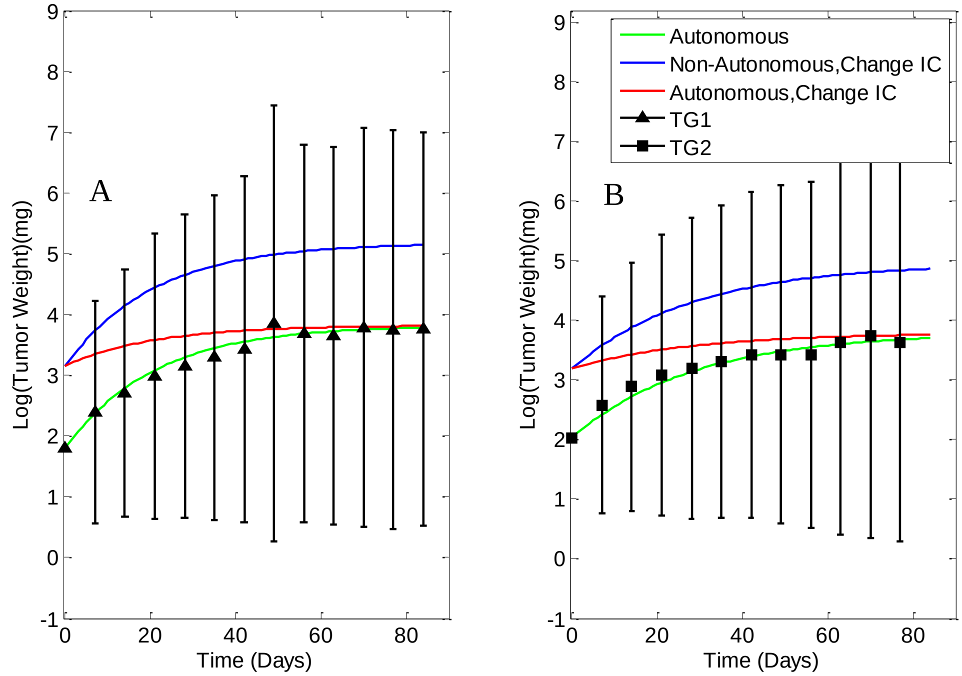

Figure 5.3 Comparison of autonomous and non-autonomous Gompertz fits of tumor growth datasets with different initial conditions (refer to materials and methods section 5.2). In (A) the initial tumor weight is 63mg and in (B) the initial tumor weight is 108mg. Green curves represent the autonomous Gompertz model fit. When the initial conditions are changed (see text) red curves represent the new autonomous Gompertz model fit and blue curves represent the new non-autonomous Gompertz fit.

To determine the ability of the purposed Gompertz model to fit a truly new dataset, TG1 dataset was used to estimate model parameters and these parameters where then used to fit the TG2 dataset. The results are shown in Figure 5.5 (B) for the autonomous Gompertz model in and Figure 5.6 (B) for the non-autonomous Gompertz model. Similarly, the TG2 dataset was used to determine model parameters and these estimated parameters where used in a Gompertz model to fit the TG1 datasets. The results of these fits are shown in Figure 5.5 (A) for the autonomous Gompertz model and in Figure 5.6 (A) for the non-autonomous Gompertz model.

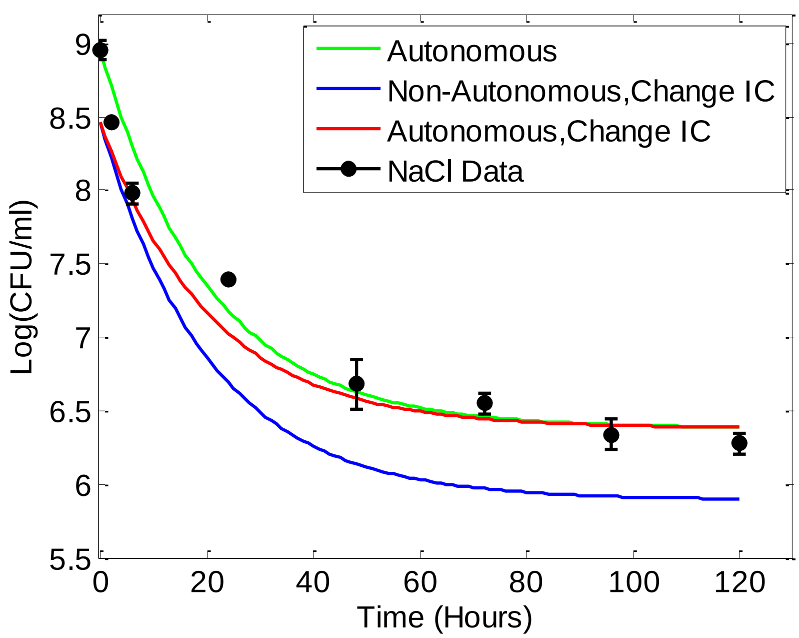

Figure 5.4 Comparison of autonomous and non-autonomous Gompertz solutions to fit *E. coli* O157:H7 inactivation when cells are exposed to NaCl at pH 3.2 and ionic strength 0.342 (circles). Green curves represent the autonomous Gompertz model fit. When the initial conditions are changed (see text) red curves represent the new autonomous Gompertz model fit and blue curves represent the new non-autonomous Gompertz model fit.

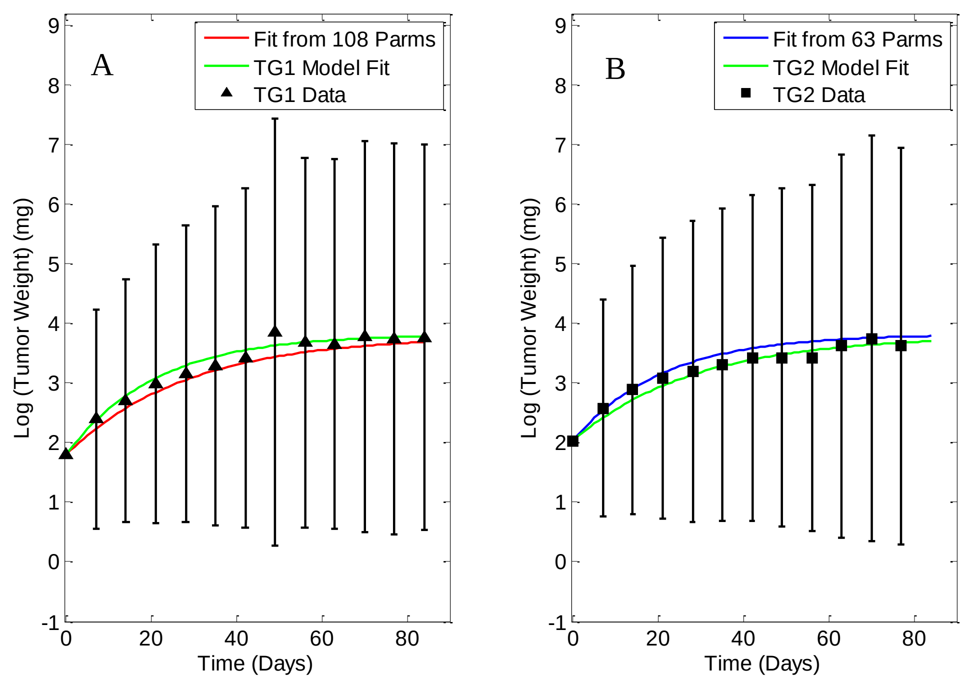

Figure 5.5 (A) Fit of the TG1 dataset with an autonomous Gompertz model whose parameters were estimated using TG2 data (red curve) shown with the original autonomous Gompertz model fit (green curve). (B) Fit of the TG2 data with an autonomous Gompertz model whose parameters were estimated using TG1 data (blue curve) shown with the original autonomous Gompertz model fit (green curve).

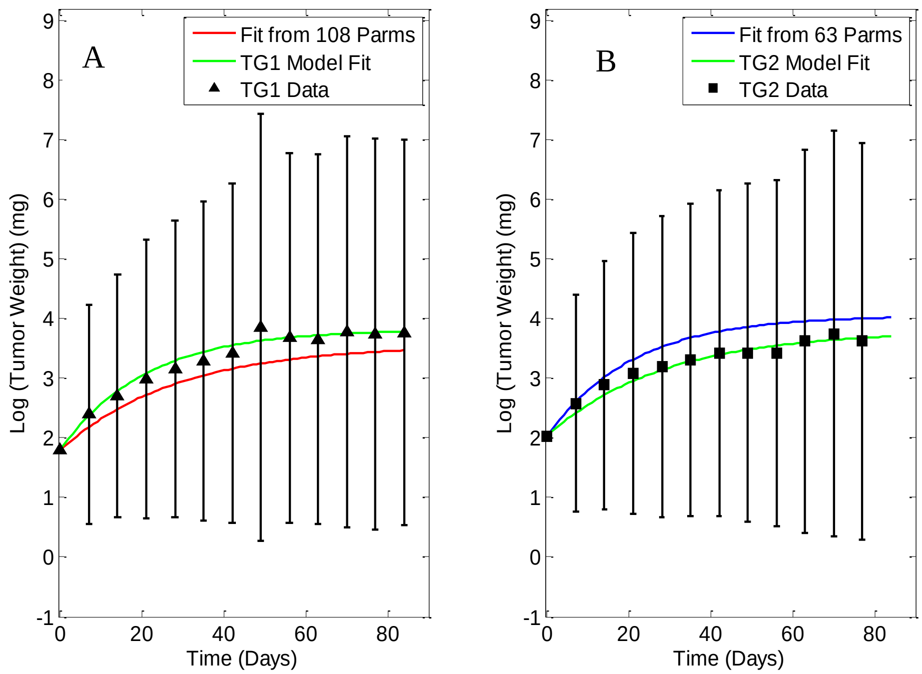

Figure 5.6 (A) Fit of the TG1 dataset with a non-autonomous Gompertz model whose parameters were estimated using TG2 data (red curve) shown with the original non-autonomous Gompertz model fit (green curve). (B) Fit of the TG2 data with a non-autonomous Gompertz model whose parameters were estimated using TG1 data (blue curve) shown with the original non-autonomous Gompertz model fit (green curve).

5.5 Discussion

Since the work purposed by Norton et al. (e.g. (119)) the literature has mainly focused on the use of non-autonomous Gompertz models to describe tumor growth. However, this investigation has shown that non-autonomous models may fail to predict new datasets. Although the solutions to the autonomous and non-autonomous Gompertz models were the same, when the initial conditions are changed the time-dependent non-autonomous model approach the same asymptotic limit as the autonomous solution (c.f. Figure 5.3 through Figure 5.5).

In Figure 5.3 the initial conditions are changed to the mean response at day 21. This presents a situation where one wants to assess the effectiveness of a cancer treatment. Given the weight of the cells before treatment, the autonomous Gompertz model solution can be used as a control to determine the pre-treatment carrying capacity. Assuming the cancer treatment produces a lower carrying capacity, the non-autonomous solution determines the magnitude of the decrease in tumor size. Conversely, the non-autonomous Gompertz solution results in an increased predicted carrying capacity, thus there is no way of determining the true efficacy of the cancer treatment. In addition, the models were assessed for their ability to predict new observations. A similar resultant is seen here, namely that the non-autonomous models fail to predict the maximum tumor weights (c.f. Figure 5.5 and Figure 5.6).

Unlike the tumor growth data, assuming a time-varying model is appropriate description for *E. coli* inactivation by NaCl may have severe consequences, since the variance among the data points are small (on the order of 0.00005 to 0.01). A model that produces a shift in the mean for the bacterial inactivation implies that the chemical used for inactivation is producing more killing that what is truly observed.

6 Conclusions

In this dissertation models were developed and examined for their ability to describe the intracellular pH and survival of *E. coli* O157:H7 in solutions similar to those found in acidified vegetable products. In Chapter 2, the Weibull model was used to describe the inactivation of *E. coli* in the presence of salt (NaCl) and acid at pH 3.2. This widely used model in field of predictive microbiology provided a good description of the killing kinetics. A secondary model to predict the survival relative to the acid and salt concentration was then created. Validation experiments were carried out and the model underestimated the time required to achieve a 5-log reduction. However, true validation experiments should be carried out in an acidified vegetable product inculcated with *E. coli* O157:H7. The analysis of the 5-log reduction time has revealed a significant correlation between survival and intracellular pH. As discussed in Chapter 2, the methods for determining the intracellular need to be re-evaluated. The silicone oil mixture used in this study could not separate the cell pellet from the supernatant when the density of these salt solutions was greater than that of the silicone oil.

In Chapter 3, a mechanistic model was created to describe the intracellular pH of *E. coli*. The model was able to describe the decrease in intracellular pH as the protonated acetic acid concentration increased. This simple model can be further extended to include a complex intracellular buffer composition. The effect of salt type and concentration on the survival and intracellular pH maintenance was observed in Chapter 4. Of the generally recognized as safe salts examined in this study, KCl produced more killing than NaCl solutions at the same ionic strength. However, the same trends were not seen for the intracellular pH values determined after a 30 minute exposure to the salt solutions. Moreover, no significant decrease in the intracellular pH was found when the temperature increased from 10^{o}C to 25^{o}C for cells subjected to NaCl or KCl at ionic strength 0.342. However, a 5 degree increase in temperature (from 25 to 30^{o}C) significantly decreased the intracellular pH. Temperature plays a critical role in controlling the survival of pathogenic bacteria. Therefore understanding the relationship between temperature, intracellular pH and survival has potential food safety implications. In addition, the relationship between the survival in acidic environments and changes in membrane potential needs to be determined.

Deterministic and stochastic models were assessed for their ability to describe the inactivation of *E. coli* in salt solutions. Of the four examined deterministic models, the Log-logistic model provided the best approximation of the data. However, because there are more parameters in this model than in the Weibull, Gompertz and Logistic models a model with fewer parameters was preferred. For the inactivation models examined here, there were inconsistencies in the good-of-fit criteria. The MSE, AIC and SBC factors were consistent in establishing a best fit model. The distributions of the proposed accuracy and bias factors established by Ross (136) as a standard measure in predictive microbiology for a “good” model, was shown here. This has not been previously examined.

A brief discussion of stochastic models for describing single cell behaviors, revealed that these models were not appropriate for the inactivation data measured in this dissertation. The mean survival behavior was able to be described with these cumulative distributions however the time-varying nature of the variance did not fit well to the observed variances. True stochastic models of microbial survival at the single cell level, requires that data is collected by methods other than plating such as the use of flow cytometry.

Chapter 5 re-examines the Gompertz and Logistic models ability to describe microbial inactivation data and tumor growth data. Comparing the results for the autonomous and non-autonomous Gompertz models showed that even though the solutions of these models are the same, when initial conditions are changed the time-varying model results in a new asymptotic limit. For modeling microbial inactivation, with variance on the order of 10^{-2}, care needs to be taken with model assumptions. When a time-varying Gompertz model is used, a change in the initial conditions implies that the chemical used for inactivation is producing more killing that what is truly observed.

REFERENCES

1. Ackers, M., B. E. Mahon, E. Leah, B. Goode, T. Damrow, P. S. Haes, W. F. Bibb, D. H. Rice, T. J. Barrett, L. Hutwagner, P. M. Griffin, and L. Slutsker. 1998. An Outbreak of *Escherichia coli* O157:H7 Infections Associated with Leaf Lettuce Consumption. The Journal of Infectious Diseases 177:1588-1593.

2. Albert, I., and P. Mafart. 2005. A modified Weibull model for bacterial inactivation. International Journal of Food Microbiology 100:197-211.

3. Armstrong, G., J. Hollingsworth, and J. Glenn Morris, J. 1996. Emerging Foodborne Pathogens: *Escherichia coli* O157:H7 as a Model of Entry of a New Pathogen into the Food Supply of the Developed World. Epidemiologic Reviews 18:29-51.

4. Axe, D. D., and J. E. Bailey. 1995. Transport of Lactate and Acetate Through the Energized Cytoplasmic Membrane of *Escherichia coli*. Biotechnology and Bioengineering 47:8-19.

5. Baranyi, J. 2002. Stochastic modelling of bacterial lag phase. International Journal of Food Microbiology 73:203-206.

6. Baranyi, J., and C. Pin. 2001. A Parallel Study on Bacterial Growth and Inactivation. Journal of Theoretical Biology 210:327-336.

7. Baranyi, J., C. Pin, and T. Ross. 1999. Validating and comparing predictive models. International Journal of Food Microbiology 48:159-166.

8. Baranyi, J., and T. A. Roberts. 1994. Review Paper A dynamic approach to predicting bacterial growth in food. International Journal of Food Microbiology 23:277-294.

9. Bell, B. P., M. Goldoft, P. M. Griffin, M. A. Davis, D. C. Gordon, P. I. Tarr, C. A. Bartleson, J. H. Lewis, T. J. Barrett, J. G. Wells, R. Baron, and J. Kobayashi. 1994. A Multistate Outbreak of *Escherichia coli* O157:H7- Associated Bloody Diarrhea and Hemolytic Uremic Syndrome From Hamburgers The Washington Experience. JAMA 272:1349-1353.

10. Bell, B. P., P. M. Griffin, P. Lozano, D. L. Christie, J. M. Kobayashi, and P. I. Tarr. 1997. Predictors of Hemolytic Uremic Syndrome in Children During a Large Outbreak of *Escherichia coli* O157:H7 Infections. Pediatrics 100:1-6.

11. Bell, T. A., J. L. Etchells, and L. H. Hontz. 1972. Low-sodium pickle products for modified diets. Journal of American Dietetic Association 60:213-217.

12. Besser, R. E., P. M. Griffin, and L. Slutsker. 1999. *Escherichia coli* O157:H7 Gastroenteritis and the Hemolytic Uremic Syndrome: An Emerging Infectious Disease. Ann. Rev. Med. 50:355-367.

13. Besser, R. E., S. M. Lett, J. T. Weber, M. P. Doyle, T. J. Barrett, J. G. Wells, and P. M. Griffin. 1993. An outbreak of diarrhea and hemolytic uremic syndrome from *Escherichia coli* O157:H7 in fresh-pressed apple cider. JAMA 269:2217-2220.

14. Beuchat, L. R. 2002. Ecological factors influencing survival and growth of human pathogens on raw fruits and vegetables. Microbes and Infection 4:413-423.

15. Beuchat, L. R. 1995. Pathogenic Microorganisms Associated with Fresh Produce. Journal of Food Protection 59:204-216.

16. Bhaduri, S. P. W. S., S. A. Palumbo, C. O. Turner-Jones, J. L. Smith, B. S. Marmer, R. L. Buchanan, L. L. Zaika, and A. C. Williams. 1991. Thermal destruction of *Listeria monocytogenes* in liver sausage slurry. Food Microbiology 8:75-78.

17. Bjornsdottir, K., F. Breidt Jr., and R. F. McFeeters. 2006. Protective Effects of Organic Acids on Survival of *Escherichia coli* O157:H7 in Acidic Environments. Applied and Environmental Microbiology 72:660–664.

18. Blackburn, C. d. W., L. M. Curtis, L. Humpheson, C. Billon, and P. J. McClure. 1997. Development of thermal inactivation models for *Salmonella enteritidis* and *Escherichia coli* O157:H7 with temperature, pH and NaCl as controlling factors. International Journal of Food Microbiology 38:31-44.

19. Booth, I. R. 1985. Regulation of Cytoplasmic pH in Bacteria. Microbiological Reviews 49:359-378.

20. Boyce, T. G., D. L. Swerdlow, and P. M. Griffin. 1995. *Escherichia coli* O157:H7 and the Hemolytic-Uremic Syndrome. The New England Journal of Medicine 333:364-368.

21. Brackett, R. E. 1999. Incidence, contributing factors, and control of bacterial pathogens in produce. Postharvest Biology and Technology 15:305-311.

22. Breeuwer, P., J. Drocourt, F. M. Rombouts, and T. Abee. 1996. A Novel Method for Continuous Determination of the Intracellular pH in Bacteria with the Internally Conjugated Fluorescent Probe 5 (and 6-)-Carboxyfluorescein Succinimidyl Ester. Applied and Environmental Microbiology 62:178-183.

23. Breidt, F., Jr., J. S. Hayes, and R. F. McFeeters. 2004. Independent effects of acetic acid and pH on survival of *Escherichia coli* in simulated acidified pickle products. Journal of Food Protection 67:12-18.

24. Breidt, F., Jr., J. S. Hayes, and R. F. McFeeters. 2007. Determination of 5-Log Reduction Times for Food Pathogens in Acidified Cucumbers during Storage at 10 and 25^{o}C. Journal of Food Protection 70:2638-2641.

25. Breidt, F., Jr., J. S. Hayes, J. A. Osborne, and R. F. McFeeters. 2005. Determination of 5-Log Pathogen Reduction Times for Heat-Processed, Acidified Vegetable Brines. Journal of Food Protection 68:305-310.

26. Breidt Jr., F. 2006. Safety of minimally processed, acidified and fermented vegetable products. CRC Press, Boca Raton, FL.

27. Brudzinski, L., and M. A. Harrison. 1998. Influence of Incubation Conditions on Survival and Acid Tolerance Response of *Escherichia coli* O157:H7 and Non-O157:H7 Isolates Exposed to Acetic Acid. Journal of Food Protection 61:542-546.

28. Brul, S., and P. Coote. 1999. Preservative agents in food: mood of action and microbial resistance mechanism. International Journal of Food Microbiology 50:1-17.

29. Buchanan, R. L. 1993. Developing and distributing user-friendly application software. Journal of Industrial Microbiology 12:251-255.

30. Buchanan, R. L., and S. G. Edelson. 1999. pH-Dependent Stationary-Phase Acid Resistance Response of Enterohemorrhagic *Escherichia coli* in the Presence of Various Acidulants. Journal of Food Protection 62:211-218.

31. Buchanan, R. L., M. H. Golden, and J. G. Phillips. 1997. Expanded models for the non-thermal inactivation of *Listeria monocytogenes*. Journal of Applied Microbiology 82:567-577.

32. Buchanan, R. L., M. H. Golden, and R. C. Whiting. 1993. Differentiation of the effects of pH and lactic or acetic concentration on the kinetics of Listeria monocytogenes inactivation. Journal of Food Protection 56:474-478.

33. Budde, B. B., and M. Jakobsen. 2000. Real-Time Measurements of the Interaction between Single Cells of *Listeria monocytogenes* and Nisin on a Solid Surface. Applied and Environmental Microbiology 66:3586-3591.

34. Butler, J. N., and D. R. Cogley. 1998. Ionic Equilibrium: Solubility and pH Calculations. John Wiley & Sons Inc., New York.

35. Buzrul, S., H. Alpas, and F. Bozoglu. 2005. Use of Weibull frequency distribution model to describe the inactivation of *Alicyclobacillus acidoterrestris* by high pressure at different temperatures. Food Research International 38:151-157.

36. Casey, P. G., and S. Condon. 2002. Sodium chloride decreases the bacteriocidal effect of acid pH on *Escherichia coli* O157:H45. International Journal of Food Microbiology 76:199-206.

37. CDC. 1995. *Escherichia coli* O157:H7 Outbreak Linked to Commerically Distributed Dry-Cured Salami--Washington and California, 1994. Morbid. Mortal. Weekly Rep. 44:157-160.

38. CDC. 1996. Outbreak of *Escherichia coli* O157:H7 infections associated with drinking unpasteurized commercial apple juice—British Columbia, California, Colorado, and Washington, October 1996. Morbid. Mortal. Weekly Rep. 45:975.

39. CDC. 1999. Outbreak of *Salmonella* serotype Muenchen infections associated with unpasteurized orange juice—United States and Canada, June 1999. Morbid. Mortal. Weekly Rep. 48:582–58.

40. CDC. 1997. Outbreaks of *Escherichia coli* O157:H7 infection and cryptospordiosis assiociated with drinking unpasteurized apple cider-Connecticut and New York, October 1996. Morbid. Mortal. Weekly Rep. 46:4-8.

41. CDC. 1997. Outbreaks of *Escherichia coli* O157:H7 infection associated with eating alfalfa sprouts-Michigan and Virginia, June- July 1997. Morbid. Mortal. Weekly Rep. 46:741-744.

42. CDC. 1993. Update: multistate outbreak of *Escherichia coli* O157:H7 infections from hamburgers-western United States, 1992-1993. Morbid. Mortal. Weekly Rep. 42:258-263.

43. Cerf, O. 1977. Tailing of survival curves of bacterial spores. Journal of Applied Bacteriology 42:1-9.

44. Chapman, B., N. Jensen, T. Ross, and M. Cole. 2006. Salt, Alone or in Combination with Sucrose, Can Improve the Survival of *Escherichia coli* O157 (SERL 2) in Model Acidic Sauces. Applied and Environmental Microbiology 72:5165-5172.

45. Chen, H. 2006. Use of linear, Weibull, and log-logistic functions to model pressure inactivation of seven foodborne pathogens in milk. Food Microbiology 24:197-204.

46. Chen, H., and D. G. Hoover. 2003. Pressure inactivation kinetics of *Yersinia enterocolitica* ATCC 35669. International Journal of Food Microbiology 87:161-171.

47. Cheville, A. M., C. Buchrieser, C.-M. Cheng, and C. W. Kaspar. 1996. *rpoS* Regulation of Acid, Heat, and Salt Tolerance in *Escherichia coli* O157:H7. Applied and Environmental Microbiology 62:1822-1824.

48. Chick, H. 1908. An investigation into the laws of disinfection. Journal of Hygiene 8:92-158.

49. Cody, S. H., M. K. Glynn, F. J. A., K. L. Cairns, P. M. Griffin, J. Kobayashi, M. Fyfe, R. Hoffman, A. S. King, J. H. Lewis, B. Swaminathan, R. G. Bryant, and D. J. Vugia. 1999. An Outbreak of *Escherichia coli* O157:H7 Infection from Unpasteurized Commerical Apple Juice. Annals of Internal Medicine 130:202-209.

50. Cole, M. B., K. W. Davies, G. Munro, C. D. Holyoak, and D. C. Kilsby. 1993. A vitalistic model to describe the thermal inactivation of *Listeria monocytogenes*. Journal of Industrial Microbiology 12:232-239.

51. Conner, D. E., and J. S. Kotrola. 1995. Growth and survival of *Escherichia coli* O157:H7 under acidic conditions. Applied and Environmental Microbiology 61:382-385.

52. Cook, G. M. 2000. The intracellular pH of the thermophilic bacterium *Thermoanaerobacter wiegelii* during growth and production of fermentation acids. Extremophiles 4:279-284.

53. Cook, K. A., T. E. Dobbs, W. G. Hlady, and e. al. 1998. Outbreak of *Salmonella* Serotype Hartford Infections Associated With Unpasteurized Orange Juice. JAMA 280:1504-1509.

54. Coroller, L., I. Leguerinel, E. Mettler, N. Savy, and P. Mafart. 2006. General Model, Based on Two Mixed Weibull Distributions of Bacterial Resistance, for Describing Various Shapes of Inactivation Curves. Applied and Environmental Microbiology 72:6493-6502.

55. Corrandini, M. G., and M. Peleg. 2009. Dynamic Model of Heat Inactivation Kinetics for Bacterial Adaptation. Applied and Environmental Microbiology 75:2590-2597.

56. Critzer, F. J., and M. P. Doyle. 2010. Microbial ecology of foodborne pathogens assocociated with produce. Critical Opinion in Biotechnology 21:125-130.

57. Diez-Gonzalez, F., and J. B. Russell. 1997. The ability of *Escherichia coli* O157:H7 to decrease its intracellular pH and resist the toxicity of acetic acid. Microbiology 143:1175-1180.

58. Diez-Gonzalez, F., and J. B. Russell. 1997. Effects of carbonylcyanide-m-chlorophenylhydrazone (CCCP) and acetate on *Escherichia coli* O157:H7 and K-12: uncoupling versus anion accumulation. FEMS Microbiology Letters 151:71-76.

59. Diez-Gonzalez, F., and J. B. Russell. 1999. Factors affecting the extreme acid resistance of *Escherichia coli* O157:H7. Food Microbiology 16:367-374.

60. Dougherty, D. P. 2002. Deterministic and Semi-Mechanistic Approaches in Predictive Fermentation Microbiology. North Carolina State University, Raleigh.

61. Dougherty, D. P., E. R. Da Conceicao Neta, R. F. McFeeters, S. R. Lubkin, and J. F. Breidt. 2006. Semi-mechanistic partial buffer approach to modeling pH, the buffer properties, and the distribution of ionic species in complex solutions. Journal of Agricultural and Food Chemistry 54:6021-6029.

62. Doyle, M. P., and L. R. Beuchat. 2007. Food Microbiology: Fundamentals and Frontiers, 3rd ed. ASM Press, Washington, D. C.

63. Entani, E., M. Asai, S. Tsujihata, S. Tsujihata, and M. Ohta. 1998. Antibacterial Action of Vinegar against Food-Borne Pathogenic Bacteria Including *Escherichia coli* O157:H7. Journal of Food Protection 61:953-959.

64. FDA. 2009. Bad Bug Book: Foodborne Pathogenic Microorganisms and Natural Toxins Handbook *Escherichia coli* O157:H7. United States Food and Drug Administration.

65. Fernandez, A., J. Collado, L. M. Cunha, M. J. Ocio, and A. Martinez. 2002. Empirical model building based on Weibull distribution to describe the joint effect of pH and temperature on the thermal resistance of *Bacillus cereus* in vegetable substrate. International Journal of Food Microbiology 77:147-153.

66. Foster, J. W., and H. K. Hall. 1991. Inducible pH Homeostasis and the Acid Tolerance Response of *Salmonella typhimurium*. Journal of Bacteriology 173:5129-5135.

67. Garren, D. M., M. A. Harrison, and S. M. Russell. 1997. Retention of Acid Tolerance and Acid Shock Responses of *Escherichia coli* O157:H7 and Non-O157:H7 Isolates. Journal of Food Protection 60:1478-1482.

68. Geeraerd, A. H., V. P. Valdramidis, and J. F. van Impe. 2005. GInaFiT, a freeware tool to assess non-log-linear microbial survivor curves. International Journal of Food Microbiology 102:95-105.

69. Gibson, A. M., N. Bratchell, and T. A. Roberts. 1987. The effect of sodium chloride and temperature on the rate and extent of growth of *Clostridium botulinum* type A in pasteurized pork slurry. Journal of Applied Bacteriology 62.

70. Gompertz, B. 1825. On the Nature of the Function Expressive of the Law of Human Mortality, and on a New Mode of Determining the Value of Life Contingencies. Philosophical Transactions of the Royal Society of London, 115:513-583.

71. Hancock, D. D., T. E. Besser, M. L. Kinsel, P. I. Tarr, D. H. Rice, and M. G. Paros. 1994. The Prevalence of *Escherichia coli* O157:H7 in Dairy and Beef in Washington State. Epidemiology and Infection 113:199-207.

72. Heldman, D. R., and R. L. Newsome. 2003. Kinetic Models for Microbial Survival During Processing. Food Technology 57:40-47.

73. Hermann, D., and J. Horst. 1970. Molecular Radiation Biology. Springer, Berlin.

74. Horiuchi, J., S. Kikuchi, J. Kobayashi, T. Kanno, and T. Shimizu. 2001. Modeling of pH response in continuous anaerobic acidogenesis by an artifical neural network. Biochemical Engineering Journal 9:199-204.

75. Horowitz, J., M. D. Normand, M. G. Corrandini, and M. Peleg. 2010. Probabilistic Model of Microbial Cell Growth, Division and Mortality. Applied and Environmental Microbiology 76:230-242.

76. Horton, H. R., L. A. Moran, K. G. Scrimgeour, M. D. Perry, and J. D. Rawn. 2006. Principles of Biochemistry. Pearson Prentice Hall, Upper Saddle River, NJ.

77. Ita, P. S., and R. W. Hutkins. 1991. Intracellular pH and Survival of *Listeria monocytogenes* Scott A in Tryptic Soy Broth Containing Acetic, Lactic, Citric, and Hydrochloric Acids. Journal of Food Protection 54:15-19.

78. Janssen, M., A. H. Geeraerd, A. Cappuyns, L. Garcia-Gonzalez, G. Schockaert, N. Van Houteghem, K. M. Vereecken, J. Debevere, F. Devlieghere, and J. F. Van Impe. 2007. Individual and Combined Effects of pH and Lactic Acid Concentration on *Listeria innocua* Inactivation: Development of a Predictive Model and Assessment of Experimental Variability. Applied and Environmental Microbiology 73:1601-1611.

79. Janssen, M., A. Verhulst, V. P. Valdramidis, F. Devlieghere, J. F. Van Impe, and A. H. Geeraerd. 2008. Inactivation model equations and their associated parameter values obtained under static acid stress conditions cannot be used directly for predicting inactivation under dynamic conditions. International Journal of Food Microbiology 128:136-145.

80. Jay, M. T., M. Michael Cooley, D. Carychao, G. W. Wiscomb, R. A. Sweitzer, L. Crawford-Miksza, J. A. Farrar, D. K. Lau, J. O'Connell, A. Millington, R. V. Asmundson, E. R. Atwill, and E. R. Mandrell. 2007. *Escherichia col*i O157:H7 in Feral Swine near Spinach Fields and Cattle, Central California Coast. Emerging Infectious Diseases 13:1908-1911.

81. Jordan, K. N., and K. W. Davies. 2001. Sodium chloride enhances recovery and growth of acid-stressed *E. coli* O157:H7. Letters in Applied Microbiology 32:312-315.

82. Jordan, K. N., L. Oxford, and C. P. O'Bryne. 1999. Survival of Low-pH Stress by *Escherichia coli* O157:H7: Correlation between Alterations in the Cell Envelope and Increased Acid Tolerance. Applied Environmental Microbiology 65:3048-3055.

83. Jordan, S. L., J. Glover, L. Malcolm, F. M. Thomson-Carter, I. R. Booth, and S. F. Park. 1999. Augmentation of killing of *Escherichia coli* O157 by combinations of lactate, ethanol, and low-pH conditions. Applied and Environmental Microbiology 65:1308-1311.

84. Kamau, D. N., S. Doores, and K. M. Pruitt. 1990. Enhanced Thermal Destruction of *Listeria monocytogenes* and *Staphylococcus aureus* by the Lactoperoxidase System. Applied and Environmental Microbiology 56:2711-2716.

85. Karpel, E., T. Alon, G. Glaser, S. Schuldiner, and E. Padan. 1991. Expression of a Sodium Proton Antiporter (NhaA) in *Escherichia coli* Is Induced by Na^+ and Li^+ Ions. The Journal of Biological Chemistry 266:21753-21759.

86. Kashket, E. R. 1985. Effects of K^+ and Na^+ of the Proton Motive Force of Respiring *Escherichia coli* at Alkaline pH. Journal of Bacteriology 163:423-429.

87. Klotz, B., D. L. Pyle, and B. M. Mackey. 2007. New Mathematical Modeling Approach for Predicting Microbial Inactivation by High Hydrostatic Pressure. Applied and Environmental Microbiology 73:2468-2478.

88. Kobayashi, H. 2003. Computer simulation of cytoplasmic pH regulation mediated by the F-type H^+-ATPase. Biochim. Biophys. Acta 1607:211-216.

89. Konings, W. N., A. Albers, S. Koning, and A. J. M. Driessen. 2002. The cell membrane plays a crucial role in survival of bacteria and archaea in extreme environments. Antonie van Leeuwenhoek 81:61-72.

90. Koutsoumanis, K., K. Lambropoulou, and G.-J. E. Nychas. 1999. A predictive model for the non-thermal inactivation of *Salmonella enteritidis* in a food model system supplemented with a natural antimicrobial. International Journal of Food Microbiology 49:63-74.

91. Kroder, M., P. M. H. Kroneck, and H. Cypionka. 1991. Determination of the transmembrane proton gradient in the anaerobic bacterium *Desulfovibrio desulfuricans* by ^{31}P nuclear magnetic resonance. Archives of Microbiology 156:145-147.

92. Kroll, R. G., and I. R. Booth. 1983. The relationship between intracellular pH, the pH gradient and potassium transport in *Escherichia coli*. Biochem. J. 216:709-716.

93. Kroll, R. G., and I. R. Booth. 1981. The role of potassium transport in the generation of a pH gradient in *Escherichia coli*. Biochem. J 198:691-698.

94. Kutalik, Z., M. Razaz, and J. Baranyi. 2005. Connection between stochastic and deterministic modelling of microbial growth. Journal of Theoretical Biology 232:285-299.

95. Laird, A. K. 1964. British Journal of Cancer 18:490.

96. Laird, A. K. 1965. Dynamics of Tumour Growth: Comparison of Growth Rates and Extrapolations of Growth Curve to One Cell. British Journal of Cancer 19:278–291.

97. Leyer, G. J., L. Wang, and E. A. Johnson. 1995. Acid Adaptation of *Escherichia coli* O157:H7 Increases Survival in Acidic Foods. Applied and Environmental Microbiology 61:3752-3755.

98. Li, H., G. Xie, and A. E. Edmondson. 2007. Evolution and limitations of primary mathematical models in predictive microbiology. British Food Journal 109:608-626.

99. Lin, J., I. S. Lee, J. Frey, J. L. Slonczewski, and J. W. Foster. 1995. Comparative Analysis of Extreme Acid Survival in *Salmonella typhimurium, Shigella flexneri, and Escherichia coli*. Journal of Bacteriology 177:4097-4104.

100. Lin, J., M. P. Smith, K. C. Chapin, H. S. Baik, G. N. Bennett, and J. W. Foster. 1996. Mechanisms of Acid Resistance in Enterohemorrhagic *Escherichia coli*. Applied and Environmental Microbiology 62:3094-3100.

101. Little, C. L., M. R. Adams, W. A. Anderson, and M. B. Cole. 1994. Application of a log-logistic model to describe the survival of Yersinia enterocolitica at sub-optimal pH and temperature. International Journal of Food Microbiology 22:63-71.

102. Lo, C., M. C. Leake, and R. M. Berry. 2006. Fluorescence Measurement of Intracellular Sodium Concentration in Single *Escherichia coli* Cells. Biophys. J. 90:357-365.

103. Lo, C. F. 2009. Stochastic Nonlinear Gompertz Model of Tumour Growth. Proceedings of the World Congress on Engineering 2.

104. McClure, P. J., C. d. W. Blackburn, M. B. Cole, P. S. Curtis, J. E. Jones, J. D. Legan, I. D. Ogden, M. W. Peck, T. A. Roberts, J. P. Sutherland, and S. J. Walker. 1994. Modelling the growth, survival and death of microorganisms in foods: the UK Food Micromodel approach. International Journal of Food Microbiology 23:265-275.

105. McDonald, L. C., H. P. Fleming, and H. M. Hassan. 1990. Acid Tolerance of *Leuconostoc mesenteroides* and *Lactobacillus plantarum*. Applied and Environmental Microbiology 56:2120-2124.

106. McFeeters, R. F., and H. P. Fleming. 1997. Balancing macromineral composition of fresh-pack cucumber pickles to improve quality and maintain flavor. Journal of Food Quality 20:81-89.

107. McKellar, R. C., and X. Lu. 2004. Modeling Microbial Responses in Food. CRC Press, Boca Raton, Fl.

108. McKellar, R. C., and X. Lu. 2003. Modeling Microbial Responses in Food. CRC Press, Boca Raton, Fl.

109. Mead, P. S., and P. M. Griffin. 1998. *Escherichia coli* O157:H7. The Lancet 352:1207-1212.

110. Membre, J., V. Majchrzak, and I. Jolly. 1997. Effects of Temperature, pH, Glucose, and Citric Acid on the Inactivation of *Salmonella typhimurium* in Reduced Calorie Mayonnaise. Journal of Food Protection 60:1497-1501.

111. Menzel, U., and G. Gottschalk. 1985. The internal pH of *Acetobacterium wieringae* and *Acetobacter aceti* during growth and production of acetic acid. Archives of Microbiology 143:47-51.

112. Michino, H., K. Araki, S. Minami, S. Takaya, N. Sakai, M. Miyazaki, A. Ono, and H. Yanagawa. 1999. Massive Outbreak of *Escherichia coli* O157:H7 Infection in Schoolchildren in Sakai City, Japan, Associated with Consumption of White Radish Sprouts. American Journal of Epidemiology 150:787-796.

113. Molenaar, D., T. Abee, and W. N. Konings. 1991. Continuous measurement of the cytoplasmic pH in *Lactococcus lactis* with a fluorescent pH indicator. Biochimica et biophysica acta 1115:75-83.

114. Monod, J. 1949. The growth of bacterial cultures. A. Rev. Microbiol 3:371-394.

115. Nannen, N. L., and R. W. Hutkins. 1990. Intracellular pH Effects in Lactic Acid Bacteria. J. Dairy Sci. 74:741-746.

116. Navon, G., S. Ogawa, R. G. Shulman, and T. Yamane. 1977. High-resolution ^{31}P nuclear magnetic resonance studies of metabolism in aerobic *Escherichia coli* cells. Proc. Nati. Acad. Sci. 74:888-891.

117. Nisbet, R. M., and W. S. C. Gurney. 1982. Modelling Fluctuating Populations. John Wiley & Sons Ltd.

118. Norton, L. 1988. A Gompertzian Model of Human Breast Cancer Growth. Cancer Research 48:7067-7071.

119. Norton, L., R. Simon, H. D. Brereton, and A. E. Bogden. 1976. Predicting the course of Gompertzian growth. Nature 264.

120. O'Neil, P. V. 2007. Advanced Engineering Mathematics, 6th ed. Chris Carson, Toronto, Canada.

121. O'Sullivan, E., and S. Condon. 1997. Intracellular pH Is a Major Factor in the Induction of Tolerance to Acid and Other Stresses in *Lactococcus lactis*. Applied and Environmental Microbiology 63:4210-4215.

122. Oh, D.-H., Y. Pan, E. Berry, M. Cooley, R. Mandrell, and F. Breidt Jr. 2009. *Escherichia coli* O157:H7 Strains Isolated from Environmental Sources Differ Significantly in Acetic Acid Resistance Compared with Human Outbreak Strains. Journal of Food Protection 72:503-509.

123. Park, S., R. W. Worobo, and R. A. Durst. 1999. *Escherichia coli* O157:H7 As an Emerging Foodborne Pathogen: A Literature Review. Critical Reviews in Food Science and Nutrition 39:481-502.

124. Peleg, M. 2006. Advanced Quantitative Microbiology for Foods and Biosystems: Models for Predictiving Growth and Inactivation. CRC Press, Boca Raton, Fl.

125. Peleg, M. 2000. Microbial survival curves - the reality of flat "shoulders" and absolute thermal death times. Food Research International 33:531-538.

126. Peleg, M., and M. Cole. 1998. Reinterpretation of Microbial Survival Curves. Critical Reviews in Food Science 38.

127. Peleg, M., and M. B. Cole. 2000. Estimating the Survival of *Clostridium botulinum* Spores during Heat Treatments. Journal of Food Protection 63:190-195.

128. Peleg, M., M. D. Normand, and O. H. Campanella. 2003. Estimating Microbial Inactivation Parameters from Survival Curves Obtained Under Varying Conditions- The Linear Case. Bulletin of Mathematical Biology 65:219-234.

129. Pitzer, K. S. 1991. Activity Coefficients in Electrolyte Solutions.

130. Rangel, J. M., P. H. Sparling, C. Crowe, P. M. Griffin, and D. L. Swerdlow. 2005. Epidemology of *Escherichia coli* O157:H7 Outbreaks, United States, 1982-2002. Emerging Infectious Diseases 11:603-609.

131. Rao, P. V. 1998. Statistical Research Methods in the Life Sciences. Duxbury Press.

132. Richard, H., and J. W. Foster. 2004. *Escherichia coli* Glutamate- and Arginine-Dependent Acid Resistance Systems Increase Internal pH and Reverse Transmembrane Potential. Journal of Bacteriology 186:6032-6041.

133. Richard, H., and J. W. Foster. 2007. Sodium regulates Escherichia coli acid resistance, and influences GadX- and GadW- dependent activation of *gadE*. Microbiology 153:3154-3161.

134. Riebeling, V., R. K. Thauer, and K. Jungermann. 1975. The Internal-alkaline pH Gradient, Sensitive to Uncoupler and ATPase Inhibitor, in Growing *Clostridium pasteurianium*. Eur. J. Biochem. 55:445-453.

135. Riondet, C., R. Cachon, Y. Waché, G. Alcaraz, and C. Diviès. 1997. Measurement of the intracellular pH in *Escherichia coli* with the internally conjugated fluorescent probe 5- (and 6-)carboxyfluorescein succinimidyl ester. Biotechnology Techniques 11:735-738.

136. Ross, T. 1996. Indices for performance evaluation of predictive models in food microbiology. Journal of Applied Bacteriology 81:501-508.

137. Ross, T., and T. A. McMeekin. 1994. Review Paper Predictive Microbiology. International Journal of Food Microbiology 23:241-264.

138. Rottenberg, H. 1979. The measurement of membrane potential and deltapH in cells, organelles, and vesicles. Methods Enzymol. 55:547–569.

139. Rottenberg, H. 1975. The Measurement of Transmembrane Electrochemical Proton Gradients. Bioenergetics 7:61-74.

140. Rowbury, R. J., M. Goodson, and T. J. Humphrey. 1994. Sodium Chloride Induces an NhaA/NhaR-Independent Acid Sensitivity at Neutral External pH in *Escherichia coli*. Applied and Environmental Microbiology 60:1630-1634.

141. Russell, J. B. 1992. Another explanation for the toxicity of fermentation acids at low pH: anion accumulation versus uncoupling. Journal of Applied Bacteriology 107:363-370.

142. Russell, J. B. 1991. Resistance of *Streptococcus bovis* to acetic acid at low pH: relationship between intracellular pH and anion accumulation. Applied and Environmental Microbiology 57:255-259.

143. Ryan, C. A., R. V. Tauxe, G. W. Hosek, J. G. Wells, P. A. Stoesz, J. McFadden, H. W., P. W. Smith, G. F. Wright, and P. A. Blake. 1986. *Escherichia coli* O157:H7 Diarrhea in a Nursing Home: Clinical, Epidemiological, and Pathological Findings. The Journal of Infectious Diseases 154:631-638.

144. Salhany, J. M., T. Yamane, R. G. Shulman, and S. Ogawa. 1975. High resolution ^{31}P nuclear magnetic resonance studies of intact yeast cells. Proc. Nati. Acad. Sci. 72:4966-4970.

145. Salmond, C. V., R. G. Kroll, and I. R. Booth. 1984. The effect of food preservatives on pH homeostasis in *Escherichia coli*. Journal of General Microbiology 130:2845-2850.

146. Shabala, L., B. Budde, T. Ross, H. Siegumfeldt, and T. McMeekin. 2002. Responses of *Listeria monocytogenes* to acid stress and glucose availability monitored by measurements of intracellular pH and viable counts. International Journal of Food Microbiology 75:89-97.

147. Shao. 1993. Linear Model Selection by Cross-Validation. Journal of the American Statistical Association 88:486-494.

148. Siegumfeldt, H., K. B. Rechinger, and M. Jakobsen. 2000. Dynamic Changes of Intracellular pH in Individual Lactic Acid Bacterium Cells in Response to a Rapid Drop in Extracellular pH. Applied and Environmental Microbiology 66:2330-2335.

149. Simpson-Herren, L., and H. H. Lloyd. 1970. Kinetics Parameters and Growth Curves for Experimental Tumor Systems. Cancer Chemotherapy Reports Part 1 54:143-174.

150. Skandamis, P. N., and G.-J. E. Nychas. 2000. Development and Evaluation of a Model Predicting the Survival of *Escherichia coli* O157:H7 NCTC 12900 in Homemade Eggplant Salad at Various Temperatures, pHs, and Oregano Essential Oil Concentrations. Applied and Environmental Microbiology 66:1646-1653.

151. Skinner, G. E., and J. W. Larkin. 1994. Mathematical Modeling of Microbial Growth: A Review. Journal of Food Safety 14:175-217.

152. Slonczewski, J. L., B. P. Rosen, J. R. Alger, and R. M. Macnab. 1981. pH homeostasis in *Escherichia coli*: measurement by ^{31}P nuclear magnetic resonance of methylphosphonate and phosphate. Proc. Nati. Acad. Sci. 78:6271-6275.

153. Smith, C. E., and H. C. Tuckwell. 1974. Some Stochastic Growth Processes. *In* P. van de Driessche (ed.), Lecture Notes in Biomathematics: Mathematical Problems in Biology (Victoria Conference), vol. 2. Springer, New York.

154. Sofos, J. N. 1983. Antimicrobial effects of sodium and other ions in food: a review. Journal of Food Safety 6:45-78.

155. Su, C., and L. J. Brandt. 1995. *Escherichia coli* O157:H7 Infection in Humans. Annals of Internal Medicine 123:698-714.

156. Taormina, P. J., and L. R. Beuchat. 1999. Behavior of Enterohemorrhagic *Escherichia coli* O157:H7 on Alfalfa Sprouts during the Sprouting Process as Influenced by Treatments with Various Chemicals. Journal of Food Protection 62:850-856.

157. Tilden, J. J., W. Young, A. M. McNamara, C. Custer, B. Boesel, M. A. Lambert-Fair, J. Majkowski, D. Vugia, S. B. Werner, J. Hollingsworth, and J. G. J. Morris. 1996. A new route of transmission for Escherichia coli: Infection from dry fermented salami. American Journal of Public Health 86:1142-1145.

158. Tsujihata, S., E. Entani, M. Asai, Y. Tsukamoto, and M. Ohta. 1998. Mathematical modeling to predict the bactericidal effect of processed vinegar on *Escherichia coli* O157:H7. International Journal of Food Microbiology 43:135-138.

159. van Boekel, M. A. J. S. 2002. On the use of the Weibull model to describe thermal inactivation of microbial vegetative cells. International Journal of Food Microbiology 74:139-159.

160. Virto, R., D. Sanz, I. Alvarez, S. Condon, and J. Raso. 2006. Application of the Weibull model to describe inactivation of *Listeria monocytogenes* and *Escherichia coli* by citric and lactic acid at different temperatures. Journal of the Science of Food and Agriculture 86:865-870.

161. Warnecke, T., and R. T. Gill. 2005. Organic acid toxicity, tolerance, and products in *Escherichia col*i biorefining applications. Microbial Cell Factories 4.

162. Whiting, R. C. 1993. Modeling bacterial survival in unfavorable enviroments. Journal of Industrial Microbiology 12:240-246.

163. Whiting, R. C., and R. L. Buchanan. 1993. Letter to the Editor: A classification of models in predictive microbiology - a reply to K. R. Davey. Food Microbiology 10:175-177.

164. Williams, R. C., S. Isaacs, M. Decou, E. A. Richardson, M. C. Buffett, R. W. Slinger, M. H. Brodsky, B. W. Ciebin, A. Ellis, J. Hockin, and W. G. *E. coli* O157:H7. 2000. Illness outbreak associated with *Escherichia coli* O157:H7 in Genoa salami. Canadian Medical Association 162:1409-1413.

165. Wong, C. S., S. Jelacic, R. L. Habeeb, S. L. Watkins, and P. I. Tarr. 2000. The Risk of the Hemolytic-Uremic Syndrome After Antibotic Treatment of *Escherichia col*i O157:H7 Infections. The New England Journal of Medicine 342:1930-1936.

166. Xie, G., and R. Xiong. 1999. Use of hyperbolic and neural network models in modelling quality changes of dry peas in long time cooking. Journal of Food Engineering 41:151-162.

167. Xiong, R., G. Xie, A. E. Edmondson, R. H. Linton, and M. A. Sheard. 1999. Comparison of the Baranyi model with the modified Gompertz equation for modelling thermal inactivation of *Listeria monocytogenes* Scott A. Food Microbiology 16:269-279.

168. Xiong, R., G. Xie, A. E. Edmondson, and M. A. Sheard. 1999. A mathematical model for bacterial inactivation. International Journal of Food Microbiology 46:45-55.

APPENDIX

Table A. 1 Diagnostics for comparing models within a salt and ionic strength treatment. Values in red represent the diagnostics which are optimal.

Ionic Strength	Salt	Model	MSE	R^2	AIC	SBC	A_f	B_f
0.342	LiCl	Weibull	0.1242	0.9976	-49.0849	-47.0017	1.0441	0.9977
		Gompertz**	0.0780	0.9985	-60.2455	-58.1624	1.0351	1.0013
		Logistic	0.1486	0.9971	-44.7737	-42.6905	1.0472	1.0004
		Cole*	0.0719	0.9986	-62.2130	-60.1298	1.0354	1.0001
	NaCl	Weibull	0.0184	0.9997	-62.9732	-60.8488	1.0142	0.9993
		Gompertz	0.0318	0.9995	-54.1994	-52.0750	1.0206	1.0058
		Logistic**	0.0161	0.9997	-65.1456	-63.0212	1.0139	0.9999
		Cole*	0.0091	0.9998	-74.1572	-72.0328	1.0097	1.0001
	KCl	Weibull**	0.0282	0.9993	-91.8239	-89.7471	1.0184	0.9977
		Gompertz	0.1181	0.9974	-54.5695	-52.4927	1.0416	1.0007
		Logistic	0.0380	0.9992	-84.0232	-81.9464	1.0223	1.0015
		Cole*	0.0238	0.9995	-96.1971	-94.1203	1.0179	0.9964
	RbCl	Weibull**	0.0559	0.9989	-65.3512	-63.2644	1.0303	0.9984
		Gompertz	0.0769	0.9984	-58.0322	-55.9454	1.0326	1.0067
		Logistic	0.0601	0.9988	-63.6902	-61.6035	1.0317	0.9997
		Cole*	0.0388	0.9992	-73.7340	-71.6472	1.0231	1.0005
	CsCl	Weibull	0.2103	0.9958	-36.4487	-34.3655	1.0553	1.0030
		Gompertz	0.3211	0.9935	-26.2824	-24.1992	1.0666	1.0080
		Logistic*	0.2019	0.9959	-37.4188	-35.3356	1.0544	1.0028
		Cole	0.2665	0.9933	-22.8298	-20.7191	1.3202	0.7582
	CaCl2	Weibull	0.0405	0.9994	-75.9787	-73.8956	1.0195	0.9989
		Gompertz**	0.0123	0.9998	-104.6100	-102.5270	1.0106	0.9986
		Logistic	0.0192	0.9997	-93.9140	-91.8308	1.0137	0.9986
		Cole*	0.0096	0.9999	-110.4120	-108.3290	1.0096	1.0003
	MgCl2	Weibull	0.0280	0.9996	-84.8118	-82.7286	1.0148	0.9994
		Gompertz**	0.0086	0.9999	-113.1530	-111.0700	1.0084	0.9994
		Logistic	0.0124	0.9998	-104.2940	-102.2100	1.0098	0.9992
		Cole*	0.0080	0.9999	-114.8830	-112.8000	1.0080	1.0003
0.684	LiCl	Weibull	0.2190	0.9953	-26.3628	-24.2521	1.0626	1.0043
		Gompertz**	0.1497	0.9968	-33.2168	-31.1061	1.0499	1.0020
		Logistic	0.1948	0.9958	-28.4692	-26.3585	1.0595	1.0032
		Cole*	0.1479	0.9968	-33.4296	-31.3189	1.0493	1.0020
	NaCl	Weibull	0.0544	0.9990	-51.4366	-49.3259	1.0280	1.0011
		Gompertz**	0.0328	0.9994	-60.5583	-58.4476	1.0189	1.0006
		Logistic	0.0355	0.9993	-59.1346	-57.0239	1.0230	1.0005
		Cole*	0.0299	0.9994	-62.1793	-60.0686	1.0184	1.0033
	KCl	Weibull	0.1279	0.9968	-36.0441	-33.9334	1.0516	1.0030
		Gompertz	0.1978	0.9951	-28.1950	-26.0842	1.0679	1.0046
		Logistic**	0.1277	0.9968	-36.0759	-33.9652	1.0544	1.0027
		Cole*	0.1198	0.9970	-37.2316	-35.1209	1.0491	1.0023
	RbCl	Weibull**	0.3446	0.9907	-18.2040	-16.0932	1.1000	1.0073
		Gompertz	0.4480	0.9879	-13.4840	-11.3733	1.1207	1.0135
		Logistic	0.3817	0.9897	-16.3675	-14.2567	1.1073	1.0099
		Cole*	0.3230	0.9913	-19.3688	-17.2580	1.1016	1.0077
	CsCl	Weibull	0.2657	0.9933	-22.8842	-20.7735	1.0817	1.0059
		Gompertz	0.4112	0.9897	-15.0232	-12.9125	1.0967	1.0088
		Logistic*	0.2640	0.9934	-22.9987	-20.8880	1.0804	1.0053
		Cole	0.2655	0.9934	-22.8967	-20.7860	1.0817	1.0053
	CaCl2	Weibull	0.0401	0.9994	-76.1897	-74.1065	1.0221	1.0170
		Gompertz*	0.0303	0.9995	-82.9715	-80.8883	1.0199	1.0031
		Logistic	0.0394	0.9994	-76.6564	-74.5732	1.0218	1.0002
		Cole	0.0313	0.9995	-82.1336	-80.0505	1.0194	1.0011
	MgCl2	Weibull	0.0191	0.9997	-94.0644	-91.9812	1.0128	0.9979
		Gompertz**	0.0054	0.9999	-124.4310	-122.3470	1.0069	0.9999
		Logistic	0.0069	0.9999	-118.4610	-116.3780	1.0082	0.9995
		Cole*	0.0050	0.9999	-126.3450	-124.2620	1.0068	1.0000

[a] *denotes best model based on the AIC values.
** denotes best two-parameter model.

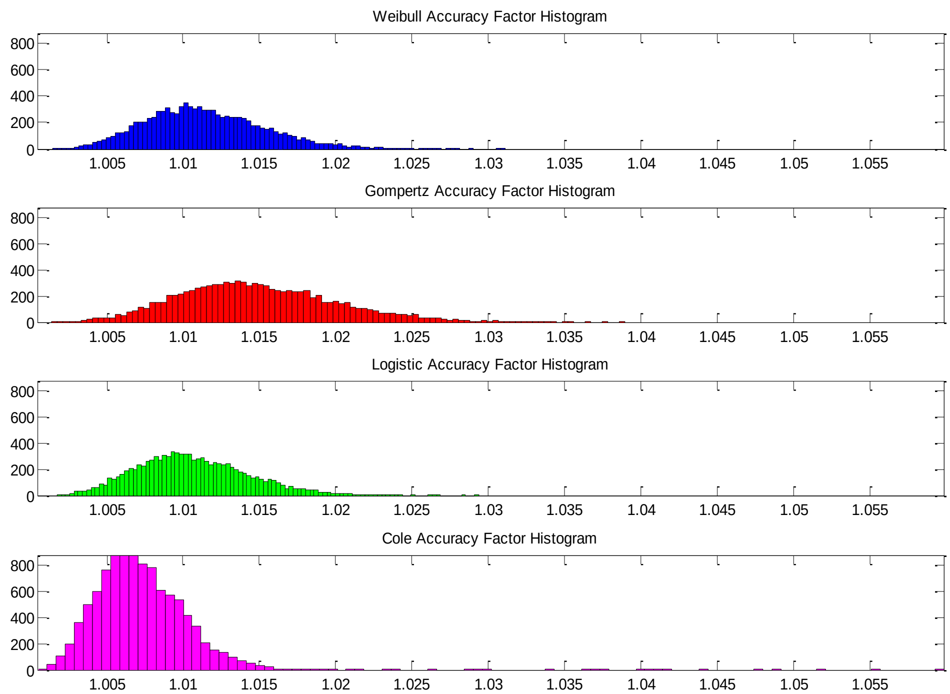

Figure A. 1 Accuracy factor histograms of 10,000 Weibull models (A), Gompertz models (B), Logistic models (C) and Cole models based on approximations of the NaCl data at ionic strength 0.342

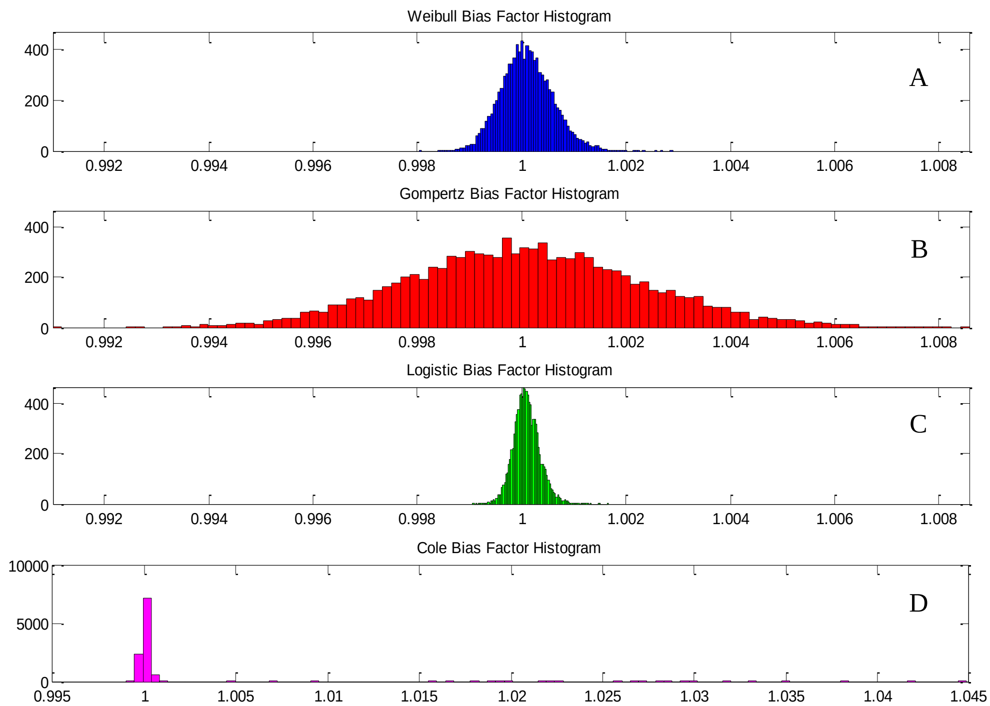

Figure A. 2 Bias factor histograms of 10,000 Weibull models (A), Gompertz models (B), Logistic models (C) and Cole models (D) based on approximations of the NaCl data at ionic strength 0.342.

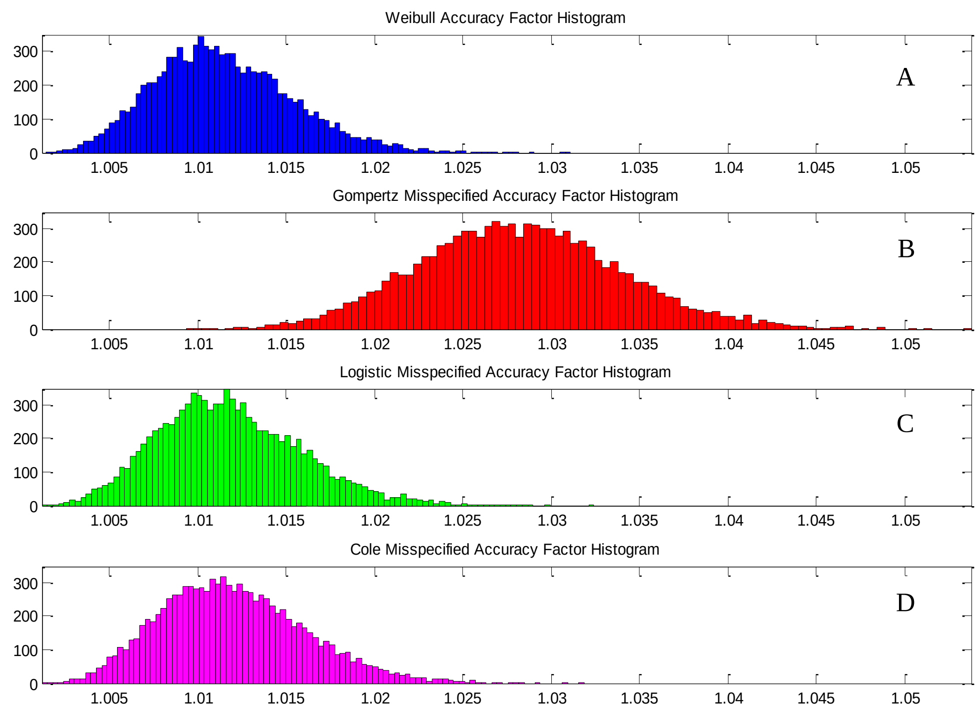

Figure A. 3 Weibull data was generated using 10,000 Weibull models based on the approximation of NaCl (ionic strength 0.342) data, with error from a normal distribution (mean 0, variance from the approximation of the Weibull fit). The generated Weibull data was then approximated with a Gompertz model (B), a Logistic model (C), or a Cole model (D) and the accuracy factor was then calculated.

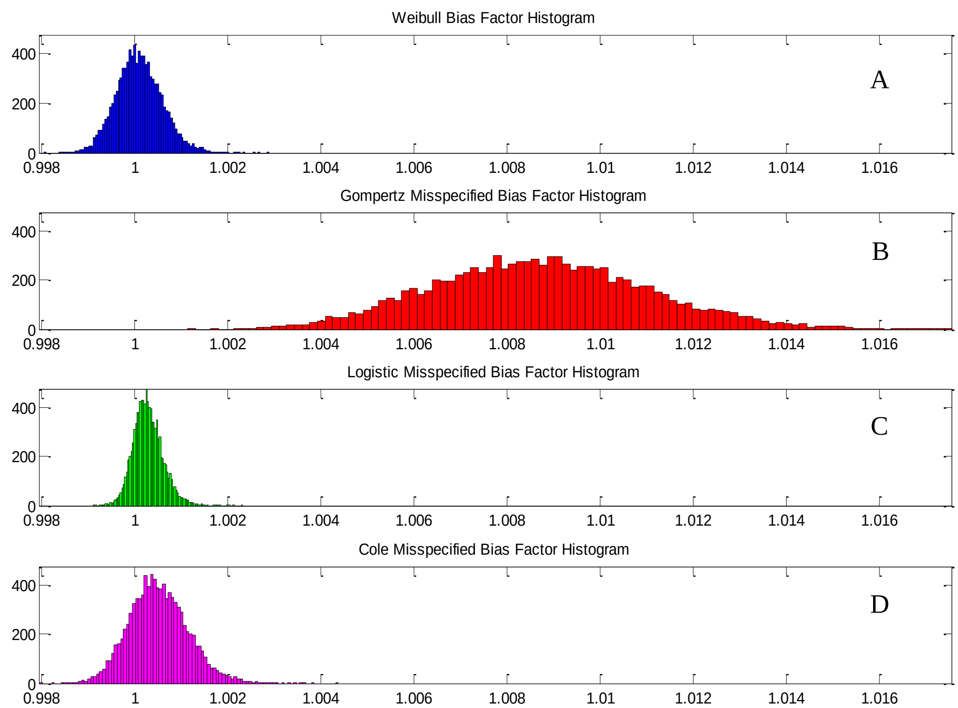

Figure A. 4 Weibull data was generated using 10,000 Weibull models based on the approximation of NaCl (ionic strength 0.342) data, with error from a normal distribution (mean 0, variance from the approximation of the Weibull fit). The generated Weibull data was then approximated with a Gompertz model (B), a Logistic model (C), or a Cole model (D) and the bias factor was then calculated.